DEVELOPMENT AND CHARACTERIZATION OF HYBRID GLASS FIBER AND EPOXY CLAY NANOCOMPOSITES

BY

AHMAD RAFIQ

A Thesis Presented to the
DEANSHIP OF GRADUATE STUDIES

KING FAHD UNIVERSITY OF PETROLEUM & MINERALS

DHAHRAN, SAUDI ARABIA

In Partial Fulfillment of the
Requirements for the Degree of

MASTER OF SCIENCE

In

MECHANICAL ENGINEERING

MAY 2014

KING FAHD UNIVERSITY OF PETROLEUM & MINERALS

DHAHRAN- 31261, SAUDI ARABIA

DEANSHIP OF GRADUATE STUDIES

This thesis, written by **AHMAD RAFIQ** under the direction of his thesis advisor and approved by his thesis committee, has been presented and accepted by the Dean of Graduate Studies, in partial fulfilment of the requirements for the degree of **MASTER OF SCIENCE IN MECHANICAL ENGINEERING**

Dr. Nesar Merah
(Advisor)

on his behalf

Dr. Zuhair M. A. Gasem
Department Chairman

Dr. Amro Al-Qutub
(Member)

Dr. Salam A. Zummo
Dean of Graduate Studies

عمادة الدراسات العليا
DEANSHIP OF GRADUATE STUDIES

Dr. Muhammad Abdul Samad
(Member)

Date 17/7/14

To those who fight to the very end.

ACKNOWLEDGEMENT

All thanks to Almighty ALLAH for giving me the strength, knowledge and courage to undertake this research and for making things easy when they appeared difficult. I am grateful to my father for keeping me strong and my mother for her relentless prayers and a never ending faith in me.

I would like to thank my advisor Dr. Nesar Merah whose guidance, support and encouragement led to timely completion of this work. I would also like to thank Dr. Muneer Al-Qadhi who always went out of his way to guide and help us. I would like to thank my committee members, Dr. Amro Al-Qutub and Dr. Abdul Samad for their input and guidance in this research work.

I would like extend special thanks to my friends Mr. Farooq Riaz Siddiqui and Mr. Nauman Zafar who supported me in all matters throughout my stay at KFUPM. Mr. Yasir Ali deserves a special mention for helping me out in every aspect of research and whose presence made the gloomy hours in lab much more bearable.

Finally, I would like to acknowledge the support provided by Mr. Lateef , Mr. Sadaqat , Mr. Sarafarz for various laboratory tasks and KFUPM as a whole for providing the facilities and means to carry out this research.

TABLE OF CONTENTS

LIST OF FIGURES

LIST OF TABLES

ABSTRACT

Full Name : Ahmad Rafiq

Thesis title : Development and characterization of hybrid glass fiber and epoxy clay nanocomposites.

Major Field : Mechanical Engineering

Date of Degree : May, 2014

In this work, electrical grade-corrosion resistant (E-CR) glass fiber mats are used to prepare glass fiber reinforced epoxy (GFRE) nanoclay composites using hand layup method followed by hot pressing. Hybrid GFRE nanoclay composites are manufactured using 0 to 5 wt% loading of I.30E nanoclay. High shear mixing is used to prepare the epoxy/clay nanocomposite. XRD analysis of hybrid GFRE nanoclay composites reveal an exfoliated/disordered intercalated morphology. The effect of nanoclay on mechanical properties is investigated by carrying out flexural and drop weight impact tests. The test results show that addition of nanoclay up to 1.5 wt% improves the flexural strength and flexural modulus by 11% and 14%, respectively. However, these properties start deteriorating when the clay content increased beyond 1.5wt%, mainly due to clay agglomeration.

Furthermore, the water barrier properties of GFRE nanoclay composites are studied at 23°C and 80°C. At 23°C there is a maximum of 1% water absorption while at 80°C the water uptake is seen to double. Addition of clay proves to be a good barrier. Subsequent flexural testing reveals that water uptake samples at 23°C cause a 7% decrease in strength and a 5% decrease in stiffness for 1.5 wt% while at 80°C, the degradation is observed to be 36% for flexural strength and 13% for stiffness. The decrease in mechanical properties is

attributed to the plasticizing effect of water and matrix swelling which also reduces the interaction between epoxy-clay and glass fibers.

Low-velocity impact is also studied for GFRE 0 wt% and GFRE nanoclay based composites for a range of energies between 10 to 50 J. It is observed that the addition of 1.5 wt% nanoclay improves the impact properties by 23%. Energy absorption increases with increasing impact energy and 1.5 wt% samples are seen to absorb the least amount of energy due to uniform dispersion of nanoclay. The stiffness of samples is determined using deflection at peak load and total impact duration, both of which are lowest for samples containing nanoclay which means that nanoclay addition makes the samples stiffer. This stiffness is maximum for 1.5 wt% after which it starts decreasing due to defects introduced by clay agglomeration and voids. The results from drop weight impact results were found to be in agreement with those obtained from flexural modulus.

The analysis of impact tested samples showed that damage occurred predominantly by delamination, matrix cracking, fiber buckling and fracture. Low impact energy resulted in delamination and matrix cracking with slight fiber breakage while samples subjected to higher impact energy went through complete perforation with a lot of fiber damage. Damage area increases with impact energy and is proportional to the amount of energy absorbed. The back side of impacted samples show the highest amount of damage as the damage proceeds towards the tensile direction.

MASTER OF SCIENCE DEGREE

KING FAHD UNIVERSITY OF PETROLEUM AND MINERALS

Dhahran, Saudi Arabia

ملخص الرسالة

الإسم الكامل : أحمد رفيق.

عنوان الرسالة : تطوير وتحسين المواد المركبة المصنوعة من الفايبر قلاس والايبوكسى.

التخصـــــص : الهندسة الميكانيكية.

تاريخ الدرجة العلمية : مايو 2014 م.

فى هذا العمل، استخدمت الياف الفايبر قلاس الكهربائية المقاومة للتاكل فى صنع مواد مركبة باستخدام تقنية الوضع اليدوى والضغط باستخدام الحرارةز مركبات مزدوجة تم تصنيعها باستخدام كميات مختلفة من الحشوات النانوطينية (من 0 الى 5 فى المائة) مصنوعة بواسطة طريقة الخلط بالقص العالى. اشعة اكس اثبتت ان درجة توزيع الحشوات النانوطينية كانت مختلطة بين تشتت عالى ومتوسط. ايضا تاثير اضافة الحشوات النانوطينية على الخواص الميكانيكية درس عن طريق اختبارى الانحناء والصدم. اظهرت النتائج ان اضافة 1.5 فى المائة ادى الى تحسن اجهاد الانحناء ومعامل المرونة بمقدار 11 و 14 فى المائة على التوالى لكن اضافة مزيد من الحشوات النانوطينية ادى الى انخفاض هذه الخواص نتيجة لتكتل الطين.

ايضا درجة اعاقة امتصاص الماء لمركب الفايبرقلاس و الحشوات النانوطينية درست عند درجة حرارة الغرفة و 80 درجة مئوية وتاثيرها على خواص الانحناء . اظهرت النتائج ان عند درجة حرارة الغرفة الامتصاص الاقصى كان عند 1 فى المائة لكن عند 80 درجة مئوية تضاعف امتصاص الماء. اضافة الحشوات النانوطينية اثبتت قدرتها على تخفيض امتصاص الماء. نتائج خواص الانحناء اظهرت انخفاض اجهاد الانحناء ومعامل المرونة بمقدار 7و 5 فى المائة عن عند اضافة 1.5 فى المائة من الحشوات النانوطينية على التوالى عند درجة حرارة الغرفة لكن عند زيادة درجة حرارة الماء ل 80 درجة مئوية لوحظ انخفاض بمقدار 36 و 13 فى المائة لاجهاد الانحناء ومعامل المرونة على التوالى انخفاض هذه الخواص الميكانيكية نتج عن التلين نتيجة لوجود الماء والذى ساعد فى تخفيض درجة الترابط بين الفايبر قلاس والايبوكسى والحشوات النانوطينية.

اختبارات الصدم عند سرعة منخفضة درس لمدى معين من الطاقة بين 10 الى 50 جول ايضا لوحظ ان اضافة 1.5 فى المائة حسن اجهاد الصدم بمقدار 23 فى المائة . امتصاص الطاقة زاد مع زيادة طاقة الصدم ولوحظ ان عند 1.5 فى المائة كان الامتصاص الادنى من طاقة الصدم نتيجة للتوزيع الجيد للحشوات النانوطينية.

صلابة العينات وجدت باستخدام الثنى عند الحمل الاقصى والزمن الكلى للصدم. لوحظ زيادة فى الصلابة عند اضافة الحشوات النانوطينية حتى 1.5 فى المائة بعد ذلك ادت العيوب مثل الفجوات والتكتل الطينى الى انخفاض الصلابة. ايضا وجد توافق فى النتائج الخاصة باختبارى الصلابة للصدم والانحناء.

اظهرت نتائج الميكروسكوب الضوئى الماسح لعينات اختبار الصدم ان الضرر كان سببه التبطين وتشقق الايبوكسى والالتواء والكسر. طاقات الصدم المنخفضة ادت الى التبطين والتشقق وانهيار جزء قليل من الفايبر لكن عند طاقات الصدم العالية لوحظ انثقاب كامل للعينات. مساحة الضرر زادت مع زيادة الطاقة الممتصة مع ضرر بالغ فى الفايبرقلاس. الجانب الاسفل من العينات المعرضة للصدم اظهرت ان الضرر الاكبر كان عند اتجاه الشد.

درجة الماجستير فى العلوم

جامعة الملك فهد للبترول والمعادن

الظهران ، المملكة العربية السعودية

CHAPTER 1

INTRODUCTION

1.1. Background

Addition of nanoclay as a filler has attracted a lot of attention as it enhances mechanical, flame retardant and barrier properties of polymer composites [1-7]. These nanocomposites may find specific use in areas such as piping industry due to the improved resistance to water and oil uptake along with considerable light weight compared to conventional composites and materials with added corrosion resistance [2-3]. The improvement in properties is generally attributed to the strong interaction between fibers and the dispersed nano sized clay particles embedded in the matrix [4].

For fiber reinforced composites, the improvement depends largely on the type of epoxy system, fibers, nano fillers and the processing technique employed [8-10]. During fabrication of fiber reinforced polymer composites the clay is first mixed with epoxy system using different methods such as mechanical, high shear mixing or ultra-sonication. This matrix is then reinforced with fibers using different techniques including hand layup, hot pressing and Vacuum Assisted Resin Transfer (VARTM) [2-3, 5-8].

Because of their improved properties, glass-fiber reinforced plastic (GFRP) have found an increasing application in industries related to oil and water handling and transportation, especially those for whom corrosion is a major concern. These materials, however, are prone to degradation by water absorption and low-velocity impacts which can occur in real-life scenarios by dropping tools etc during their service life.

1.2. Nano-Composites

Composite materials are a result of bringing together two or more materials with different properties to produce a material with entirely new and desired properties. Shown in Figure 1.1 are the common types of matrix namely metals, ceramics and polymers. There are a wide variety of reinforcements available which can be added to these matrix to get desired properties. The current work deals with polymer matrix composites with nanoclay and glass fiber fillers. The expressions 'hybrid composite' and 'hybrid nanocomposite' will be used to describe the materials throughout this thesis.

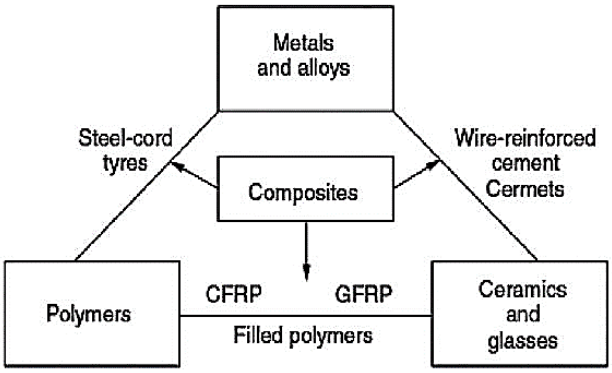

Figure 1.1 Common classes of composites.

One of the most common matrix for Glass Fiber Reinforced Plastics (GFRP) is the epoxy resin which is a thermoset polymer. As mentioned before, these polymers exhibit very good mechanical and thermal properties but these properties are easily degraded in the presence of water laden atmosphere as the water acts as an efficient plasticizer [11-12]. Reinforcing epoxy/fiber system with layered silicate nanoclay is one way to improve the barrier properties. Nanoclay are considered suitable reinforcements due to their low cost and high aspect ratio [13]. The water absorption or permeability of such nanocomposites depends

on the amount of clay content, the type of clay content (which translates to the aspect ratio) and the degree of dispersion of clay (will be discussed in more detail later). The addition of these nano silicate layers have been shown to be an effective barrier against water absorption and give a substantial improvement over naturally hydrophilic epoxy based composites [14].

The term ‘nanocomposite’ is used for the composites in which any one of the constituent materials has at least one of the dimensions less than 100 nm. Figure 1.2 gives a perspective of the size of objects as compared to nanoscale. Polymer nanocomposites have the advantage of exhibiting superior properties due to the very high surface to volume ratio and very high aspect ratio but their uniform dispersion is an issue which remains to date. Due to this high aspect ratio, the interfacial area between the matrix and reinforcement is many times greater in nanocomposites than in conventional composites which means that the matrix properties are substantially affected in areas in close vicinity of the reinforcement. Another implication of nano-size is that only a minute amount of nano reinforcement is enough to have a noticeable effect on the final composite [15].

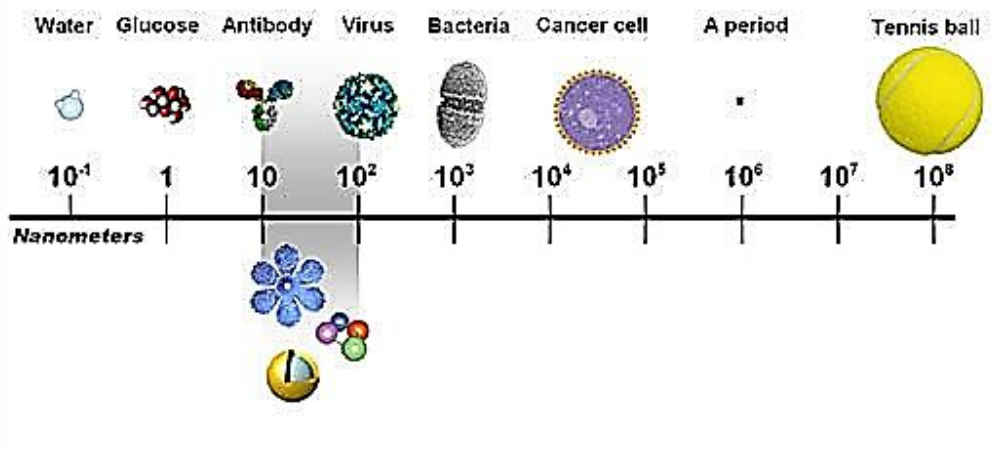

Figure 1.2 Scale comparison [61].

1.3. Objectives

The overall objective of this study is to develop a hybrid glass fiber/epoxy nanoclay composite (GFREnc) with improved mechanical and water uptake resistance properties which can be used for manufacturing GFRE pipes for water transportation. This study also aims at bringing a better understanding of different mechanical and physical properties by conducting an in depth testing and analysis of these nanocomposites under impact and flexural loading. The results of this study will benefit the scientific community and industry at large which will help to manufacture better and more economical GFRE pipes. The specific objectives of the proposed work are:

1. To develop a hybrid glass fiber and epoxy nanoclay composite while maintaining or improving its physical and mechanical properties.

2. To study the effect of clay addition on flexural properties and determine optimum clay loading.

3. To determine optimum clay loading as a barrier for water uptake process at different temperatures.

4. To investigate the effect of water ingress on the flexural properties of GFREnc hybrid composites.

5. To study the effect of nanoclay loading on the resistance of GFREnc composite to low velocity impact.

1.4. Motivation and Justification

The application of this research focuses mainly on the GFRE pipe manufacturing industries. There are big manufacturing groups operating in the Kingdom most notably, the

Saudi Arabian Amiantit and the Future Pipe Industries of Saudi Arabia. These companies manufacture commercial quantities of completely epoxy based GFRP pipes and accessories which are used extensively in oil and water transportation and handling. Where epoxy itself was lacking the desired mechanical properties, the addition of fiber reinforcements have shown much promise and with improved corrosion resistance (and thus long life) the GFRE based pipes are quickly replacing the metal pipes originally used by companies in the Kingdom of Saudi Arabia. However, as mentioned before, the vulnerabilities of epoxy based pipes such as water absorption still remains a concern which needs to be thoroughly addressed.

Figure 1.3 GFRE pipe being produced using filament winding.

Another major concern of using laminated structures is the damage induced by impact of foreign materials which are expected to be encountered during the service life. Damage induced by impacts can cause a drastic reduction in the strength of the structure. Of particular interest is the low-velocity impact situation which is quite common for piping

structures, such as tool drops, hail storms and runway debris. For this reason, impact on composite laminated structures has been the subject of extensive research but not much work has been carried out in the realm of nanocomposites and hybrid nanocomposites. Impact resistance of polymer nanocomposites is amongst the least understood and the most important mechanical properties of such composites [16]. This research focuses on different types of low-velocity impacts, impact characteristics and damage characterization.

The relatively low cost of clay and its availability makes this work economically feasible. The nanocomposite will give local designers working in pipe industries greater flexibility in making pipes. It is believed that the development of such nanocomposite and the possibility of furthering its production at the industrial level will help existing and future Saudi industries compete in the worldwide market.

1.5. Research Methodology

The previously stated objectives will be approached by dividing them into sub tasks dealing with (1) literature Review, (2) development of GFRE based clay nanocomposites, (3) structure characterization (4) water uptake and (5) mechanical testing (flexural & impact tests). These sub tasks will be briefly discussed in the following sections.

1.5.1. Literature Review

Literature review will be covered in chapter 2 of this thesis in which the existing scientific literature has been reviewed relevant to the topics. In order to do an extensive study, the literature review has been further divided into (1) material characterization (2) GFRE development (3) mechanical properties and (4) water absorption.

1.5.2. Development and Material Characterization

The commonly used development methods like vacuum infusion, vacuum bagging and hand layup were studied. Hand/wet layup method followed by hot pressing is chosen for this work. High Shear Mixing (HSM) technique is adopted to mix different clay loadings (0-5%) were used for making GFRP sheets in order to determine the optimum clay loadings. SEM and XRD are used for studying GFREnc morphology and structure while Pixera microscope camera is used for studying impact damage. Chapter 2 will deal with development and material characterization in more detail.

1.5.3. Water Absorption

Water absorption will be studied for GFRE based clay nanocomposite sheets for different clay loadings. Samples are cut according to ASTM D570 [66] and immersed into tap water for a period of four months at ambient and high temperatures. The change in weight is measured with time. More details on this will be treated in chapter 3 and 4.

1.5.4. Mechanical Testing

The effects of clay addition and water uptake on mechanical properties of GFRE nanoclay composites are amongst the main focus of this research. Flexural and impact tests were studied according to ASTM standards and the samples are meticulously prepared and tested to ensure repeatability.

CHAPTER 2

LITERATURE REVIEW

The following review deals with the latest research carried out largely in the field of fiber reinforced epoxy clay nanocomposites with focus on the work related to the previously defined objectives concerning the development and enhancing the physical and mechanical properties of glass fiber reinforced epoxy clay nanocomposites.

2.1. Material Characterization

Since the greatest improvement comes with the exfoliation of nano-clay, it is therefore necessary to be able to characterize different samples based on their morphology and the dispersion of nano-clay or to determine the nanostructure of the samples. Of these techniques, wide angle x-ray diffraction (XRD), Scanning Electron Microscopy and Transmission Electron Microscopy (TEM) are commonly used.

2.1.1. Morphology: Intercalated and Exfoliated Nanocomposites

As said earlier, the main advantage of using nano particles (nanoclay in this case) is their high surface area/ aspect ratio. This requires that the nanoclay is properly dispersed inside the epoxy matrix otherwise they may agglomerate and all the advantages of using the nano particles will be lost. This agglomeration can act as stress concentrations and can thus act as defects. The distribution is marked by homogenous distribution of the nanoclay while dispersion is how effectively the clay platelets (individual layers of clay) have been dispersed without being agglomerated. Figure 2.1 shows two types of morphologies intercalated and exfoliated. Exfoliated morphology is the most desired form in which the

clay layers are completely separated and distributed within the matrix which allows the polymer to completely seep in between the platelets [3].

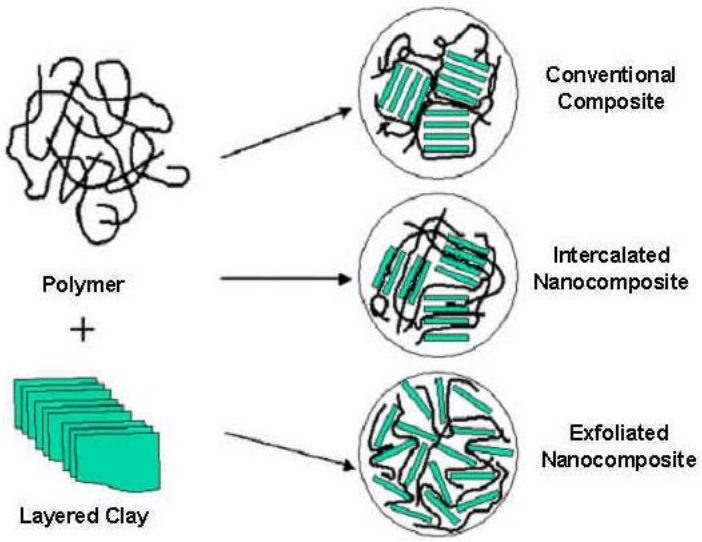

Figure 2.1 Morphologies of clay particles.

The distance between any two platelets is commonly known as the 'basal spacing' and that is the major difference between intercalated and exfoliated nanocomposite. The main purpose of mixing is to increase this basal spacing. If the spacing does not increase then the polymer chain does not go in between the clay platelets and results in conventional or intercalated morphology. This degree of exfoliation (conventional to fully exfoliated) depends on the processing technique and has a profound effect on the final properties.

2.1.2. X-Ray Diffraction (XRD)

The technique most commonly used to characterize the degree of dispersion of MMT in a polymer is perhaps the wide angle X-Ray diffraction or WA XRD for short. The wide angle

x-ray diffraction measures the spacing between the silicate layers by measuring the intensity as the function of diffraction angle (2 θ) of the incident x-rays.

This diffraction is given by Bragg's law [3].

$$\boldsymbol{2d \sin \theta = n \lambda} \qquad (2.1)$$

Where *d* is the interlayer spacing between the silicate layers.

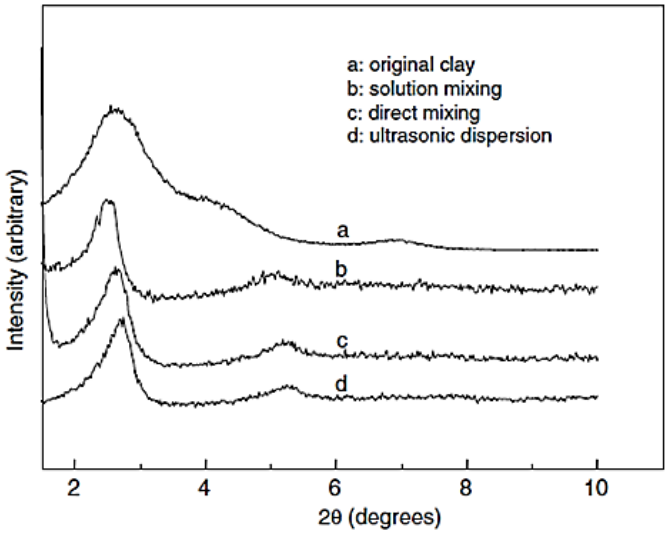

Figure 2.2 Typical XRD spectra showing the effect of mixing techniques on morphology [20].

Figure 2.2 shows XRD spectra for epoxy clay samples prepared using different mixing techniques. It can be seen that for (a) the peak is as the left most which means that it has the highest *d*-spacing according to Equation 2.1.As XRD can provide information on the particle size, therefore the size of nano particles have a profound effect on the diffraction pattern. Generally, the smaller the particle size the broader the peak.

Generally there are three definitions associated with the dispersion of nano clays based on the observed *d* spacing [3].

(i) *Immiscible* – No change in *d* spacing meaning no polymer has entered the space between the clay layers.

(ii) *Intercalated* – Increase in *d* spacing indicating that polymer has entered the space between clay layers.

(iii) *Exfoliated* – No peak is observed (out of range of XRD) which indicates that a lot of polymer has entered into the space between clay layers. However, in this case it is recommended to proceed to TEM as well in order to make sure that it is indeed exfoliation due to which there is no peak as it can instead be a case of disordered intercalation.

The wide use of this technique is because XRD is nondestructive and does not require intricate sample preparation.

2.1.3. Scanning Electron Microscope (SEM)

Scanning Electron Microscope (SEM) is a type of microscope which uses electron beam as opposed to light beam in a conventional microscope to scan the surface of the sample. When the electrons from the SEM interact with atoms of the sample, signals are generated in the form of electrons and characteristic X-Rays which are used to identify the surface topography, composition and other properties [4, 20].

SEM requires that the samples be electrically conductive. Sample preparation of SEM is comparatively more time consuming than XRD and involves steps such as cutting, polishing and etching.SEM is capable of providing very high resolution images up to 1 nm which makes it a very suitable imaging technique for nano-scale particles. The surface structure of polymer nanocomposites, dispersion of clay and fracture surfaces all can be

seen through SEM in a great detail. A typical SEM micrograph for GFRE is shown in Figure 2.3 which shows the surface characteristics of different samples for different clay loadings. The image shows epoxy-clay matrix adhesion with the fibers. SEM images also allow the clay dispersion in the bulk to be estimated.

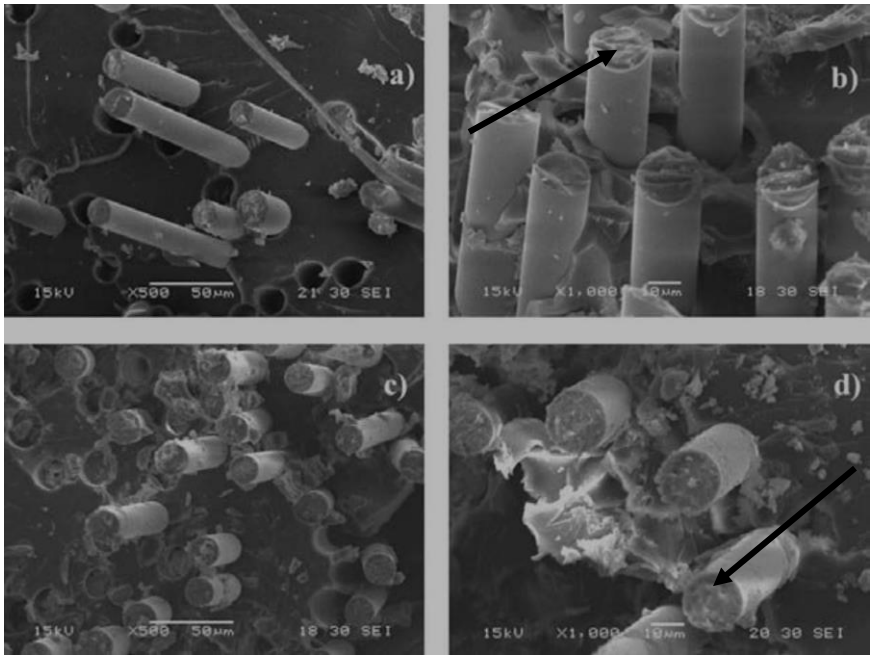

Figure 2.3 A typical SEM Image [6].

2.1.4. Transmission Electron Microscope (TEM)

Transmission Electron Microscope also works using the electron beam but, as the name states, it works on the transmission of electron beam through the sample [2]. This beam of electron interacts with the sample as it passes through it. Typically, a TEM consists of an electron gun and a group of lenses for focusing the electron beam on the sample.

Usually the specimen preparation involves cutting thin sample slices, punching to get the required size, dimpling to decrease the thickness to the order of a few microns and finally penetrating the sample using ion-milling.

A typical TEM image is shown in Figure 2.4 which shows the intercalated platelets dispersed in the polymer composite in an orderly fashion.

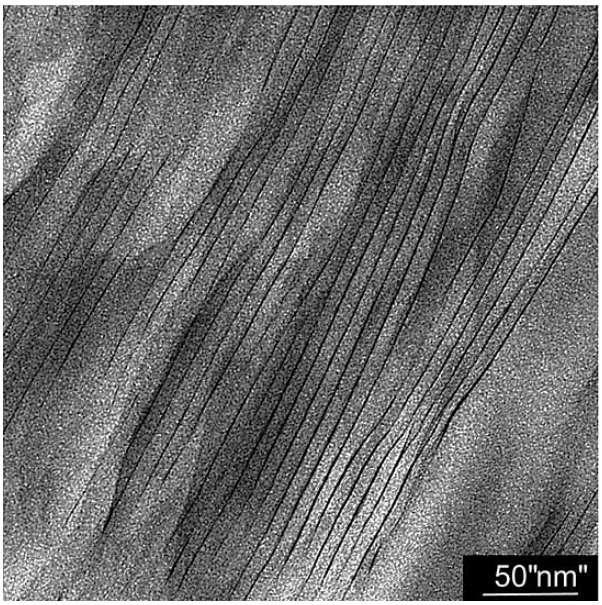

Figure 2.4 A typical TEM image [7].

Transmission Electron Microscope produces a high resolution image which allows easy observation of nanoclay dispersion. The observed structure under TEM can be classified as *immiscible* for large and undispersed clay particles, *intercalated* for ordered stacks of clay layers and *exfoliated* for individual clay layers [3].

It should be noted that since the sample size is very small, different samples can give different results and thus one sample is not a good measure or representative of the whole material. As TEM alone cannot measure *d*-spacing therefore it is necessary to use this in conjunction with XRD to determine the actual situation of clay dispersion.

2.2. GFRE Development

This section will serve as foundation to the upcoming experimental procedures and will deal with different GFRP manufacturing techniques, their advantages and disadvantages.

2.2.1. General Composite Manufacturing

Composite manufacturing methods spans to a huge variety depending on their applications. However, all of those methods can be divided into 4 basic manufacturing steps being done in different ways [3].

Impregnation

Here, the fibers and resins are mixed together to form a laminate. Fibers and resins are available in many different forms and types. Impregnation is done in different ways for different methods. For filament winding, the fiber from the spool is passed through resin bath and thus soaking it with resin. In wet layup however, each layer of fibers is wetted manually with resin using an applicator like roller or spray gun etc. Some of the factors effecting the impregnation are viscosity of resin, surface tension and capillary action.

Lay-Up

Once we have the impregnated fibers ready it is time to place them relative to each other in the desired angle or layers. In filament winding the fibers are wound due to a relative motion between mandrel and carriage. In case of hand or wet layup, the impregnated layers of fibers are stacked on top of each other at desired angles.

Consolidation

Consolidation is done to ensure intimate contact between layers of laminate to ensure air removal. This improves quality of final part by removing voids. Consolidation is done by application of pressure e.g. vacuum bagging.

Solidification

Curing or solidification is the final step which may take from a few minutes to few hours depending on the type of resin and hardener used. Solidification is usually done under

application of heat and pressure. The factors governing solidification include resin type curing kinetics, temperature and pressure.

2.2.2. Manufacturing Techniques

Composite production techniques utilize different kinds of raw materials including prepregs, mats, fibers, fabrics and resins for fabrication of parts. Each method has its own advantages and disadvantages with regard to processing, time, cost etc. The main purpose of this section is to provide detailed information on the processes used commonly to produce Fiber Reinforced Composites in lab scale according to the literature.

Hand/Wet Layup

Layup methods are one of the oldest methods used for manufacturing composites and are still widely used for making products such as boat hulls. Layup methods are easiest to carry out but are labor intensive. Layup processes have the advantage of a very simple mold design especially since these are open mold methods in which curing is mostly done at room temperatures and pressures.

The method itself consists of applying mold release to the mold after which a gel coat is applied if extra finish is needed (Figure 2.5). The resin is applied using a brush or roller after which the fiber layer is introduced. The fiber layer is pressed manually to ensure wetting. More layers of resin and fibers are applied until the required thickness is achieved. The process is finished off by vacuum bagging or hot pressing.

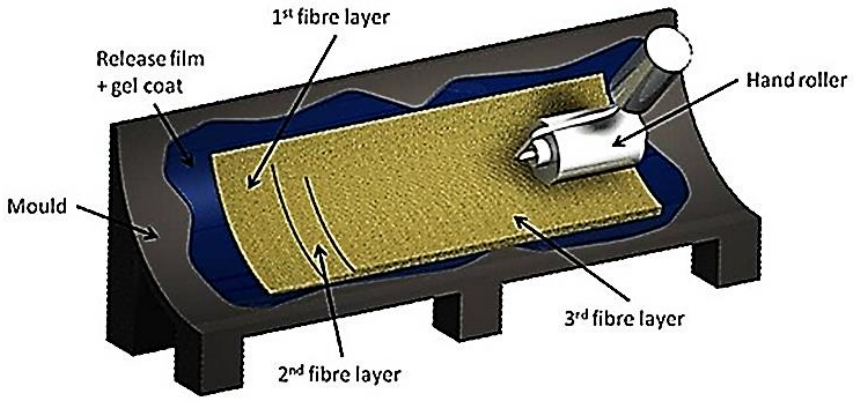

Figure 2.5 Hand Layup

As mentioned before, this process is cheap, versatile and simple. The raw materials are usually the only significant cost which also are cheaper compared to prepegs used in VARTM process. But this process cannot be tightly controlled as some variables depends on the experience and judgment of the person itself which means that the products are not always exactly similar.

VARTM (Vacuum Assisted Resin Transfer Molding)

Vacuum Assisted Resin Transfer Molding method uses external pressure to consolidate the laminates. It is this reason that this process results in a higher fiber volume percentage of parts as well as a better surface finish. This method can also produce more parts as compared to hand/wet layup. These characteristics make it an attractive candidate for aerospace industry.

Unlike hand layup, VARTM requires an elaborate mold for carrying out the composite making. Although any material like aluminum, steel, plastic or wood can be used for mold making but its rigidity must be ensured to withstand the process pressure. Also, the mold

design must take into account miscellaneous parameters such as thermal expansion, sealing etc.

To begin with part making first a mold release is applied to the mold surface. Then a preform is fabricated and is placed inside the mold and clamped as shown in Figure 2.6. The resin and catalyst (if any) is then placed in the dispenser tanks. The mold is heatd and suitable vacuum is created which drives the resin mixture from the tank to the mold and wets the fibrous preform. In case of open mold one side is vacuum bagged and then the part is allowed to cool.

VARTM offers important advantages such as automated production, improved finish, and formation of complex and high fiber volume parts. However, the cost of the product is very high as compared to hand layup and the process itself requires a lot of trial and error (even simulations) in order to perfect the parameters otherwise there would be improper fiber wetting which leads to high porosity and dry parts. The most important limitation is that of clay filtration as discussed in previous sections.

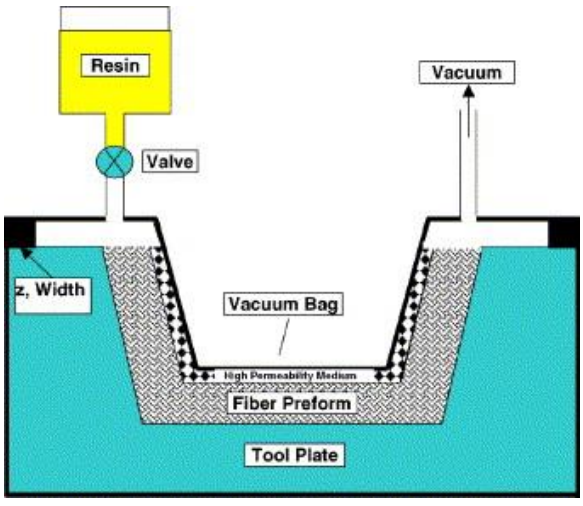

Figure 2.6 VARTM Process

2.3. Mechanical Properties

Fiber reinforced polymers (FRP) can be mechanically characterized using a variety of techniques to determine their mechanical performance under different loading conditions. Static tests include flexural, fracture, tensile and impact tests while transient and cyclic tests include creep and fatigue tests. Static tests provide a good measure of strength, modulus and elongation to failure. Quasi-static tests like drop weight impact determines damage resistance for different impact energies. For the engineering applications targeted in this research the mechanical properties of primary concern are flexural properties and impact resistance [17-19].

2.3.1. Flexural Properties

The flexural test is usually carried out to determine the flexural properties for materials such as strength, modulus and flexural strain. Flexural properties of polymer and nanocomposites may vary with specimen preparation and with testing parameters. Therefore, to determine repeatable and comparable statistical results, these factors must be carefully controlled. During the preparation of specimen the dimensions should be similar to those dictated by the standards, like ASTM D790 [66].

Kornmann et al. [7] presented results based on GFRE nanoclay samples prepared using hand layup followed by vacuum bagging and hot pressing. The increase in flexural modulus and strength were attributed to stronger interface between epoxy and fibers due to sticking of silicate layers to glass fibers. They also reported an increase in water uptake and a decrease in T_g with clay loading which was attributed to decrease in crosslink density. Manfredi et al. [6] used pultrusion for making glass fiber reinforced clay nanocomposites and reported an increase of upto 29% in flexural strength and a similar

increase in flexural modulus due to better adhesion of epoxy clay mixture to fibers. Figure 2.7 shows that water uptake had a negative effect on the flexural properties due to matrix swelling, plasticization and hydrolysis of the material.

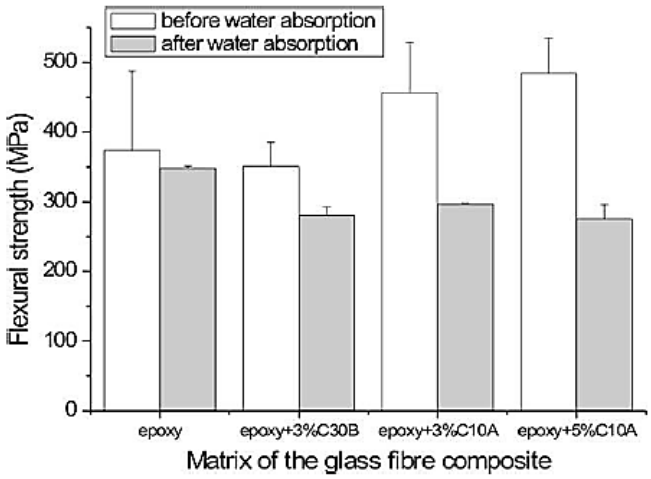

Figure 2.7 Effect of water uptake on flexural strength of GFRE based clay nanocomposites with different clay types and loadings [6].

Sharma et al. [10] prepared glass fibers reinforced clay nanocmposites using hand layup. Contrary to what was reported by Kornmann [7] they found 140% improvement in flexural strength using 3 wt% of C.30B clay. However, they did not find any substantial improvement in mechanical properties by increasing the clay content beyond 3 wt%. They found a 75% decrease in flexural strength when exposed to water uptake for 3 wt%. The reduction was higher for samples without nanoclay. Lin et al. [20] used VARTM (Vacuum Assisted Resin Transfer Molding) to prepare glass fiber reinforced clay (C.15A) nanocomposites in which they found increase in mechanical properties, upto 12 % in flexural modulus, for fibers placed in longitudinal direction and no observable improvement in fibers placed in transverse direction. They also observed nanoclay filtration problem which is inherent with the VARTM process.

Lefevere et al. [22] has presented a detailed argument on the problem of filtration using an experiment in which they used different particle and pore sizes. The fiber used was PET with unsaturated polyester resin, while glass bead particles were used for good interaction between the two. They concluded that an intermediate particle size is required for a given pore size in order to avoid filtration. If the particle size is too small there will be no retention and if the particle size is too large there will be filtration. Both of these cases are undesirable as they do not lead to any improvement in mechanical properties. Quaresimin and Varley [21] prepared glass fiber reinforced clay nanocomposite samples using hand layup and found a significant increase in compressive strength and impact strength while no improvement was observed in tensile properties. They argued that only the properties in which clay and matrix played role were improved.

Subramaniyan and Sun [23] used VAWL (Vacuum Assisted Wet Layup) instead of VARTM (Vacuum Assisted Resin Transfer Molding) for preparing the glass fiber reinforced clay nanocomposites inorder to minimize the filtration of clay fillers by the fibers. They observed improvement in compressive elastic modulus and compressive strength for upto 5 wt% clay loading. Xu and Hoa [24] used hot melt (prepregs) along with vacuum bagging to make carbon fiber reinforced clay (I.30E) nanocomposites. They found upto 85% improvement in interlaminar fracture toughness for upto 4 phr clay content. They attributed this behavior to the presence of clay particles in between the laminates which restricted their movement as well as to more epoxy in 4 phr sample.

Bozkurt et al. [25] prepared 1, 3, 6 and 10 wt % samples of K10 clay and E-glass fibers using hand layup. The improvement in flexural strength and fracture toughness were found to be around 6 wt % after which they decreased. Muhammad Zulfi et al. [5] prepared E-

glass samples using 2 to 8 wt % Organically Modified Montmorillonite Clay (OMMT) 1.28 E clay and hand layup. It was found that all properties like flexural strength, flexural modulus, fracture toughness and impact strength increased with the most optimum being for 4 wt %. Figure 2.8 shows that there is a 19.0% increase in flexural modulus and 9.0% increase in flexural strength.

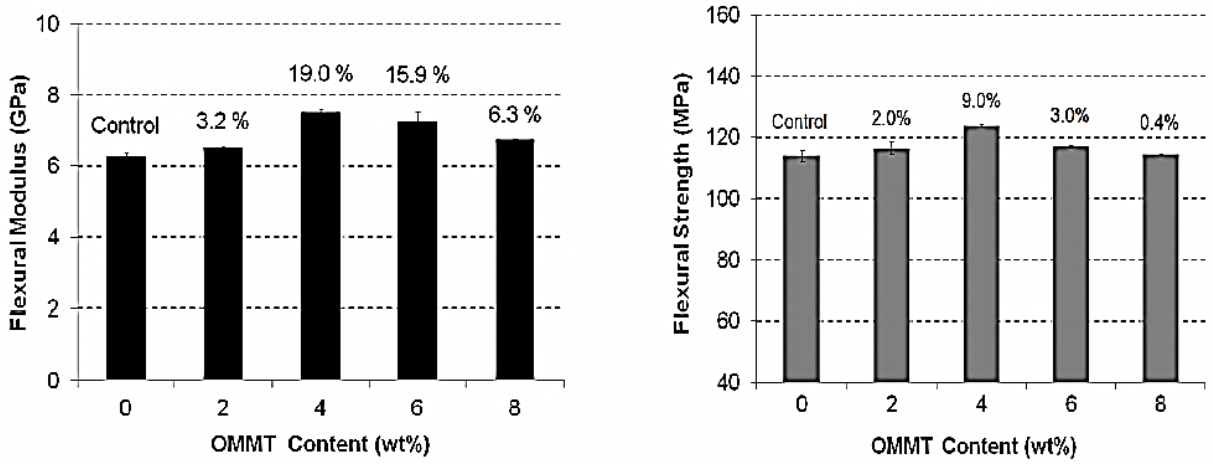

Figure 2.8 Flexural Modulus and Flexural Strength of DGEBA based epoxy-clay nanocomposites [5].

Zhou et al [26] tested 0, 1, 2, 3, 4 wt % K10 clay epoxy nanocomposites with carbon fibers manufactured using VARTM. It was found that 2 wt % showed the highest improvement (13.5%) in the flexural strength. The trend observed was similar to that found by other researchers [5, 25]. The onwards decrease was attributed to the agglomeration of clay particles. Suresh et al. [27] manufactured carbon fiber reinforced composites with 0, 1.5, 3 % 5 wt % clay. It was observed that tensile strength and hardness increased with addition of clay. Mohammed F. Uddin & C.T. Sun [28] used VARTM and sol-gel technique to fabricate 15 wt% silica fiber glass nano composite with fiber volume percentage of 50% maximum. Upto 40% improvement was shown for tensile strength and a similar improvement was reported for flexural strength and flexural modulus.

Chaudhry et al [29] used VARTM to produce 0, 1, 2 and 3 wt % composites of carbon fiber reinforced epoxy clay (I.28E) composites. These composites showed maximum improvement in flexural strength of 14% as compared to pristine GFRE at 2 wt % after which there was a decrease. Similar trend was observed by Alamri et al [30] prepared 0, 1, 3 and 5 wt % C.30B nanoclay samples for determining the mechanical properties of recycled cellulose fibers and concluded that 1 wt % clay loading showed the largest increase in flexural strength. For higher clays, the poor dispersion of nano clay and increased viscosity of matrix (which led to increased amount of bubbles and voids) was the cause of lower flexural strength. No improvement in fracture toughness was seen on addition of clay and higher impact strength was observed for 1 wt %.

2.3.2. Drop Weight Impact

Hybrid composites are used in applications in which they may be/are exposed to impact like conditions e.g tool dropping or flying fragment impacting the composite. Resulting damage can severely change the mechanical properties of the composite. Such a situation is most commonly simulated using drop weight impact. Drop weight impact tests determine the ability of composite laminated plates or pipe sections to resist impact damage. In this test, an impactor which is available in different shapes and sizes, impacts the fiber composite laminate at a specified energy, velocity or height. The resulting impact determines the damage resistance by the laminate and is then measured in terms of physical damage measurements and other quantitative measurements such as energy absorbed, load and deflection. There are a variety of standards available for drop-weight impact measurements for different applications however, it has been seen that proprietary sample and test parameters are usually used [65].

Low velocity impact damages have the tendency to generate internal damage which is easy to overlook. The effect of nanoclay addition to epoxy and carbon fiber based nanocomposite on the low velocity impact tests were found to have significant improvement in damage resistance with less damage area. The results obtained by Iqbal et al. [31] are represented in Figure 2.9 which shows that laminates with 3wt% clay showed highest incipient energy and highest energy absorbed as compared to 0 and 5 wt%. This was attributed to exfoliated dispersion of 3 wt% clay in the epoxy matrix. It was also noted that 3 wt% clay showed the least damage area while the damage increased with increasing impact energy. The types of impactors may also have a profound effect on the damage resistance of composites as investigated by Sevkat et al [32]. The amount of area in contact between the test plate and impactor was found to be the deciding factor. For a flatter impactor, like charpy, the impact damage was sustained by a larger number of fibers as compared to the spherical impactor. It was also observed that the smaller the contact area (spherical impactor) the higher the contact duration for the impactor.

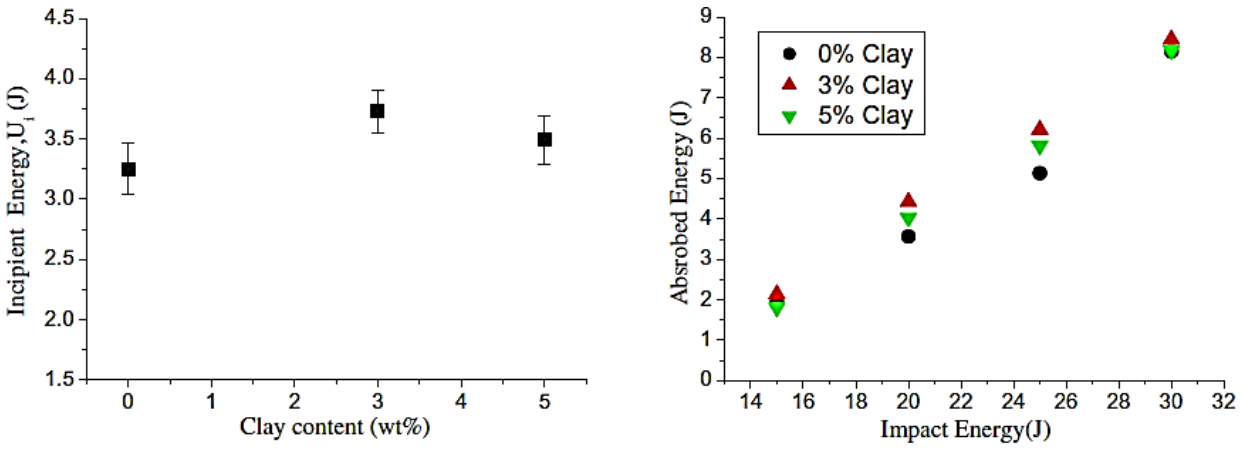

Figure 2.9 Incipient and absorbed energy for different clay loadings [31].

Avila et al. [33] investigated the effect of addition of montmorillonite (MMT) clay layers on impact behavior and response of glass-fiber (S2 type) reinforced epoxy clay composites. It was found that clay addition increased both stiffness and impact damage resistance upto 5%. The damage type was found to alternate between interlaminar and intralaminar delamination. Lower energy samples were found to have absorbed most damage with the back damage being more than the front damage due to the back being in tension. Similar results were reported by Alomari et al. [34] when they performed low-velocity impact tests on nanoclay reinforced Kevlar based nanocomposites. They found that higher filler content increased the impact damage resistance but higher clay loadings were not as efficient in resisting delamination as lower clay loadings. They attributed this to clay agglomeration which acted as stress concentrators. The samples with higher clay loadings showed upto 71% increase in damage as compared to lower clay loadings. Delamination was found to be the prevalent form of damage which improved when clay was added to the matrix.

The effect of clay dispersion and morphology on impact characteristics ere studied by Lin et al. [36] for different low velocities. Addition of C30B nanoclay improved the impact strength as they formed a tortuous path but this was found to be good only for clay loadings lower than 5wt%. Higher clay loadings deteriorated the properties and were no better that those of neat epoxy and this was also attributed to nanoparticle agglomeration. Matrix cracking was the predominant mode of failure but with introduction of clay partial cracking was observed. Hosur et al. [37] prepared foam cores made of carbon fiber with polyurethane and nanoclay (SC-15) to determine the low-velocity impact effect. Nanoclay infused structures generally resulted in higher peak loads and had smaller damage area as compared to neat foams. 0.5% clay absorbed lesser energy with a higher peak load as

compared to neat epoxy and 1% clay. The nanoclay based foams were found to have become stiffer and had brittle fracture on impact.

Avila et al. [38] prepared glass fiber sandwich plates with faceplates made of epoxy-clay while the core was composed of Styrofoam. Low-velocity impact tests were performed but the rebound brakes were not activated and the striker was allowed to hit the test specimen multiple times until it came to rest. The stiffness of composite panels were observed to have increased upto 5% clay addition after which it decreased when clay loading was increased to 10%. It was explained that the saturation limit of epoxy-clay system was somewhere between 5-10% due to which addition of subsequent clay beyond 5% only acted as stress concentrator and the composites turned les stiff. At higher velocities the core crushing and face sheet tearing was observed while at lower velocities barely visible damage was seen.

Reis et al. [39] made a comparison between impact filler properties of cork and nanoclay. The addition of both fillers improved the damage tolerance and maximum load bearing capacity on impact. Addition of nanoclay, however, increased the damage area as compared to cork. Opposite trend was seen for displacement in which nanoclay filled composites performed better. Matrix cracking and delamination were found to be the main modes of failure. Aymerich et al. [40] also found nanoclay based composites to have higher energy absorbing capabilities with reduction in peak force during low-velocity impact. The higher energy absorption also led to higher damage in nanoclay based composites due to high energy dissipative mechanisms. The stiffness of the composites was also observed to have changed significantly. Matrix cracks, delamination and fiber breakage were the significant failure modes observed.

2.4. Water Uptake

Epoxy resins show promise in mechanical properties such as strength and stiffness etc but are vulnerable to significant degree of moisture absorption which degrades their structural integrity and thus their mechanical properties. Moisture absorption is basically the measure of a material's ability to resist moisture penetration. For this reason, the combination of nanoclay and fibrous reinforcements are of a great interest as they can enhance the mechanical properties and act as barrier to water absorption as well. These barrier properties are now proving useful in coatings and dielectric materials [41].Generally, ASTM D570 standard is used to measure the water absorption for plastics.[66]

Chow [42] prepared I.30E nanoclay based glass fiber reinforced DGEBA epoxy composites using hand layup to study water absorption properties. The studies were conducted for epoxy matrix without fibers, epoxy matrix with fibers and epoxy-clay matrix with fibers for comparative analysis of water uptake properties. The samples reached complete saturation in 35 days with highest absorption gradient for neat epoxy samples. As shown in Figure 2.10 below, the addition of fibers reduced the water uptake to 1.1% as compared to 2.3% of neat epoxy. Subsequent addition of 3% nanoclay (I.30E) resulted in 1.25% water uptake which is an improvement over neat epoxy but showed increased water absorption as compared to fibers in neat epoxy.

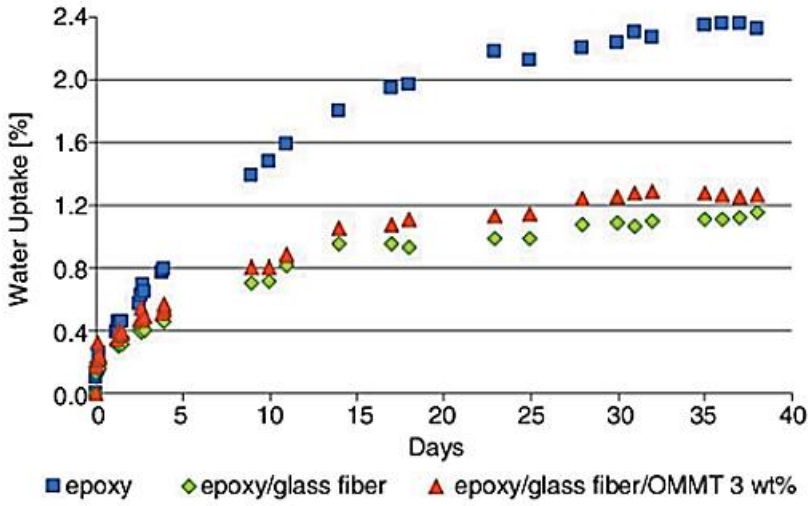

Figure 2.10 Typical water uptake behavior of GFRE clay nanocomposites as compared with other systems [42].

Mohan and Kanny [43] determined the water uptake behavior for sisal fiber reinforced DGEBA epoxy composites using resin infusion technique. They found a steep increase in water uptake in the beginning during diffusion period which gradually became constant over the time. The total equilibrium water uptake also decreased with addition of higher nanoclay content because of increased tortuous path. No clear trend was observed for diffusivity with added clay. The rate of water uptake for 5% nanoclay was observed to be 3 times less than unfilled composites. Authors also compared 5% of micro clay which fell in between 1% and 3% nanoclay by performance which is due to improper dispersion of microclay in matrix.

Kim et al. [44] studied the moisture absorption properties of epoxy clay nanocomposites using three different types of organoclay namely KH-MT-TJ2, C20A and I30P. Amongst the three, C20A and I30P showed better barrier properties due to larger interlayer distance between the silicate layers and much more uniform dispersion. The diffusivity was found to be decreasing with increasing clay content. There was some deviation from Fickian

behavior and it was attributed to exfoliation and dispersion of the organoclay. Nanoclay I30P was found to be the most effective in resisting water permeability due to its high aspect ratio. As expected from the tortuous path model, the water permeation resistance was found to have increased with increased clay content. Liu et al. [19] conducted study of water absorption at different temperatures and different clay loadings to determine the effect on water absorption. The curves were in good agreement with Fick's law at lower temperatures but at higher temperatures they showed some deviation. The maximum water absorption level decreased with increased clay loading and clay dispersion which improved tortuosity. The diffusion constant decreased with increasing clay loading but increased by the order of 100 when the environment temperature was raised from 23°C to 80°C.

Dhakal et al. [45] investigated the effect of water absorption on the mechanical properties of hemp fiber reinforced polyester composites when immersed in water at room temperature and at boiling temperature. It was found that moisture uptake increased as fiber volume fraction increased due to the presence of more voids and higher fiber cellulose content. At room temperature, these composites were found to follow Fickian behavior, whereas at the elevated temperature the absorption behavior was non-Fickian. At high temperatures, the water uptake is significant because of moisture induced degradation. As for the effect of moisture absorption on mechanical properties, significant drops in tensile and flexural properties were observed due to the degradation of the fiber–matrix interface.

Alamri and Low [1] tested 0, 1, 3 & 5 % C30B samples for water uptake and found that the behavior was fickian for all samples and the water uptake rate is rapid in the beginning and slows down when it reaches saturation level. Water uptake decreased with increase in clay weight percentage but due to hydrophilic nature of recycled cellulose fiber, the water

uptake was higher as compared to neat epoxy sample. The weight gain with time was minimum for 5 wt % as it increases the hindrance in water uptake path. Flexural modulus degraded significantly on exposure to moisture. In another investigation by Alamri and Low [62] on the effect of nanofillers on water absorption and subsequent effect on mechanical properties, they added nanoclay (C30B), halloysite nanotubes (HNTs) and nano-silicon carbide (n-SiC) particles in epoxy based nanocomposites without the inclusion of any fibers. Fickian behavior was observed in water uptake and all types of nanofillers exhibited excellent barrier properties with reduced amount of water uptake as compared to neat epoxy samples. Addition of 5% n-SiC particles showed best barrier properties with least water uptake. Furthermore, with increased addition of all types of nanoparticles also decreased the water absorption. Nanoclay based composites showed highest flexural strength and modulus values followed by n-SiC and HNT. Water absorption had a negative effect on flexural properties of these composites.

Becker et al. [41] compared the water uptake properties of three different high-performance epoxy systems when mixed with I.30E nanoclay. They tested diglycidyl (DGEBA), triglycidyl (TGAP) and tetraglycidyldiamino (TGDDM) based systems for water uptake at 80°C. The results showed that DGEBA based epoxy clay nanocomposites showed least amount of water absorption amongst the three epoxy types and this difference was attributed to polarity of polymers which has an impact on bound water rather than the free water trapped in the micro-voids. There was an overall reduction in equilibrium water uptake with increased clay loading but there was no specific trend.

CHAPTER 3

EXPERIMENTAL PROCEDURE

This chapter deals with complete synthesis and experimental procedure adopted to produce the GFRE nanocomposites as well as the materials and equipment used in various tasks throughout the course of this work.

3.1.Materials Used

This section will deal with the different materials used in the development of GFRE clay nanocomposites. Properties and general information related to epoxy, clay, hardener/curing agent and fiber glass used will also be detailed in this section.

3.1.1. Epoxy

Since the target application of this work is the pipe manufacturing industry, therefore, the epoxy used is according to that recommended by major pipe manufacturing companies in Saudi Arabia e.g Amiantit and Future Pipe Industries. Araldite 6010 is used for this work which is provided by JANA, KSA. Araldite 6010 is an unmodified liquid epoxy resin based on Diglycidyl Ether Bisphenol A (DGEBA). This epoxy is a derivative of Bisphenol A (Figure 3.1) which has two hydroxyphenyl groups and is both colorless and insoluble in water. The properties of this epoxy resin supplied by the manufacturer are listed in Table 3.1.

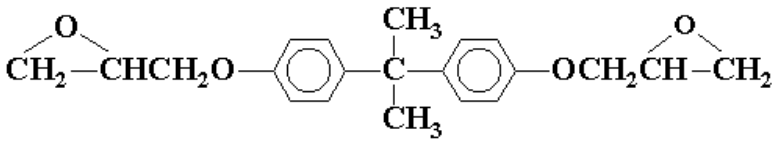

Figure 3.1 Chemical Structure of Bisphenol A.

Table 3.1 Araldite GY 6010 properties

Property	Value
Appearance	Clear No Contamination
Physical State	Liquid
Color APHA	125 Max
Epoxy value	0.5208 - 0.5495 eq/100g
Weight per epoxide	182-192 g/eq
Water Content (KF)	0.08 % Max.
Viscosity@ 25°C (77°F)	11,000 - 14,000 cP
Aging Resistance Temperature	150°C
Glass Transition Temperature	160°C
Flexural Strength (kg/cm^2)	900-1000

3.1.2. Curing Agent

The curing agent used for this epoxy is Aradur 42 (Figure 3.2) which is supplied by Bondstrand, KSA as a product of HUNTSMAN, USA. Aradur 42 is based on isophoronediamine (IPDA).The mixing ratio with Araldite GY 6010 used is 100:24. The properties and chemical structure are given in Table 3.2.

TABLE 3.2 Aradur 42 (IPDA) properties

Property	Value
Appearance	Clear No Contaminaton
Physical State	Liquid
Viscosity at 25 °C	10 – 20 cP
Density at 20 °C	0.92 g/cm3
Mixing Ratio (GY 6010)	100:24

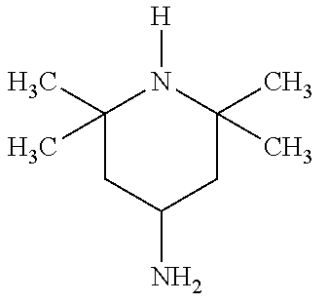

Figure 3.2 IPDA chemical structure.

3.1.3. Clay

The nano filler material used in this study is organically modified motmorillonite (OMMT) clay particles. These clays come from smectite family and have a 2:1 ratio, meaning that it has 2 tetrahedral sheets sandwiching a central octahedral sheet as shown in Figure 3.3 [47]. This sandwich structure gives them a huge ability to exchange ions which allows its chemical properties to be modified. Isomoprhous substitutions in these sheets makes them negatively charged which allows for charge exchange with cations (alkylammonium cations) in order to make them organophilic. This ion exchange also helps turn the clays from hydrophilic to hydrophobic. Organophilicity and hydrophobicity allows for a more

homogenous dispersion (exfoliation) of clay platelets by making them more compatible with the polymer matrix [7].

These clay particles are broken down into plate shaped sub particles called clay platelets whose diameter is approximately one micrometer [47]. These platelets maintain a planer profile with 1 nm thickness and other dimensions in the order of $10^2 - 10^3$ nm. This gives them an aspect ratio between 100-1000 which is the main source of effectiveness of nano fillers.

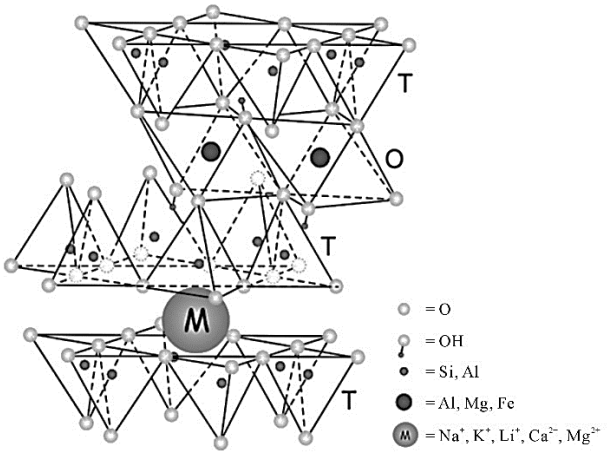

Figure 3.3 Structure of montmorillonite clay. T: Tetrahedral, O: Octahedral.

There are a wide variety of organoclays available by many different suppliers. The clay type used in this study is I.30E is chosen based on the work by Al-Qadhi et al [46]. I.30E clay is supplied by Nanocor, Inc, USA. The physical properties of I.30E, as provided by the manufacturer, are given in the Table 3.3.

Table 3.3 Nanomer I.30E Properties.

Property	Value
Appearance	White Powder
Mean Dry Particle Size	8-10 (microns)
Specific Gravity	1.71
Moisture	3 % (max)
Mineral Purity	98.5 % (min)

3.1.4. Fibers

Fibers are used as reinforcement in composites. These fibers generally occupy 20%-70% of the matrix volume in composites [48-49]. The fibers can be chopped, woven or stitched. The most common types of fibers used in composites are the glass and carbon fibers.

Glass fibers are the most widely used reinforcement material mainly due to their low cost, high strength-weight ratio and good corrosion resistance. There are many types of glass fibers which are listed below.

1. A-glass (alkali) is a high alkali containing glass which is very resistant to chemicals but has lower electrical properties.
2. C-glass (chemical) is best resistant to chemical attacks and is mainly used in the form of tissue in outer layer of laminates in pipes carrying chemicals.
3. D-glass (dielectric) has a low dielectric constant with superior electrical properties. However, its mechanical properties are not so good as E-or S-glass.
4. E-glass (electrical) has much lower alkali content and is stronger than A glass. It has good tensile and compressive strength and stiffness, good electrical properties

and relatively low cost. E-glass is the most common form of reinforcing fiber used in polymer matrix composites.

5. ECR-glass (electrical,chemical resistant) is a specialized type of E-glass without any Boron content. This type of glass has higher mechanical properties (stiffness, strength, density) as compared to E-glass and has excellent corrosion resistance.
6. S-glass (strength) is a high-strength glass with a 33% higher tensile strength than E-glass.

The glass fiber types used in this study are provided by Amiantit Fiberglass Industries Limited. The fiber is Chopped Strand Mat type ECR-glass because of the high mechanical and corrosion resistant properties desired for this application i.e water and oil transportation pipes. This type of fiber is 2 oz type with weight of about 600 g/m^2 (measured) and density of 2.66 g/cm^3.

Figure 3.4 ECR-glass chopped strand mat used in this work.

3.2. Mold Design and Assembly

A total of two molds are used for this work. A smaller mold (90 mm x 100 mm) is used for the initial development of GFRE clay nanocomposites as it is easier to use, which allows

more flexibility in terms of its operation and there is also less material wastage. However, this mold has important size limitations which is not suitable for making standard drop weight impact samples.

A new mold is therefore designed to make samples of 130 mm x 180 mm with a minimum thickness of 3.8 mm. It also has a top plate which can be bolted with the mold in order to compress the sample from the top. This allows the samples to have uniform thickness and also for the matrix to spread evenly across the fibers with fiber volume composition at 30%. The mold is fabricated using aluminum alloy and all of the parts were grinded and later hand polished using 1000 Emery paper for mirror finish.

The mold consists of three plates – bottom, middle and top. The bottom and middle plates are first bolted together and after the layup is complete the top plate is attached to compress the sample to required thickness. All of these plates were joined with each other by placing a gasket in between to prevent leakage at high temperature and for easy separation. The middle plate defines the length and width of the sample while the difference in thickness between middle and top plate defines the thickness of the fabricated hybrid composite sample. The detailed mold drawings are illustrated in Figure 3.5 below and Figure 3.6 is a photograph of the finished mold.

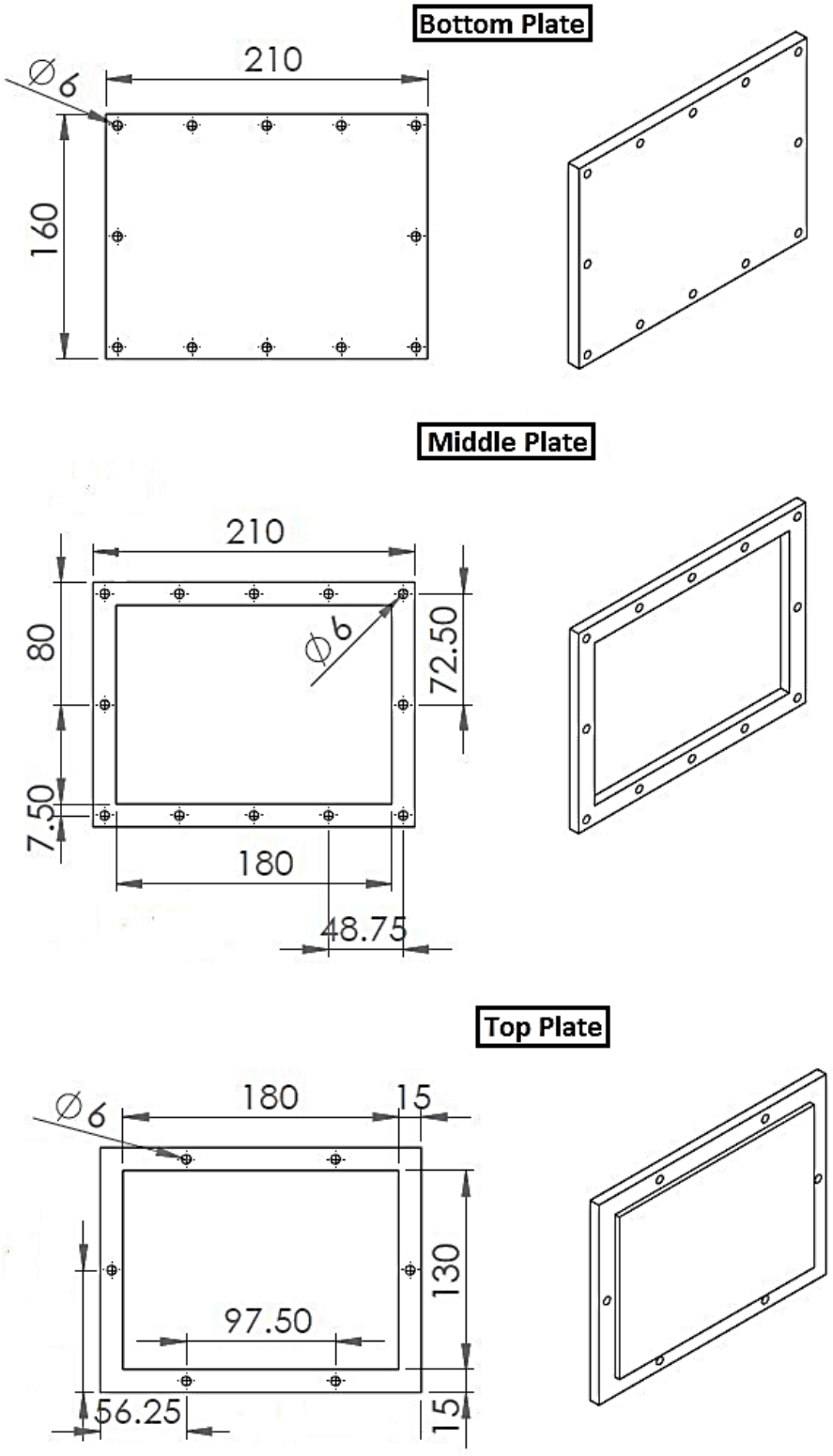

Figure 3.5 Drawings for mold fabricated for this work.

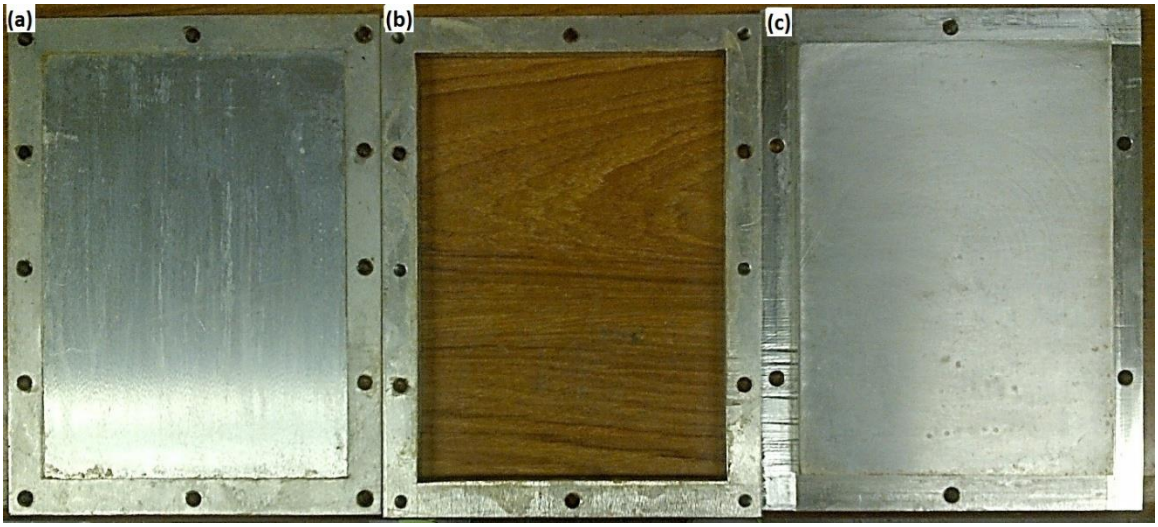

Figure 3.6 Exploded view of mold (a) Bottom Plate (b) Middle Plate (c) Top Plate.

3.3. Synthesis of Glass Fiber Reinforced Epoxy-Clay Nanocomposites

This part deals with synthesis of epoxy-clay mixture to be used as matrix later on in the second part for preparing the glass fiber reinforced composites.

Step-1: Mixing

The required amount of epoxy and nanoclay (0-5 wt%) is first weighed into a beaker and is then carefully hand mixed together thoroughly for exactly five minutes. After this, the mixture is placed under high shear mixing machine with the aim of exfoliating the epoxy into nanoclay platelets and to uniformly disperse the platelets in the epoxy matrix. The high shear mixing machine used for this operation is L5M-A high shear mixer, supplied by Silverson, UK, having maximum mixing speed of 10000 rpm. The epoxy-clay nanocomposite samples are mixed for 1 hour at 6000 RPM. During this process the mixture temperature is monitored using a thermocouple and is maintained between 35 and 45^{o}C by using a water bath as shown in Figure 3.7. This maintains the viscosity of the mixture and

prevents excessive temperature from being induced into the material which could lead to material degradation or outright burning.

Figure 3.7 Step-1: High Shear Mixing using L5M-A for uniform dispersion.

Step-2: Degassing

During high shear mixing a lot of bubbles are generated, The presence of bubbles are known to be a source of decrease in strength as they act as defects and they also absorb more water which further deteriorates their mechanical properties. In order to avoid these bubbles the mixture is degased in a vacuum oven at high temperature. For this purpose a Shellab vacuum oven (Figure 3.8) is used. Pre-degassing is performed for 4 hours at 120° and post-degassing is done for 8 hours at 65° [46].

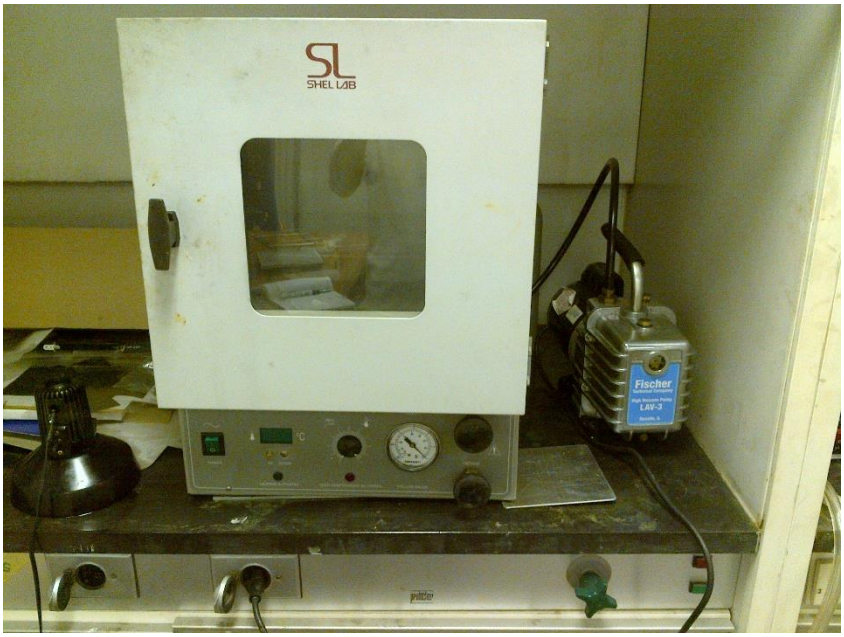

Figure 3.8 Step-2: Degassing using Shellab vacuum oven.

Step-3: Hand Lay Up

After degassing the IPDA hardener is added to the mixture in the ratio 100:24. The final mixture is then gently stirred for 5 minutes. The gentle stirring is to ensure that a minimum amount of bubbles are generated during this operation so that the final composite has the least number of voids.

Once the final nanocomposite has been prepared it is then used to make fiber reinforced epoxy clay nanocomposites (hybrid). For this purpose wet/hand layup method is used followed by hot pressing. The layup starts by first cutting the required number of fiber mats from the fiber roll. First, a layer of mold release agent is applied to the bottom of the mold in order to facilitate the release of final composite once it is completely cured. Then a layer of epoxy clay mixture is applied followed by a mat of fiber glass which is then pressed by a roller or a metallic compactor for uniform distribution of epoxy clay mixture and for

proper wetting. A total of five layers are applied and then the top of mold is bolted providing the necessary pressure for epoxy-nanoclay to uniformly penetrate the glass fiber layers.

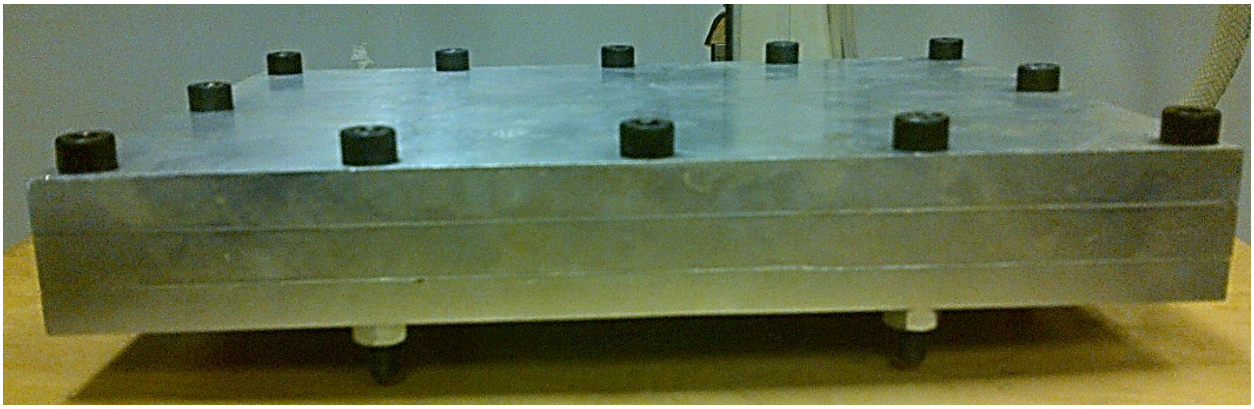

Figure 3.9 Mold completely closed after wet-layup.

Step-4: Curing

Once the mold is completely closed it is then placed in vacuum oven for curing. Pre-curing is carried out at 100° for 60 minutes and post curing at 170° for 60 minutes, as optimized by Al-Qadhi et al [50]. Post curing is done in order to ensure complete cross-linking which also improves the mechanical properties.

Once the part has been fully cured it is then carefully removed by opening the mold. The final composite has dimensions of 130 mm x 180 mm x 4 mm.

3.4. Testing Program

Once the samples are manufactured, a number of tests are performed which will be discussed in detail in this section.

3.4.1. Sample Preparation

Samples required for testing are cut from the prepared sheets using diamond cutters and close dimensional accuracy is maintained in all of the samples. Water uptake samples are cut to the dimensions of 80 mm x 30 mm x 4 mm (ASTM-D570) which are subsequently cut to 80 mm x 10 mm x 4 mm (ASTM-D790) for flexural tests later on. Drop weight impact tests are performed on sheets clamped in a propriety fixture which exposes an area of 110 mm x 110 mm (ASTM-D7136M) [65-66].

3.4.2. Water uptake

Water uptake is performed by immersing GFRE and GFREnc samples in tap water at room temperature and at 80°C. For both of these tests the ASTM-D570 standard is followed with dimensions of 80 mm x 30 mm x 4 mm [66]. The prepared samples are immersed in water for a period of 4 months after which flexural tests are performed. The samples immersed in water at room temperature are placed individually in small containers filled with water as shown in Figure 3.10 while the samples immersed in high temperature water are all kept together in a plastic container (Figure 3.11) and are then put in a thermostat controlled oven with temperature fixed at 80°C. Care is taken that all the samples are completely immersed in water. At regular intervals the samples are taken from the container and were dried using a tissue before being placed in for measurement. The samples are weighed using Mettler Toledo AG285 analytical balance with readability of 0.01mg. The percentage water absorbed was measured using equation 3.1.

$$\boldsymbol{M_t = \frac{(M - M_o)}{M_o} \times 100} \qquad (3.1)$$

Where M and M_o are respectively, the instantaneous and initial weights of exposed specimens.

Figure 3.10 Samples immersed in water for ambient testing.

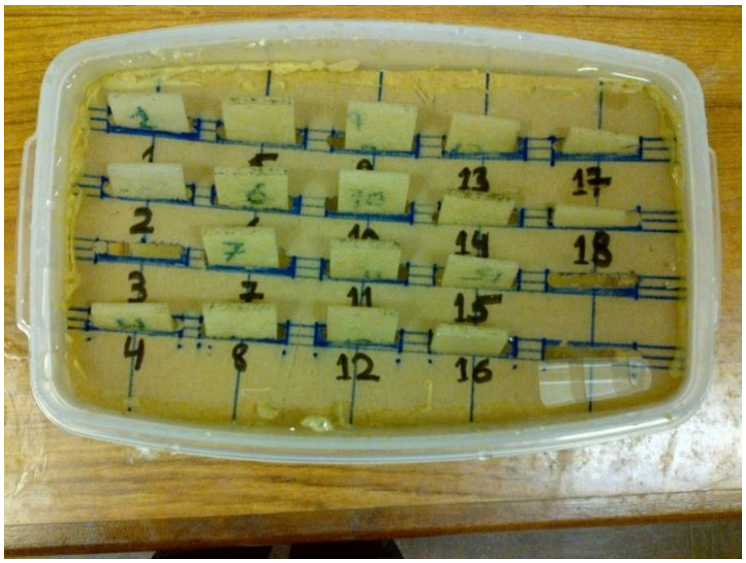

Figure 3.11 Samples immersed in water for high temperature testing.

3.4.3. Flexural Tests

Flexural tests are performed using the Instron 3367 testing machine as shown in Figure 3.12. This machine has load measurement accuracy of ± 0.5% of reading down to 1/100 of load cell capacity. ASTM-D790 (3-point bending) standard is used and a minimum of 6 samples are tested for dry samples while 4 samples are tested for wet samples. The Instron software bundled with the machine was used to record the flexural strength and modulus of the test specimens. The span is kept at 64 mm with cross head speed of 1.7 mm/min with sample dimension of 80 mm x 10 mm x 4 mm.

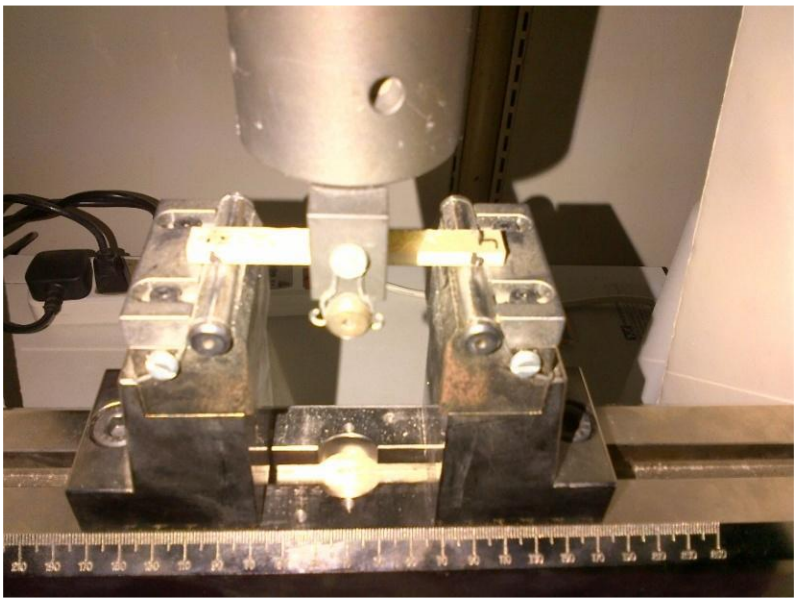

Figure 3.12 Flexural testing on Instron machine.

3.4.4. Drop Weight Impact

Drop weight impact tests are performed using the instrumented Instron Dynatup 9250G machine shown in Figure 3.13. This machine has a speed accuracy of 0.1% and a position

accuracy of +/-0.02 mm. Low-velocity impact tests are performed on GFRE samples containing 0, 1.5 and 3 wt% clay. The impact energy is varied between 10 and 50 J by varying the height of the impactor. 4 tests are performed for each sample type.The results are recorded using Impulse^{TM} Impact Software for energy absorbed, impact energy and transient curves for load and deformation etc.

Figure 3.13 Instron Dynatup 9520G machine used for drop weight impact test.

The impact tests are performed using the spherical tup with 12.5 mm diameter. The load is calibrated for each batch of samples and the rebound brakes are kept activated for all the

tests so that the impactor only struck the sample once. For each sample the height/energy reference is calibrated. The samples are carefully placed so that the tup always strikes the sample at its center (Figure 3.14 (a)). The fixture used for keeping the sample in place is shown in Figure 3.14 (b), it has a rectangular opening of 110 mm x 110 mm and the sample is constrained on all sides.

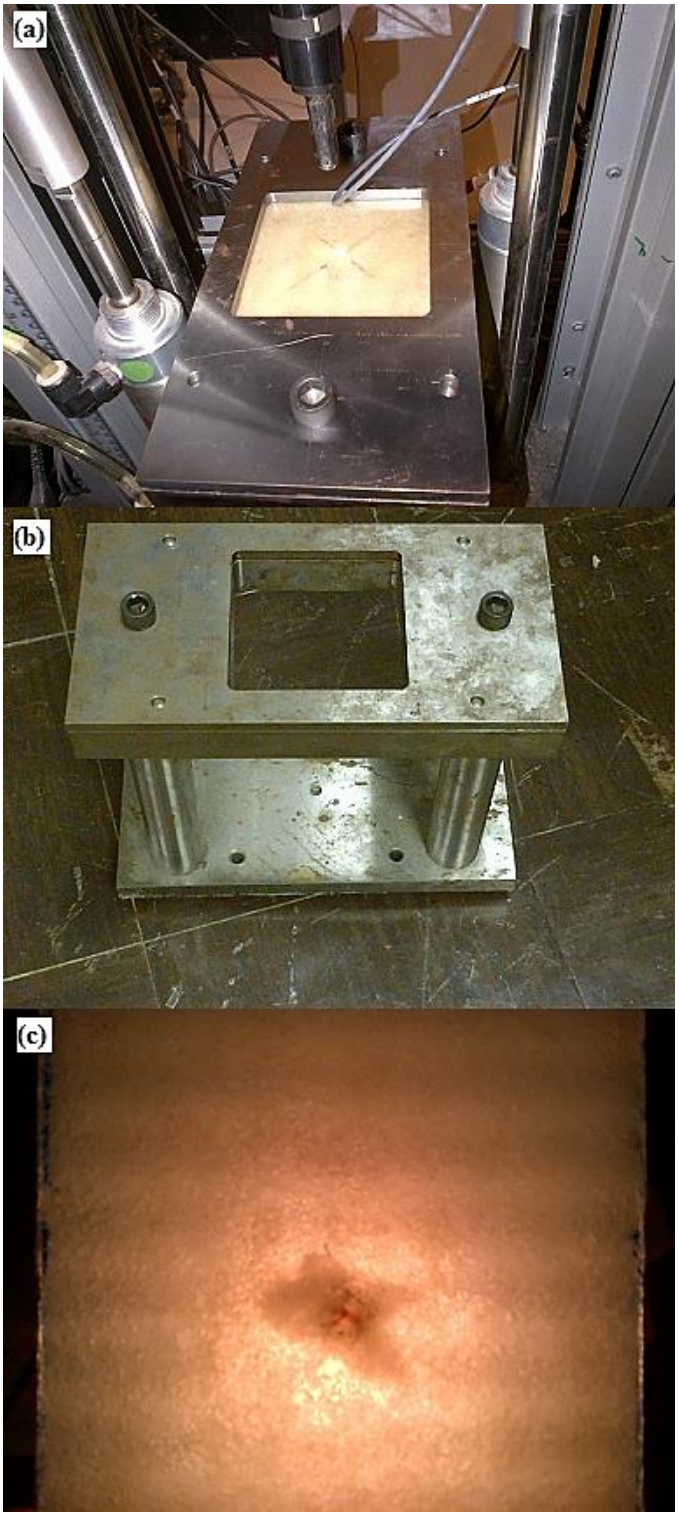

Figure 3.14 Drop Weight Impact Tests (a) Sample calibration (b) Fixture (c) Damage Identification.

After impact the damage is observed using both non-destructive (Figure 3.14 (c)) and destructive techniques. Strong backlighting source is used to determine the delamination/damage area. Damaged area is characterized using ASTM-D7136M [65]. Afterwards the samples are fractured using liquid nitrogen in order to create surfaces which are later observed using SEM for internal damage.

3.5. Characterization

Characterization is a very important part of this work and a number of equipment is used for this purpose. Technical details and specifications of the used equipment are detailed in the following sections.

3.5.1. X-Ray Diffraction (XRD)

Bruker D8 Advance is used for XRD during this work. It is equipped with auto-positioning of 9 specimen holders. The source of the X-ray was Cu Kα radiation having a wavelength of 1.5406Å. All samples are scanned between 2 and 10 degrees using a step of 0.02º. The X-ray diffraction is conducted on the pure nanoclay, neat epoxy and nanocomposites. The nanoclay sample is in the powder form, while small pieces in the form of blocks (10 x 10 x 2.5 mm) are cut for the sheets of neat epoxy and nanocomposites and placed in sample holders and mounted in the sample chamber of the X-ray diffraction equipment.

Figure 3.15 Bruker D8 Advance XRD used in this work.

3.5.2. Scanning Electron Microscope

Jeol JSM-6460LV high resolution scanning electron microscope with a magnification range of 5 to 100,000X (10 nm resolution) running the AnalySIS® imaging software is used to inspect the surface of all composites. The electron gun of this SEM has a voltage between 0.3 to 30 kV with tungsten hairpin filament. The surfaces of the specimens are coated with gold using a Quorum TechK 550X sputtering equipment to make the surface of the sample electrically conductive.

Figure 3.16 Photograph of Jeol JSM-6460LV SEM.

CHAPTER 4

RESULTS AND DISCUSSIONS

4.1.Microstructure Examination

The surface of the prepared nanoclay/epoxy composites was examined by the optical microscope. Figure 4.1 shows these optical micrographs of the surface for the nanocomposites containing different clay loadings. As shown in the figure, the size of the clay clusters increases with increase in clay loading. Figures 4.1 (a) & (b), show the difference in sizes of the agglomerated clay clusters for nanocomposites containing 1% and 2% of clay loading. It can be observed that there is not much difference in the sizes at these clay loadings but the difference is more apparent when compared with high clay loadings like 5 wt% as shown in Figure 4.1 (c) . At 5 wt% the clay cluster sizes increase to as much as 40 μm [46]. As will be seen later, these clusters will negatively affect some of the mechanical and physical properties of the nanocomposites.

The XRD spectra for I.30E clay powder, pure epoxy and epoxy/nanoclay composites are shown in Figure 4.2. It can be seen that there are no peaks for pure epoxy and epoxy/clay nanocomposites and their relative intensities increase with clay loadings. The increase in relative intensity can be explained by larger size of agglomerated clay clusters and higher percent of clay loading as reported by some researchers [19, 60]. The representative peak of I.30E occurs at a diffraction angle of about 4.4˚ corresponding to an interlayer spacing of approximately 20.08 Å. The samples containing epoxy and clay did not show any peak, irrespective of clay loading, in the XRD range of 2˚ to 10˚. This is an indication that the

polymer was able to enter between the clay platelets resulting in possible exfoliated or disordered intercalated nanocomposite structure.

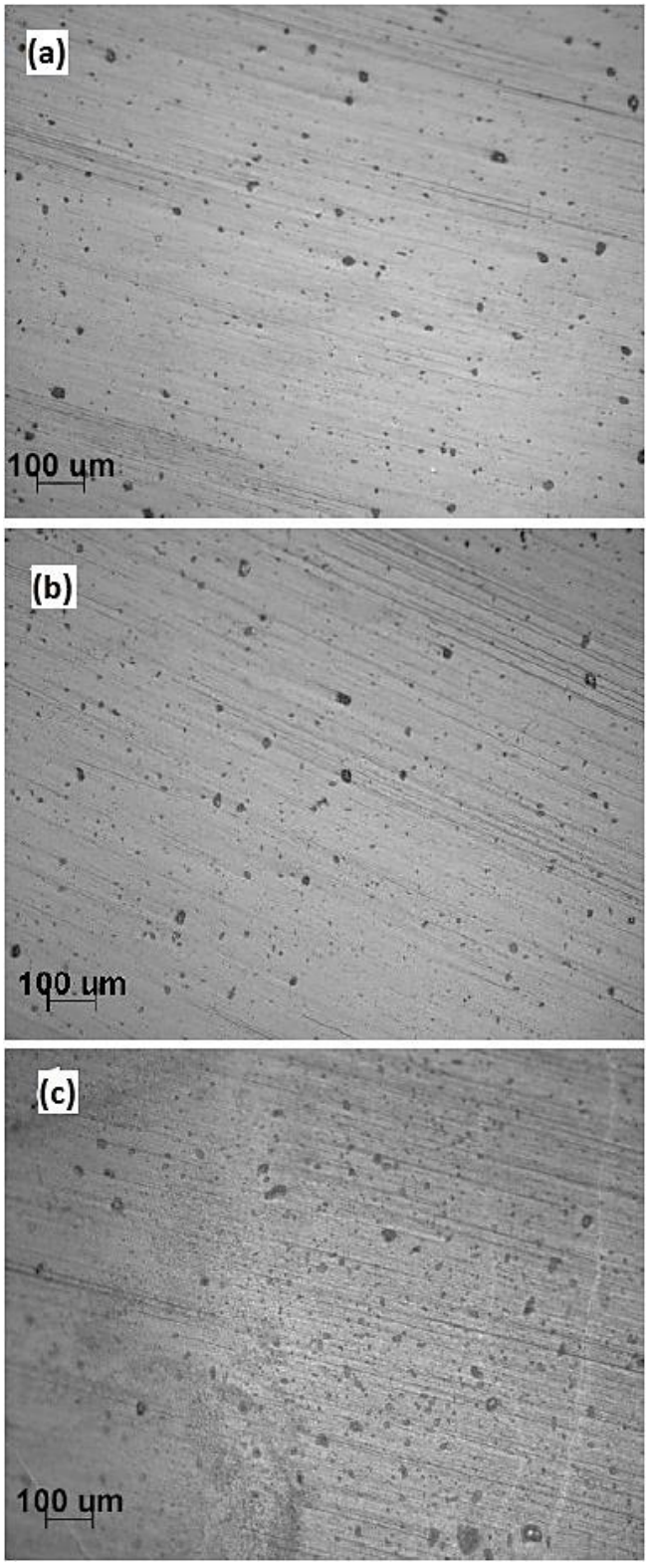

Figure 4.1 Optical micrographs for nanocomposites containing different clay loadings (a) 1 % (b) 2 % (c) 5 %

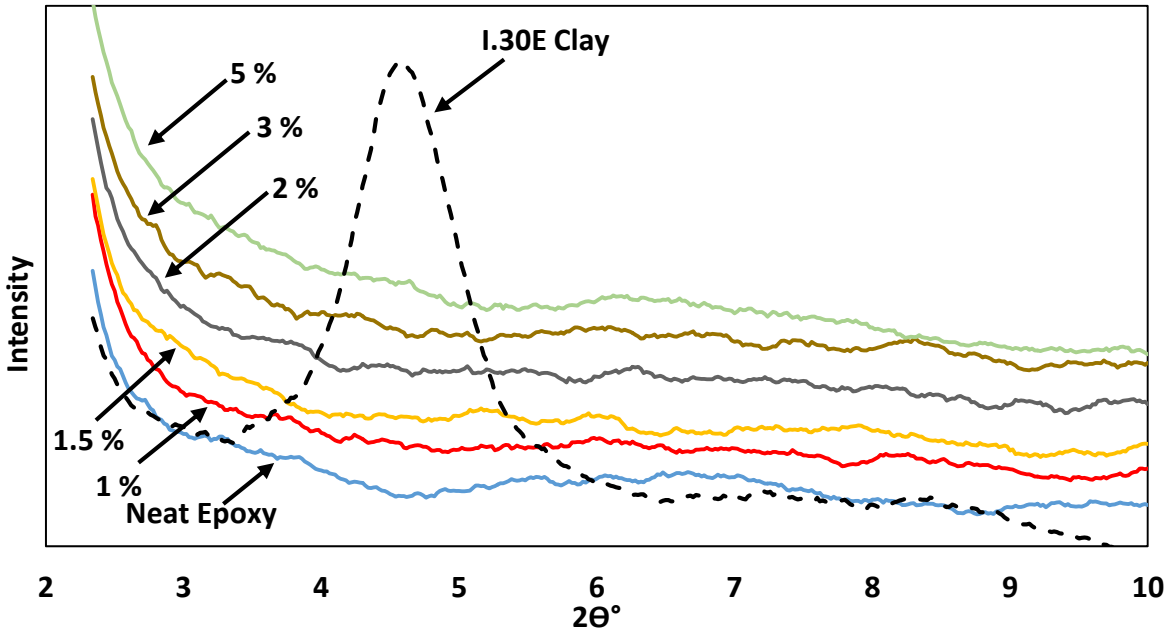

Figure 4.2 XRD Spectra of epoxy clay nanocomposites.

In general, the absence of diffraction peaks can be attributed to either (a) exfoliated structure or (b) disordered intercalated structure. Al-Qadhi et al [46] have shown that both morphologies are present in nanocomposites prepared following the same procedure. Figure 4.3 (a) shows the disordered intercalation marked by white arrows where the black lines are the clay platelets forming a valley inside which the epoxy is seen, while Figure 4.3 (b) shows the exfoliated region representing complete platelet separation. Therefore, it is expected that the resulting morphology of the prepared nanocomposites consists of both disordered intercalation and exfoliation structures. As explained before, the layers still bear a well-defined spatial relationship to each other in intercalated morphology while these individual layers are completely distributed in exfoliation structure.

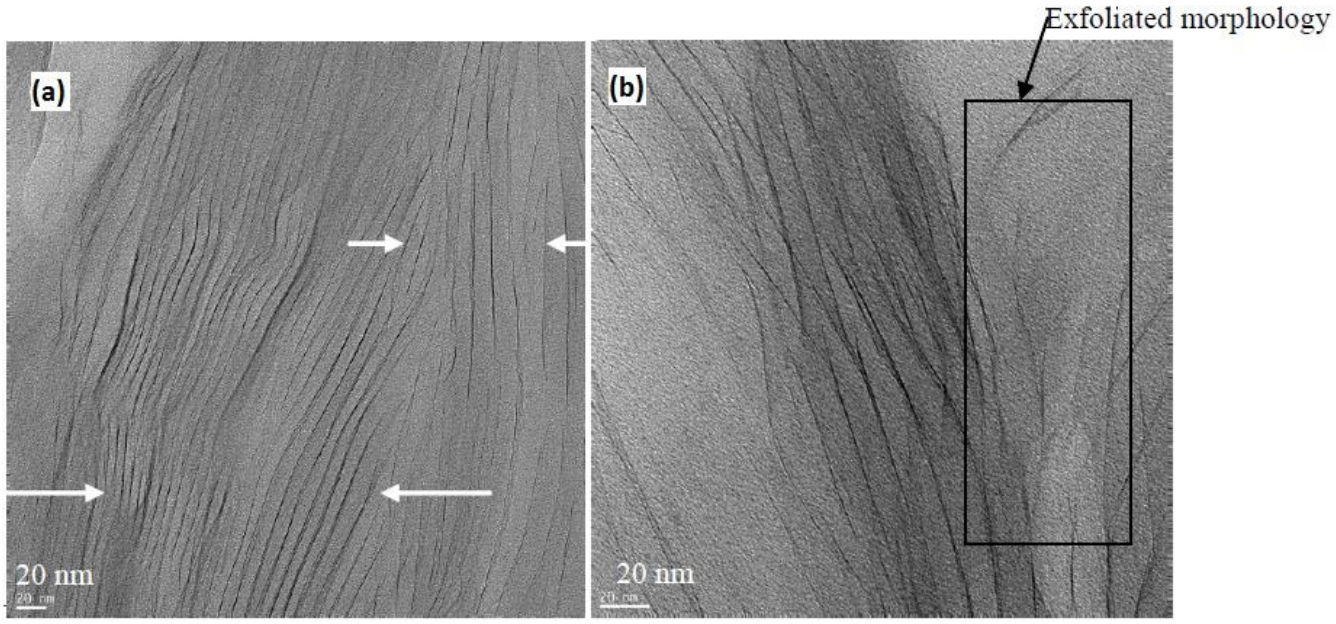

Figure 4.3 TEM images of nanocomposites containing 2% clay showing (a) Disordered intercalation and (b) Exfoliation [46].

4.2.Effect of Glass Fiber and Clay Loading on Flexural Properties

4.2.1. Flexural Properties in Dry Conditions

Table 4.1 lists the average values of flexural properties for samples tested in dry conditions using ASTM D-790 specifications. This is elaborated in Figure 4.4 which shows the effect of clay loading and glass fiber on flexural strength of fiber reinforced epoxy composites. Addition of only 30 vol% glass fiber has resulted in more than 100% improvement in flexural strength, and further reinforcement by nanoparticles has resulted in more than 11% increase in strength at the clay loading of 1.5 wt%. Clay loadings higher than 1.5% resulted in gradual decrease of flexural strength reaching to about 5% at a clay loading of 5 wt%. This positive effect of clay addition on flexural strength can be readily seen from the plot of Figure 4.4.

Table 4.1 Average properties of flexural properties of dry GFRE samples.

Clay Loading %	Flexural Strength (MPa)	Standard Deviation	Flexural Modulus (GPa)	Standard Deviation
0	208.89	3.52	8.30	0.27
1	221.00	5.78	8.96	0.34
1.5	232.56	1.88	9.46	0.13
2	226.22	2.53	9.13	0.05
3	213.77	2.32	8.81	0.13
5	198.83	5.42	8.47	0.14

The improvement in flexural strength upto 1.5 wt% is because of the exfoliated nanocomposite structure as explained earlier. The presence of clay is known to improve the adhesion of the nanocomposite with the surface of glass fibers resulting in better interfacial bonding of the final laminate [5]. Good interfacial adhesion provides better stress transfer and the inherent property of clay as the carrier of superior compression properties improves the flexural properties as well [8, 20]. The negative effect of addition of clay beyond 1.5 wt% can be attributed to agglomeration of clay which acts as stress concentrators. The morphology of the nanocomposite at different clay loadings will be discussed in detail at the end of this section. This negative effect is more profound at higher clay loadings because of the increase in viscosity of the matrix which makes processing

and degassing more much difficult. This also results in tiny air gaps or micro voids which reduces the mechanical properties of the samples [30].

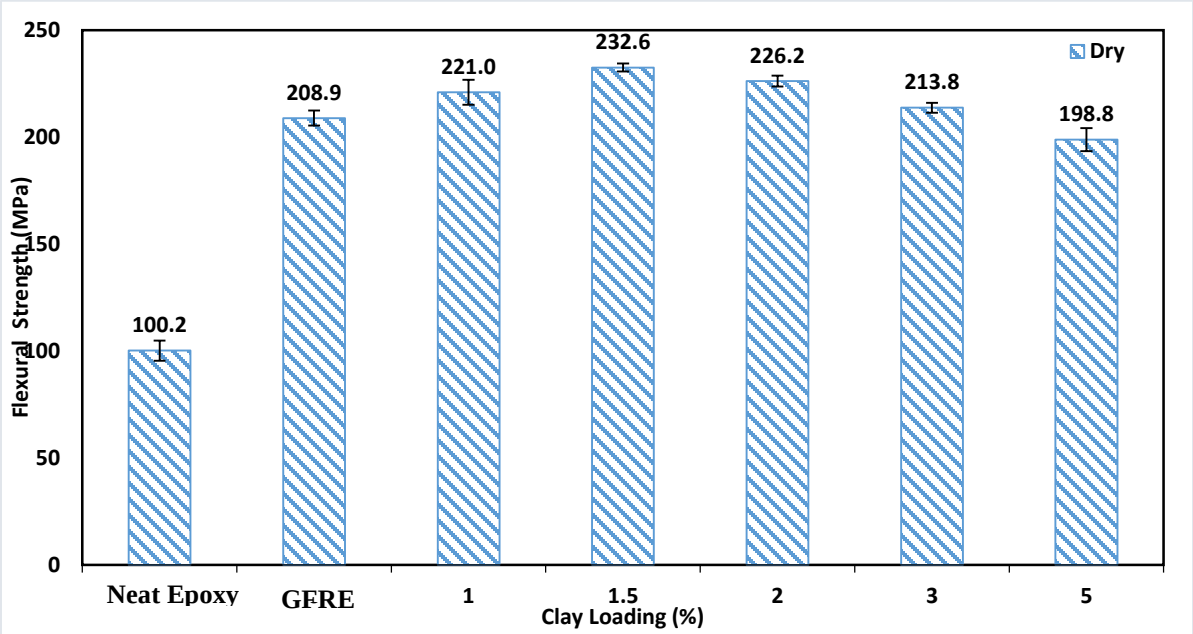

Figure 4.4 Flexural strength as a function of clay loading for dry samples.

As mentioned before, good interfacial adhesion between glass fibers and epoxy clay matrix is the main source of improvement for GFRE clay nanocomposites. This effect is shown by SEM micrographs of flexural fracture surfaces presented in Figure 4.5 where the fiber surface of nanocomposites with and without clay are compared. Figure 4.5 (a) shows the fibers of GFRE 0% nanoclay samples where no clay particles can be seen on the surface. The smooth surface of fibers without nanoclay adhesion does not allow the matrix to have a strong interaction. Arrows in Figure 4.5 (b) illustrates that absence of clay particles on fiber surface reduces the adhesion and makes them loosely bonded which is seen by the

large gaps between the fibers and the matrix. Lesser adhesion also results in a larger number of fiber pullouts which explains the lesser strength [5].

In comparison, Figure 4.5 (c) and (d) shows a bundle of fibers in 1.5 wt% sample where the clay adhesion is prominent. This clay adhesion is due to the interaction between epoxy clay matrix and fiber glass strands. The presence of clay increases the adhesion which allows stronger contact between fiber and matrix by providing a better ‘grip’ and thus improves the mechanical properties. The effect of clay loading on adhesion can be seen in Figure 4.5 (e) and (f) which shows 1.5 and 3 wt% samples where there is significantly less fiber pull out and the fibers are closely sticking to the epoxy matrix which allows for higher flexural properties as compared to neat epoxy samples.

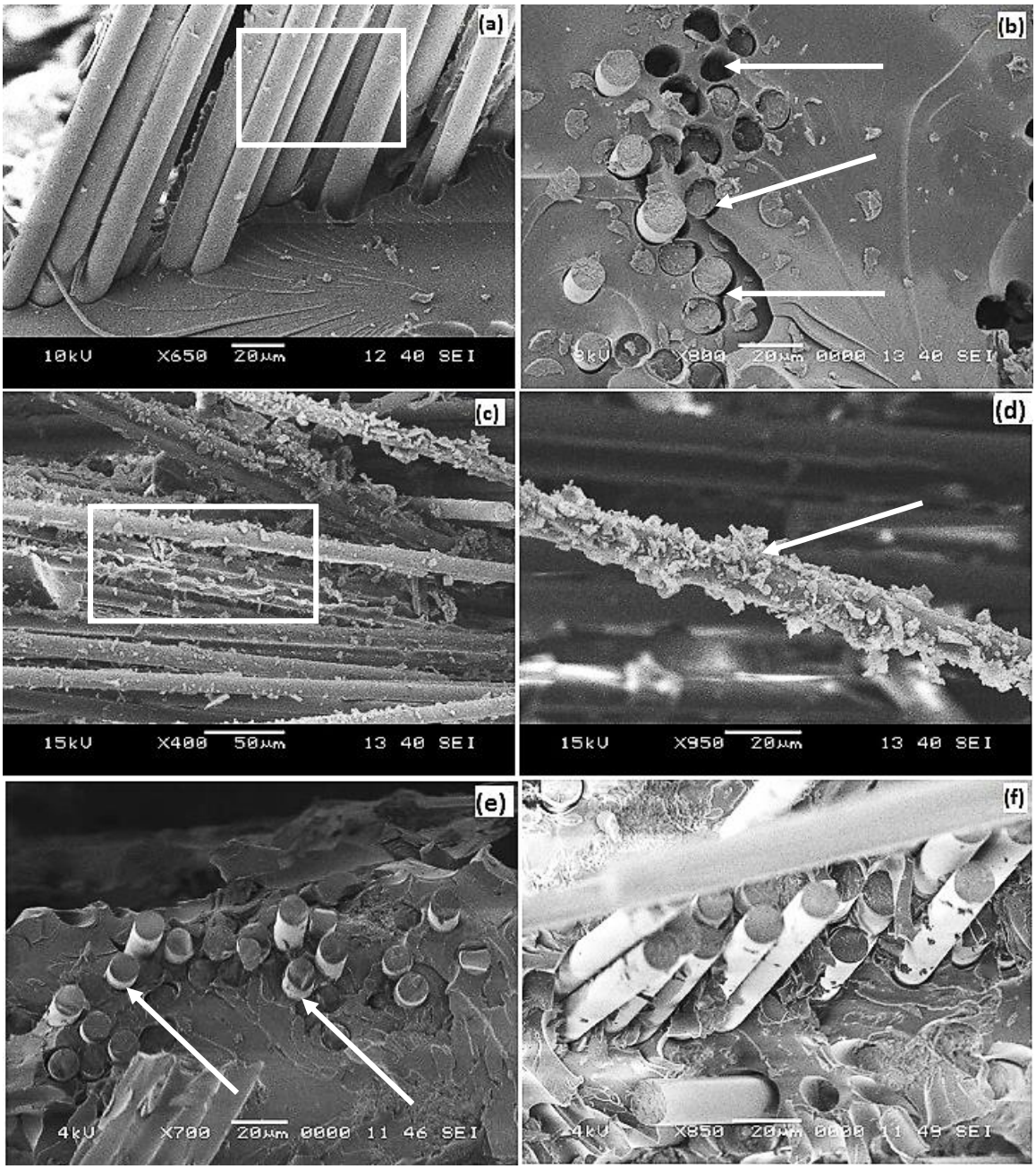

Figure 4.5 SEM of flexural surfaces of (a) & (b) 0 wt%, (c) & (d) 1.5 wt%, (e) 1.5 wt% (f) 3 wt%.

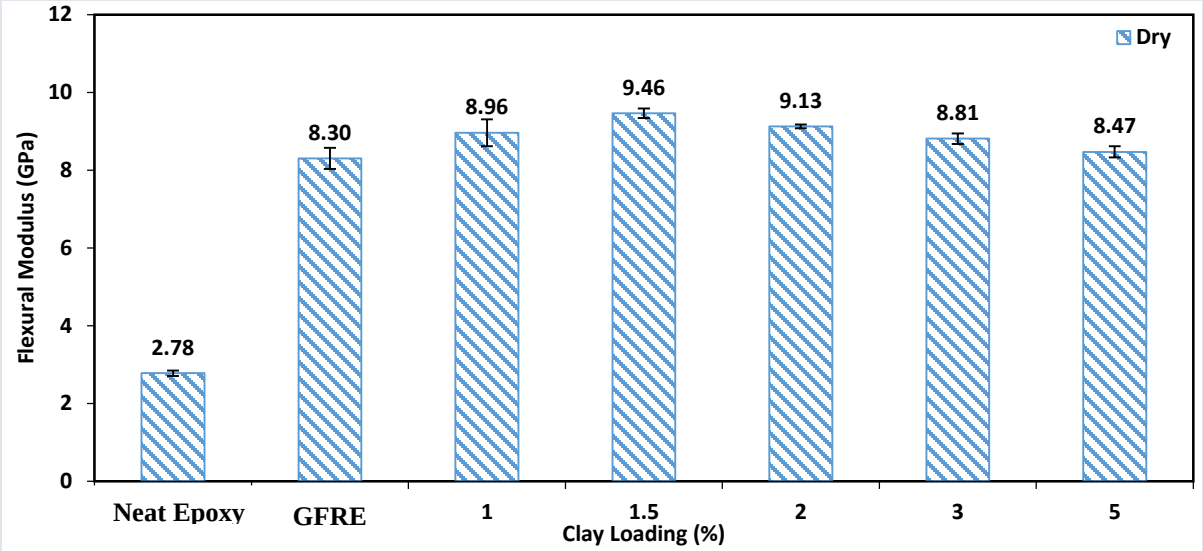

Figure 4.6 Flexural modulus as a function of clay loading for dry samples.

The flexural modulus results presented in Table 4.1 are plotted in Figure 4.6 to illustrate the effects of glass fiber and clay on the stiffness of hybrid nanoclays. It can be seen that flexural modulus follows the same general trend observed for flexural strength. As expected the addition of glass fiber to neat epoxy samples increased the modulus by 200%. This is due to the superior flexural modulus of E-CR glass fibers (~ 5 GPa).The highest value of flexural modulus is obtained with the optimum clay loading of 1.5 wt% with an improvement in stiffness of 14%. Beyond 1.5 wt% the addition of clay gradually decreased the flexural modulus until eventually it reached 5wt% which is comparable to the GFRE 0 wt% sample in terms of its properties. This behavior is different from the expected increase in flexural modulus with increase in clay loading.

The improvement in flexural modulus for GFRE nanocomposites is due to the higher stiffness of clay (~ 170 – 180 GPa) and improved interfacial adhesion of clay when added to these composites as explained earlier. The morphology of the resulting laminate also has

been reported to have a substantial effect on the properties with exfoliated/disordered intercalated being the most effective [5]. At higher clay loadings (beyond 1.5 wt% in this case), the tendency of clays to agglomerate increases which forms lumps and acts as stress concentrators and thus loses their reinforcing ability. Similar trends of flexural strength and flexural modulus were observed by Zulfi et al. [5], Yasmin et al. [9] and many other researchers [8, 51-52] including kornmann [7] who found no increase in flexural modulus at all on addition of nanoclay.

4.2.2. Material Morphology, Clay Agglomeration and Voids

Figure 4.7 shows the SEM micrographs taken of flexural fracture surfaces for different clay loadings. The images show clay agglomeration in different nano composites. Figure 4.7 (a) is a micrograph presenting GFRE samples which shows absence of clay agglomeration as there is no clay present. Figure 4.7 (b) shows micrograph for 1.5 wt% clay surface on which small patches of clay agglomeration were found. Clay agglomeration can be spotted by rougher surface as compared to its surroundings which is because of lump formed by clay. Even though 1.5 wt% is the optimum clay loading there is still clay agglomeration but it is lesser than that at higher clay loadings as shown in Figure 4.7 (c). In 3 wt% samples and higher the clay agglomeration was found to be spread in a larger area and was more frequent which explains its negative effect on flexural properties.

In order to ascertain that those agglomerated clusters seen in Figure 4.7 are indeed clay aggregates, energy dispersive spectroscopy (EDS) was used to identify and quantify the elemental composition of these clusters. Figure 4.8 shows SEM image of nanocomposite containing 5% of clay loading including the suspected agglomerated clay cluster. Table 4.2 lists the components of all spectra shown in Figure 4.8, which shows that spectrum 1 and

spectrum 2 ,which are inside the suspected agglomeration area , contains 15% and 9% Silicon while other spectrums lying outside the suspected region has no Silicon content, thus proving that it is indeed agglomerated clay cluster.

As mentioned before, the viscosity of the matrix is increased during processing and at higher clay loadings, which makes processing/degassing difficult. According to Yasir et al [67] there is a 33% increase in viscosity after hand mixing and a 120% increase in viscosity after high shear mixing. Addition of clay from 3 wt% to 5 wt% increases the viscosity by 55 % due to increased amount of clay present. This explains the difficulty in degassing resulting in more micro voids at higher clay loadings which decreases the flexural properties. The regions marked A, B and C in SEM micrographs of Figure 4.9 show voids found in nanocomposite samples containing 2 and 3 wt% nano-clay.

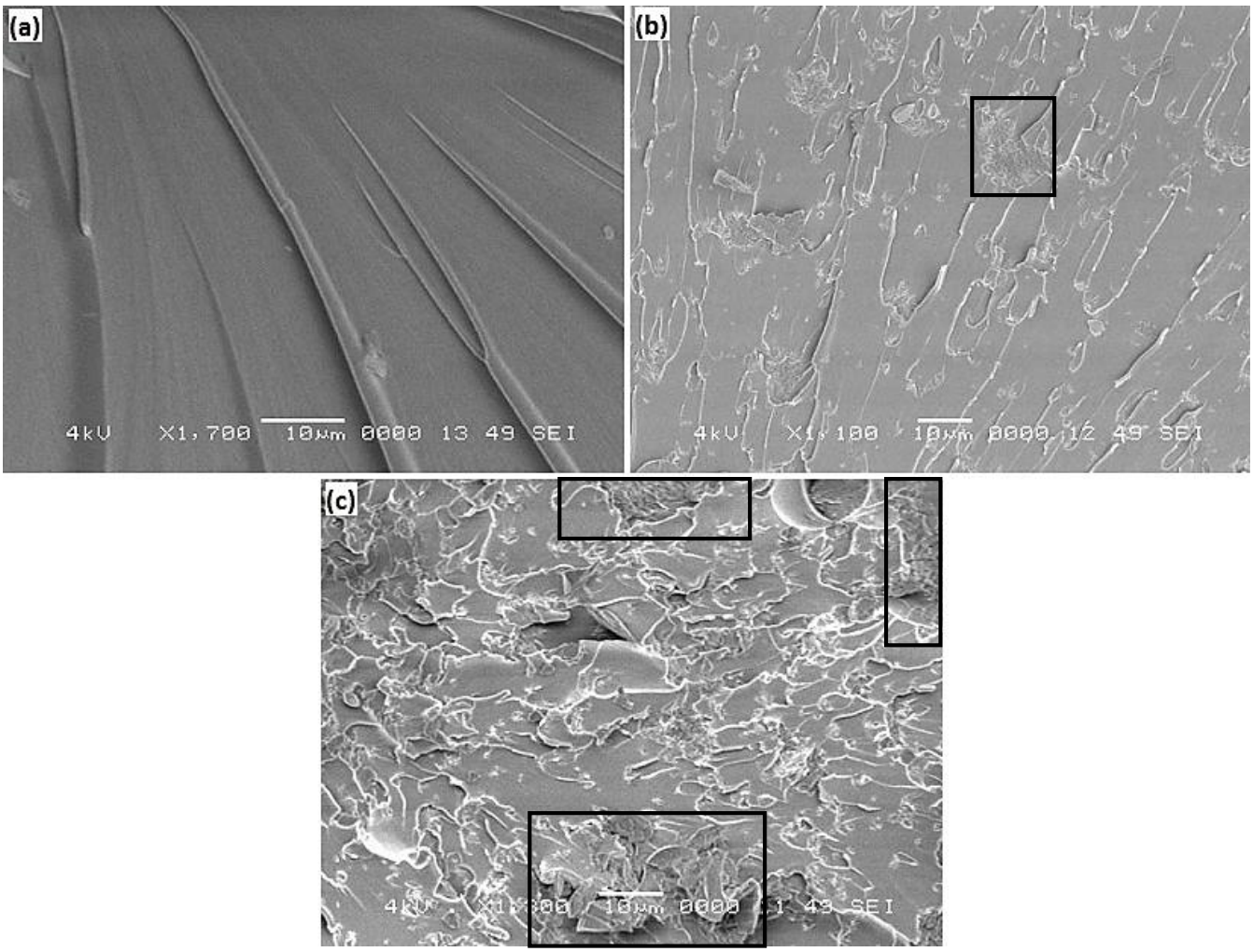

Figure 4.7 SEM showing morphology of (a) 0% (b) 1.5%, and (c) 3% epoxy clay nanocomposites.

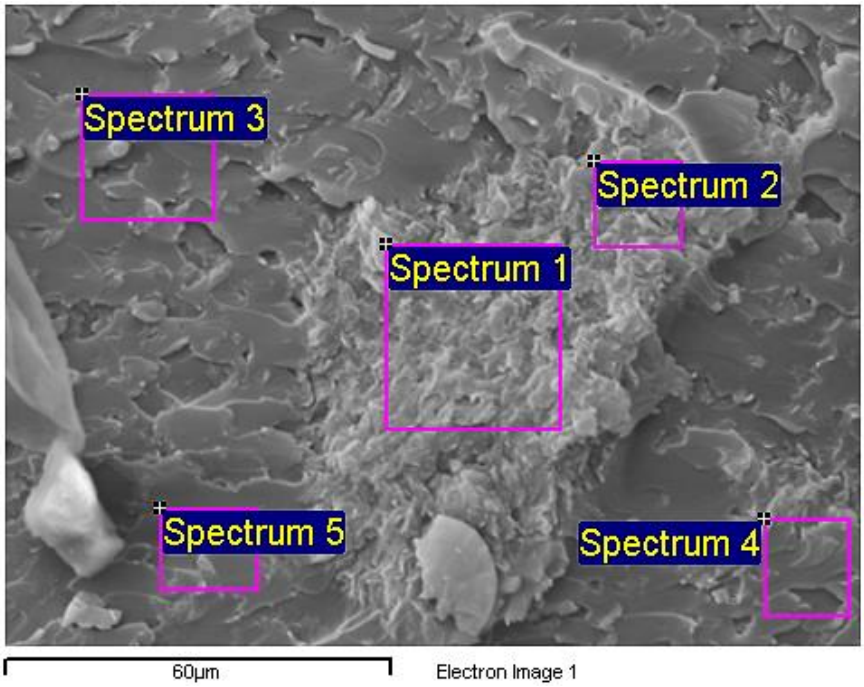

Figure 4.8 SEM image of nanocomposite having clay aggregate used for EDS analysis.

Table 4.2 Quantitative composition of spectrums in Figure 4.8

Spectrum	C%	O%	Mg%	Al%	Si%	Ca%	Fe%	Total
1	56.95	22.21	0.62	3.84	15.42	0.35	0.61	100
2	60.66	26.24	0.76	2.99	8.89	0.46	-	100
3	77.97	22.02	-	-	0.01	-	-	100
4	78.63	21.37	-	-	-	-	-	100
5	76.94	23.05	-	-	0.01	-	-	100

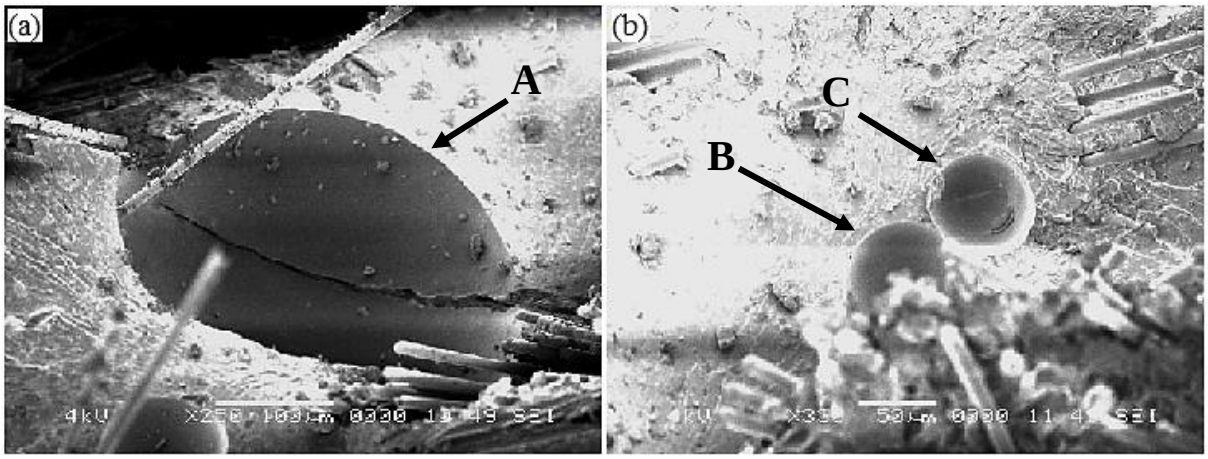

Figure 4.9 Voids in nanocomposites containing (a) 2 wt% and (b) 3 wt% clay.

4.2.3. Water Uptake of GFRE Nanocomposites

In order to determine the water uptake behavior and its effect on flexural properties, the fiber reinforced epoxy clay nanocomposites are immersed into tap water at room temperature for a period of about 4 months. Figure 4.11 shows the variation of percentage weight gain (M_t) with square root of time ($\sqrt{t}$) where (M_t) is calculated from equation 4.1.

$$\boldsymbol{M_t = \frac{(M - M_o)}{M_o} \times 100} \qquad (4.1)$$

Where M and M_o are respectively, the instantaneous and initial weights of exposed specimens.

It is observed that none of the samples reached saturation after the exposure duration of 120 days. Previous work by Al-Qadhi et al. [53] suggests that a period of about a year is required for this epoxy clay system to reach complete equilibrium. Each of the curves in Figure 4.11 show two distinct regions, with the first being diffusion controlled while the second region represents a gradual increase in water uptake. The linear region of weight gain versus square root of time indicates that it is Fickian diffusion behavior, which for

these samples is observed to occur for the first two days. The Fickian diffusion behavior is governed by the following equation

$$\frac{M_t}{M_\infty} = 4\sqrt{\left(\frac{D}{\pi h^2}\right)} \times \sqrt{t} \qquad (4.2)$$

Where M_t is the weight gain in time t, M_∞ is the weight gain at saturation, D is the diffusivity constant in mm^2/s, h is the thickness of sample in mm.

The second stage where the diffusion process starts to slow down is associated with molecular motion and polymer relaxation. This stage is known to be effected by the presence of fibers which constraints the segmental motions [6]. Water uptake is influenced by the hydrophilic character of constituents in composite (matrix and the fibers), the crosslinking of matrix itself, the adhesion between the fibers and the matrix, and most importantly, the presence of voids in the material [6]. Water uptake is due to the ability of water molecules to penetrate through the epoxy matrix. The water absorption behavior is considered to depend on the free and bound water. The amount of free water is determined by the free volume of an epoxy clay matrix and that is why the water uptake reaches true equilibrium only when all the micro-voids are completely filled. The bound water is the water molecules which interacts with the polymer matrix. In the case of epoxy matrices, water molecules have strong affinity for the hydrophilic functional groups such as hydroxyl or amine as shown in Figure 4.10. The water molecules might interact with epoxy molecules by forming hydrogen bonding with hydrophilic groups [42].

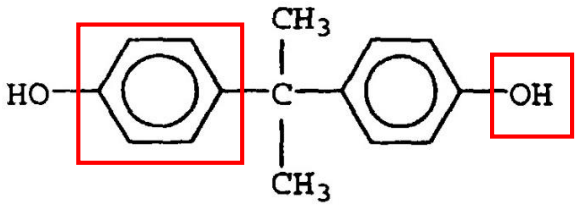

Figure 4.10 DGEBA structure highlighting hydrophilic groups.

Table 4.3 shows the maximum water uptake, improvement and difference in improvement percentage for different clay loadings. As shown, the addition of clay results in decreased water uptake. The samples with nanoclay loading of 5 wt% show the most improvement of about 25% however the improvement is seen decreasing with increasing clay loading due to processing difficulties at higher clay loadings which results in clay agglomeration. The same behavior has been observed by other researches where the presence of high aspect ratio nano-fillers can create a tortuous pathway for water molecules to diffuse into the composites [1].

Table 4.3 Improvement in water uptake with addition of clay in GFRE nanocomposites.

Clay Loading %	Water Uptake % (Max)	Improvement %	Difference %
0	1.00	0	0
1	0.89	11	11
1.5	0.85	15	4
2	0.80	20	5
3	0.77	23	3
5	0.75	25	2

The results of Fig. 4.11 show that GFRE without clay has a maximum of 1% weight gain while the minimum weight gain of 0.7% is found for the hybrid composite with 5% clay loading. Figure 4.12 reveals that GFRE 0 wt% samples show 47% less water uptake than neat epoxy samples. This is mainly because due to the presence of 30 % less epoxy clay mixture than neat epoxy samples. Secondly, the presence of fibers might also have aided in increasing the tortuosity of the water uptake path [7, 42]. The addition of 1 wt% of nanoclay has brought about 11% improvement in water barrier. It is evident that the clay platelets create an impermeable medium which creates a hurdle in the path of water flow and forces it to take a tortuous path. This results in an increased time for water uptake, resulting in decreased water content in composites filled with nanoclay [43].

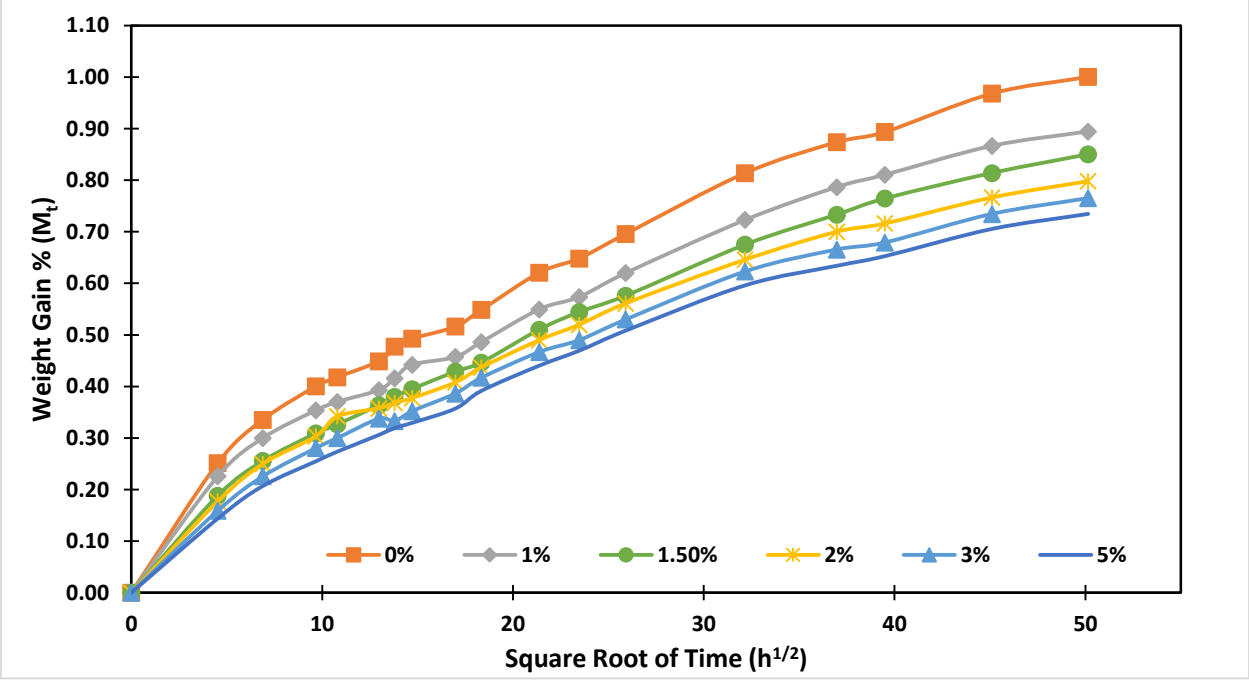

Figure 4.11 Water uptake behavior of GFRE at 23°C with different nanoclay loadings.

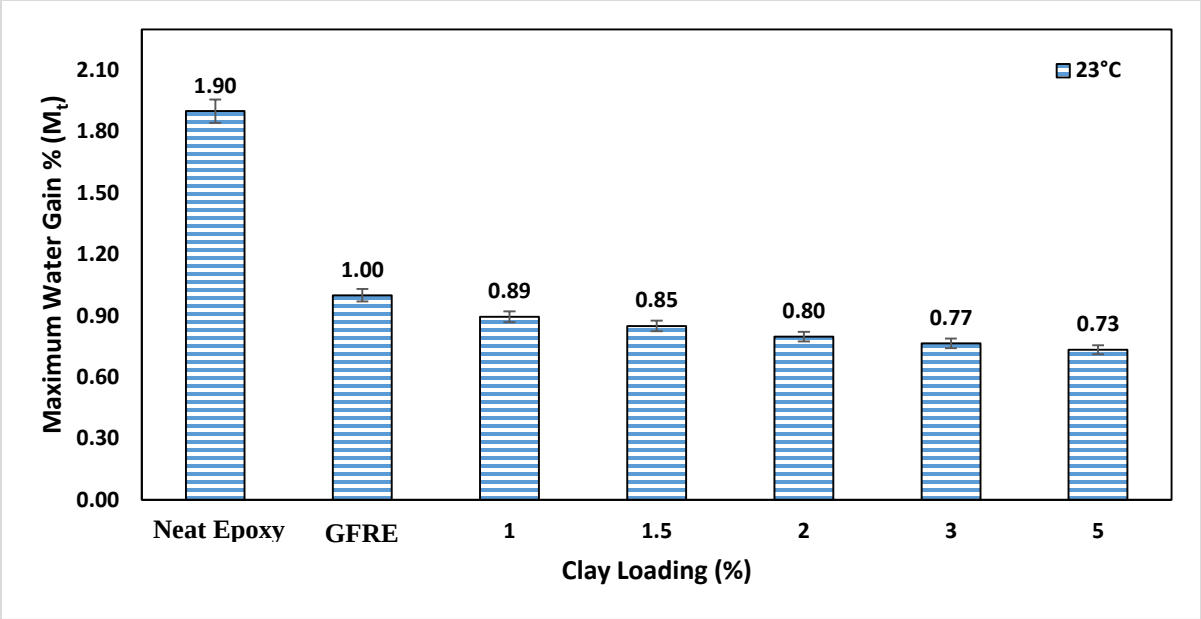

Figure 4.12 Maximum water uptake for different clay loadings at 23°C.

Figure 4.13 shows the water uptake behavior of the same composites at 80°C. Like previous observations, these samples also display a two-step behavior. During the first few days water ingress occurs mainly by diffusion process governed by Fick's law while in the second phase there is a steady increase in water absorption. The total amount of water absorbed at the end of test period is about twice for 80°C samples as compared with those exposed at room temperature. It can also be seen that at the end of test period these samples also did not reach complete equilibrium.

Table 4.4 shows that addition of clay loading decreased the water uptake but, as illustrated in the last column by the difference in improvement percentage, this improvement is seen to decrease overall at higher clay content due to clay agglomeration which decreases its effectiveness. As mentioned above, the reduction in water absorption with increasing clay loading was attributed to tortuous path created by clay platelets which means that water

molecules would need to get around the platelets and will need more time to reach complete saturation.

Table 4.4 Improvement in water uptake with addition of clay in GFRE nanocomposites.

Clay Loading %	Water Uptake % (Max)	Improvement %	Difference %
0	1.826	0	0
1	1.719	6	6
1.5	1.626	11	5
2	1.528	16	5
3	1.446	21	5
5	1.363	25	4

As shown in Figure 4.14 GFRE 0% samples absorb 31% less water than neat epoxy samples. As explained for the room temperature exposure, this is due to the fact that there is less epoxy-clay mixture in GFRE samples and fibers also improve the water absorption barrier properties. The GFRE 0% nanoclay samples absorb 1.80% water which is about 80% more as compared to room temperature samples. In similar works Manfredi et al. [6] prepared GFRE composites of 30% fiber using C.30B nanoclay and found a maximum water uptake of 1.60% which compares well to the results found by this work. Kornmann et al [7] has also shown that high temperature increases the water uptake.

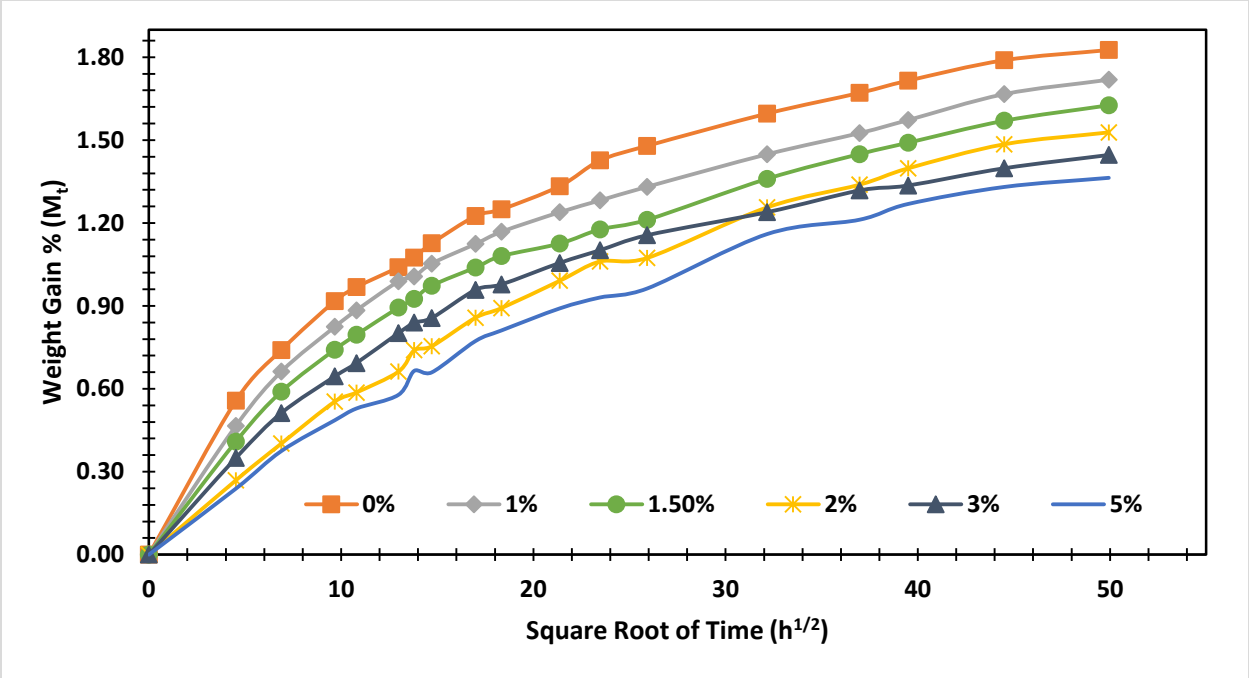

Figure 4.13 Water uptake behavior of GFRE at 23°C with different nanoclay loadings.

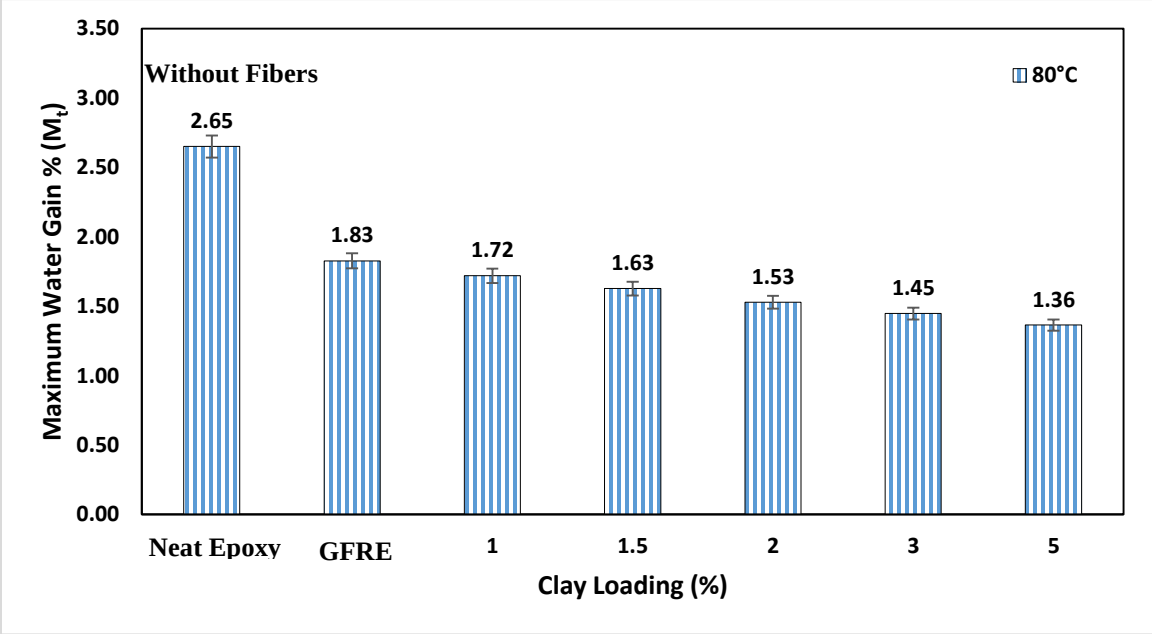

Figure 4.14 Maximum water uptake for different clay loadings at 80°C.

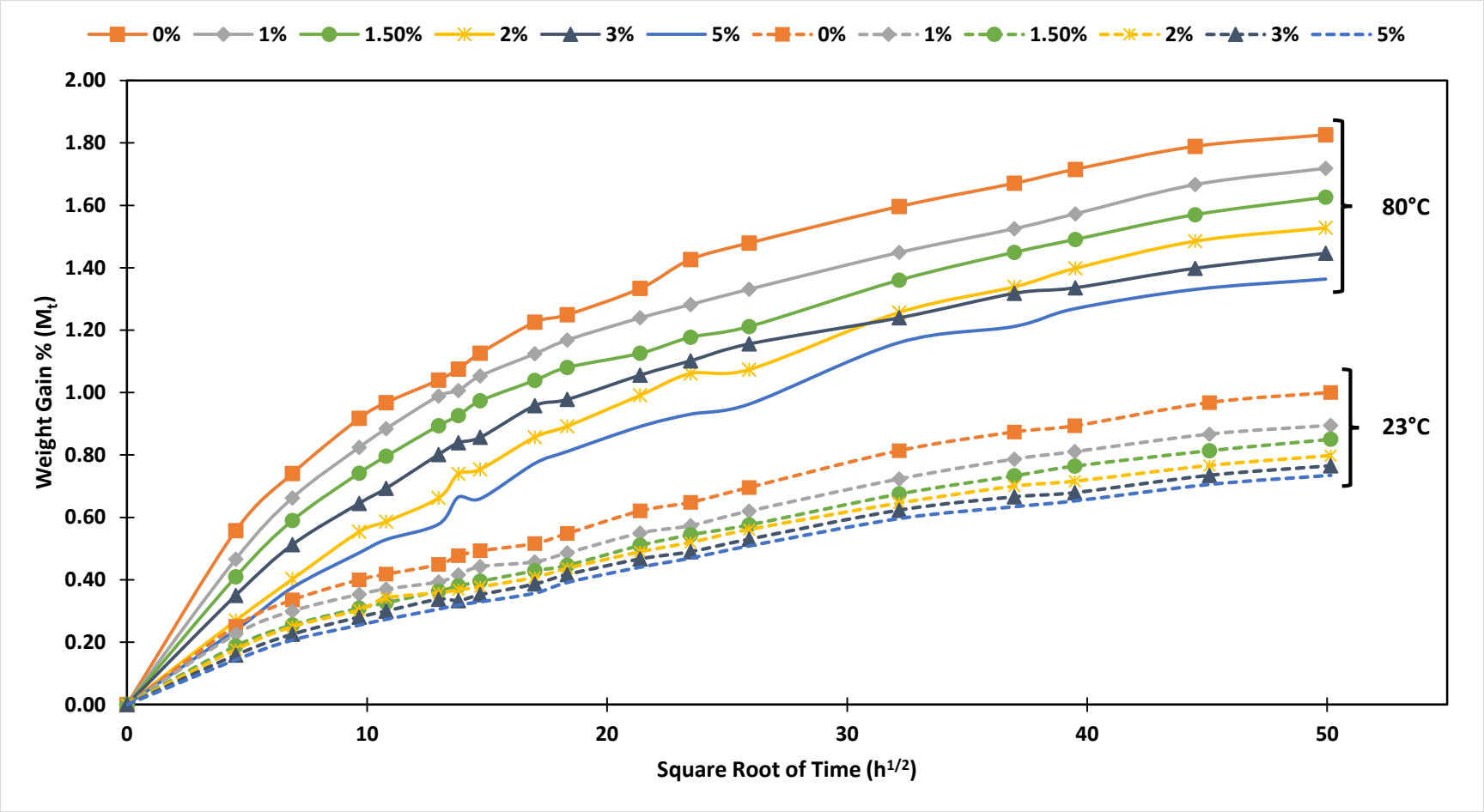

Figure 4.15 Water uptake behavior of GFRE at 23°C and 80°C for different nanoclay loadings.

The change in water uptake behavior can be explained using the rate of diffusion at different temperatures. The gradient of linear portion of the curve is related to diffusivity according to Fick's law (Equation 4.2). Table 4.5 lists the rate of diffusion calculated from the gradient of the liner portion of curves shown in Figure 4.15. It can be observed that samples immersed at 80°C had more than twice the rate of diffusion as compared to the sample immersed at 23°C. The higher gradient means higher water diffusivity which explains the higher water uptake for samples at higher temperature and therefore the samples at room temperature have lower rate of diffusion and lower water content as observed in the previous plots.

Table 4.5 Rate of water diffusion in GFRE nanocomposites at different temperatures.

Clay Loading (%)	**Rate of Diffusion (s^{-1})**	
	80°C	**23°C**
0	3.41E-06	7.55E-06
1	3.06E-06	6.32E-06
1.5	2.55E-06	5.55E-06
2	2.40E-06	3.65E-06
3	2.15E-06	4.74E-06
5	1.95E-06	3.24E-06

4.2.4. Effect of water uptake on flexural properties

The plasticizing effect of moisture ingress in the epoxy matrix of the exposed GFRE and GFRE nanoclay composites resulted in the reduction of flexural properties as shown in Figure 4.16 and 4.17. The previously presented flexural test results of results of dry specimens have also been added for comparison. The flexural strength and modulus are seen to be reduced by water uptake with higher M_t resulting in more degradation. Again, 1.5 wt% nanoclay addition showed highest improvement in flexural strength and also showed fairly less reduction in properties as compared to most clay loadings. Beyond 1.5 wt% the strength decreases owing to clay agglomeration and voids. Even though the water uptake is slightly less for higher clay loadings but the decrease in flexural properties is higher indicating the significance of clay agglomeration in nano composites.

The flexural strength for room temperature water uptake samples is observed to be 6-10%, depending on clay loading, less than those without water uptake. Neat epoxy samples lose the most strength in the presence of water and the nanoclay based samples show significant improvement. Even after 4 months water exposure the 1.5 wt% samples are still 3% better than GFRE 0% dry samples. As mentioned, the overall observed reduction in flexural properties on water exposure can be directly associated with plasticizing effect of water which can lead to diminishing interfacial interaction between epoxy and clay nanoparticles [1]. Further aggravation in negative effect can be caused by matrix swelling and hydrolysis [6]. For the samples immersed in water of 80°C water exposure samples, on average, the reduction in strength is about 36% as compared to the unexposed samples and about 30% as compared to 23°C water uptake samples. The combined effect of moisture absorption with high temperature has a strong influence on the matrix structure which leads to

significant decrease in flexural strength. Again, the GFRE 0 wt% samples are the worst while samples with nanoclay performs up to 14% (1.5 wt%) better which justifies the addition of nanoclay as reinforcement even at high temperatures. Manfredi et al. [6] observed a similar profound decrease when GFRE nanoclay samples were tested for high temperature water absorption.

A similar trend is found for flexural modulus as shown in Figure 4.17 where the flexural modulus of both water uptake at room temperature as well as 80°C is shown. Water absorption has a negative effect on flexural modulus and this effect is even more significant at high temperatures. At 1.5wt% the flexural modulus is highest which is 15% for 23°C and 14% for 80°C. Furthermore, it is observed that at this optimum clay loading the reduction in flexural modulus is amongst the lowest. At 1.5wt% the flexural modulus is still higher than that of dry neat epoxy which justifies the manufacturing of hybrid composites. Flexural modulus for room temperature water immersion nanoclay based samples decreased by a maximum of 5% while that for high temperature samples decreased by 11-13% because of synergetic effect of water absorption and high temperature.

Table 4.6 Average properties of flexural properties of dry GFRE samples.

Clay Loading %	Flexural Strength (MPa)		Standard Deviation		Flexural Modulus (GPa)		Standard Deviation	
	23°C	80°C	23°C	80°C	23°C	80°C	23°C	80°C
0	187.70	127.30	1.91	3.58	7.61	7.11	0.13	0.29
1	203.55	140.08	0.72	1.67	8.50	7.81	0.05	0.12
1.5	216.11	147.98	7.95	3.08	9.01	8.27	0.27	0.04
2	208.75	144.48	5.77	4.32	8.72	8.02	0.43	0.15
3	200.22	137.32	2.43	4.64	8.41	7.76	0.03	0.04
5	186.05	128.59	3.59	2.01	8.08	7.49	0.02	0.07

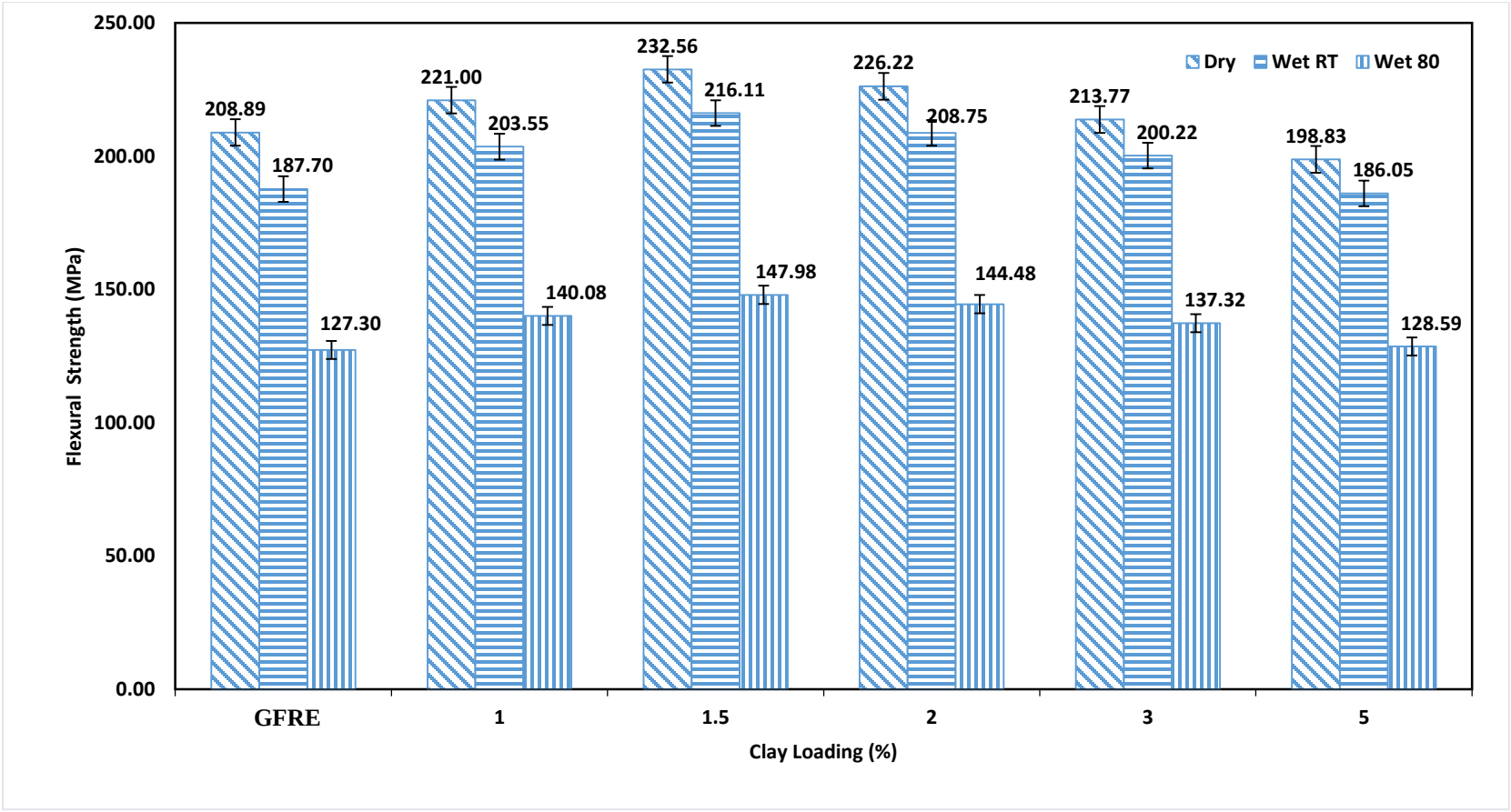

Figure 4.16 Effect of water uptake on flexural strength of GFRE and GFRE nanoclay composites at 23°C and 80°C water exposure.

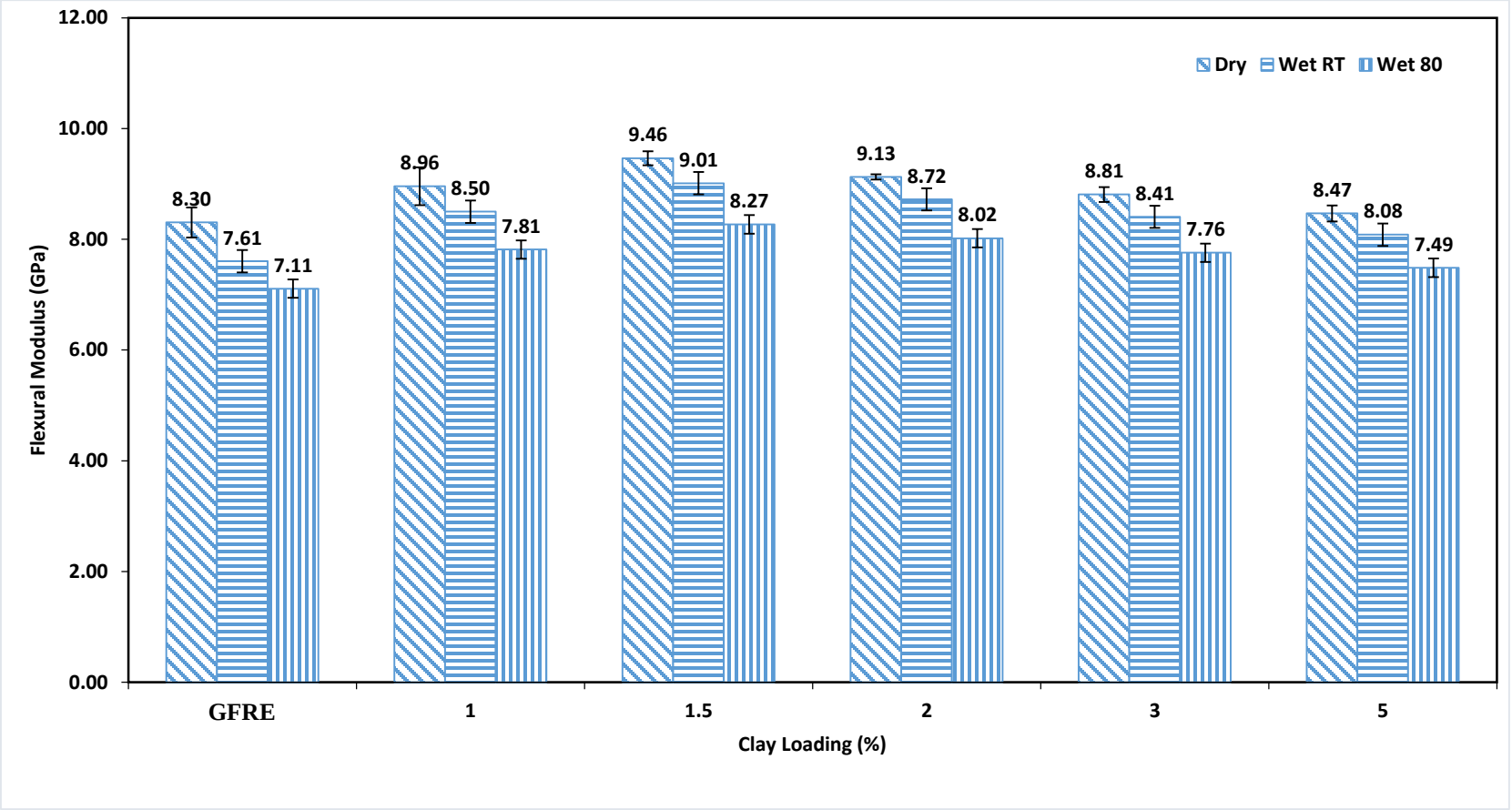

Figure 4.17 Effect of water uptake on flexural modulus of GFRE and GFRE nanoclay composites at 23°C and 80°C water exposure.

4.3.Drop Weight Impact

Hybrid composites are used in applications in which they may be/are exposed to impact like conditions for example, tool dropping or flying fragment impacting the composite. Resulting damage can severely change the mechanical properties of the said composite. Such a situation is most commonly simulated using drop weight impact. Drop weight impact test determines the ability of composite laminated plates to resist impact damage. In this test an impactor, which is available in different shapes and sizes, impacts the fiber composite laminate at a specified energy, velocity or height. The resulting impact determines the damage resistance by the laminate and is then measured in terms of physical damage and other quantitative measurements such as energy absorbed, load and deflection.

As mentioned before, flexural results showed that 1.5% clay loading samples are the best in terms of their properties and therefore the drop weight impact test focused on determining the impact response of these clay loading samples. For comparison, these samples are tested along with GFRE without nanoclay (0%) and GFRE with higher clay loading (3%). Four different drop weight energies are selected in between the range of 10 to 50 J based on preliminary testing. The 10 J impact energy is selected in order to study the Barely Visible Impact Damage (BVID), 20 J represents Clearly Visible Impact Damage (CVID) while 35 J and 50 J represents complete perforation and are selected to observe the impact response at and beyond the threshold energies.

4.3.1. Load, Energy and Displacement Responses

(a) Load-Time Response

Figure 4.18 shows the load vs. time response of the laminates with different clay loadings when subjected to drop weight impact. These impact damage resistance plots can be

characterized by incipient damage or damage initiation (P_i) and maximum or peak load (P_p) as marked in Figure 4.18 (a). Incipient damage is identified by the first sudden drop in the load-time curve. Beyond this point, the remaining strength of the laminate is mainly influenced by the impact energy which is the main cause of damage growth within the laminate. The peak load (P_p) that a laminate can take for a particular energy is apparent by the peak value read off the load-time chart [31].

The first plot shows that incipient load of all the three nanocomposites are nearly identical with 1.5 and 3% having only slightly higher values than 0% nanoclay. Afterwards, the difference is more apparent in peak load where the 1.5% clay loading samples performed substantially better than 3 and 0 wt%. As shown in Table 4.7, the improvement observed for 1.5 wt% samples goes up to 23% while for 3 wt% the improvement reaches 14%. The improvement percentage is also seen to decrease with increasing impact energy because the samples approach the threshold energy that it can absorb. This increase in impact resistance is mainly due to the enhancing effect of nanoclay addition to GFRE. A similar trend can be seen for the 20 J, 35 J and 50 J impact energies. It can also be seen from the results of Table 4.7 that there is a gradual increase in P_i and P_p as the impact energy increases [39].

Figure 4.18 (a) and (b) shows a gradual load drop over the time which is a qualitative indication that not so severe damage or localized form of damage has occurred. This type of bell-shaped load–time curve shows a relatively smooth and symmetrical loading and unloading portions, which indicates that the loading is within the elastic range of the coupon. Fig 4.19 (c) and (d) however shows a comparatively sharper load drop indicating that a higher amount of damage or even perforation have happened [36]. The relatively

symmetrical loading and unloading curves (a) and (b) are also a qualitative indication of less amount of damage as compared to (c) and (d) [59].These curves also contain oscillations which are created by the vibrations of the samples due to collision between the impactor and sample [64].

In general, increasing both the impact energy and clay loading increases the peak load and 1.5 wt% shows the maximum load bearing capacity amongst the three clay loadings tested. The reason for 1.5 wt% samples showing marked improvement over 3 wt% samples can be associated with agglomeration and voids found in the 3 wt% samples (Figure 4.7), as already explained in flexural properties. Agglomerations act as internal flaws with stress concentration which can reduce the impact resistance capability of the laminates. Clay agglomeration and voids also affect the interaction of fibers with matrix which results in less than optimum stress transfer during impact [35].

In this work a peak load of over 4 kN has been observed for glass fiber reinforced epoxy-clay system which is a substantial improvement over what has been reported by some of the researchers including Avila et al. [33] who found a maximum peak load of 1.5 kN for glass fiber 0 wt% samples which is the highest as there is no improvement with clay (I.30E) addition.

Table 4.7 Initial and peak load for different laminates.

Energy (J)	Clay (%)	P_i (kN)	P_p (kN)	Standard Deviation	Improvement (%)
10	0	0.249	2.67	0.41	-
	1.5	0.274	3.29	0.17	23.22
	3	0.260	3.04	0.18	13.86
20	0	0.256	3.37	0.21	-
	1.5	0.349	3.81	0.15	13.05
	3	0.338	3.51	0.36	4.15
35	0	0.478	3.68	0.17	-
	1.5	0.514	3.99	0.15	8.42
	3	0.495	3.80	0.18	3.26
50	0	0.494	4.12	0.11	-
	1.5	0.550	4.22	0.21	2.42
	3	0.548	4.15	0.14	0.73

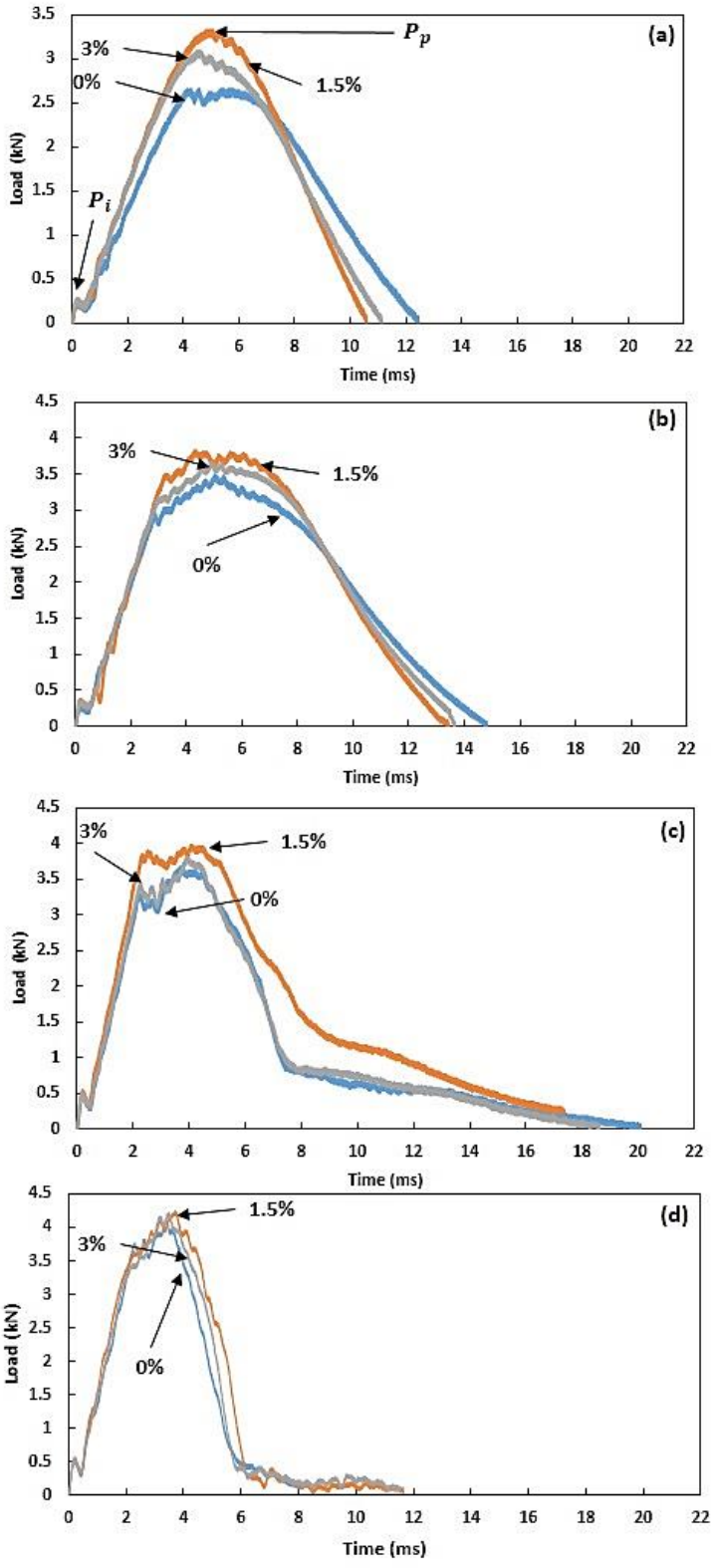

Figure 4.18 Load vs Time plots of samples impacted with (a) 10 J (b) 20 J (c) 35 J and (d) 50 J

(b) Energy-Time Response

The plots of Fig. 4.19 illustrate the variation of the impact energy with time. The impact energy (E_i) is divided into elastic energy (E_e) and absorbed energy (E_a) as shown in Figure 4.19 plot (a). Elastic energy is the part of impact energy which is stored elastically in the specimen and is transferred back to the impactor while absorbed energy is the fraction which is absorbed by the specimen and accounts for the damage produced [54]. It can be seen from subsequent plots (a) to (d) that increase in impact energy promotes a decrease of the elastic recovery. Figure 4.19 (c) and (d), show that practically all of the impact energy is converted into absorbed energy and, consequently, the damage changes from localized to complete perforation. The beginning of the plateau of the curve coincides with the loss of contact between the striker and the specimen, so, this energy coincides with that absorbed by the specimen [35].

As shown in Figure 4.19, the samples with 1.5 wt% nanoclay loading absorb less energy as compared to 3 wt% and GFRE (0%) samples. In general, the addition of clay decreases the energy absorption capability of the laminates. Less energy absorption is desired for the use of such laminates as the amount of damage is proportional to the amount of energy absorbed and therefore less internal damage will have a substantial effect on the service life.

This behavior is further explained in Figure 4.20 and 4.21 which shows that maximum absorbed energy for samples is 35 J, which defines the threshold limit. It can also be seen, as mentioned before, that 1.5 wt% samples absorb the least amount of energy and thus are expected to have the least damage as will be explained later. From Figure 4.21 it can be observed that for impact energies below 35 J, i.e. (a) 10 J and (b) 20 J, there is a finite

amount of absorbed energy and that laminates can still absorb energy higher than impact energy. But this threshold is reached when impact energy is 35 J or higher, Figure 4.21 (c) 35 J and (d) 50 J after which the absorbed energy is nearly the same.

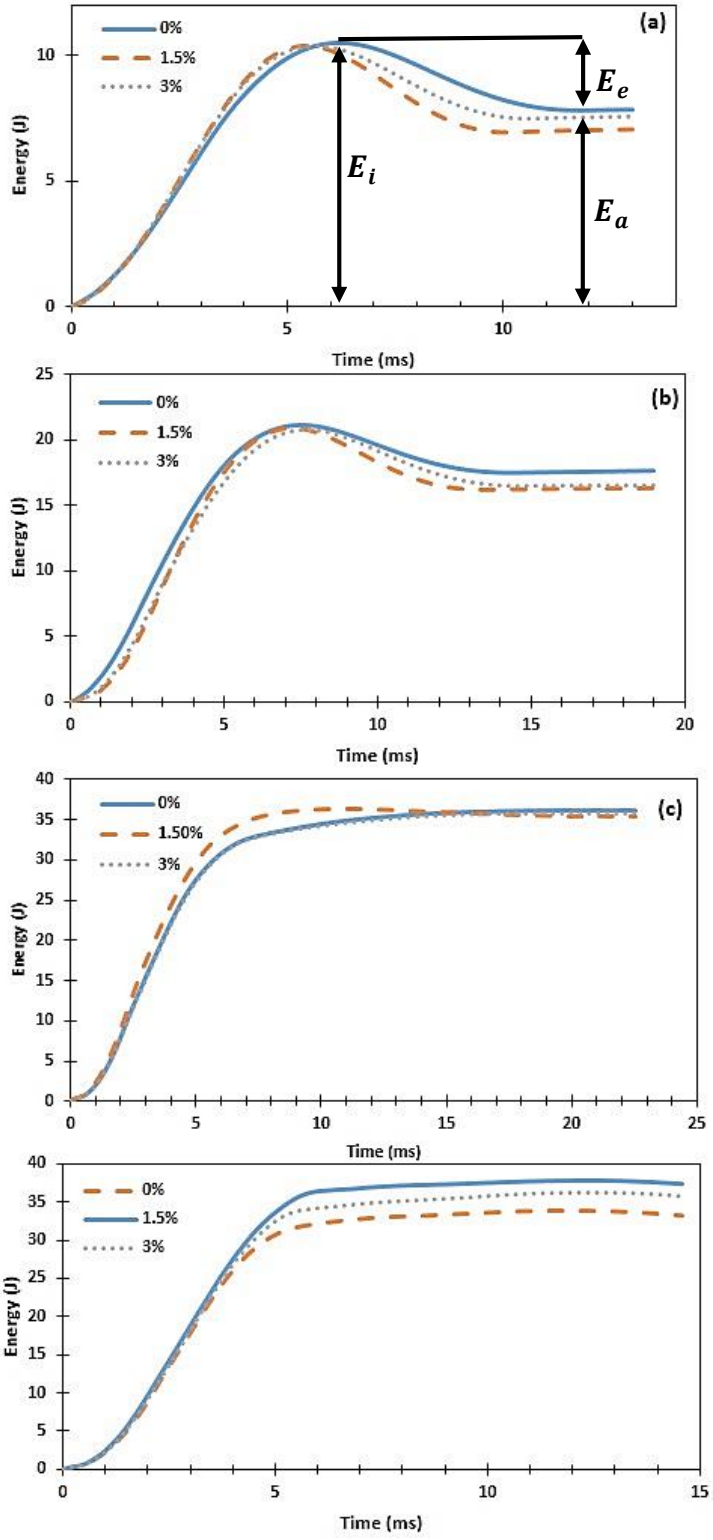

Figure 4.19 Energy profile with time for laminates impacted with (a) 10J (b) 20J (c) 35 J and (d) 50 J.

Table 4.8 Impact and absorbed energy for different GFRE nanocomposites.

Impact Energy (J)	Clay (%)	Absorbed Energy (J)	Standard Deviation
10	0	7.83	0.38
	1.5	7.01	0.16
	3	7.55	0.27
20	0	17.54	0.33
	1.5	16.28	0.21
	3	16.49	0.22
35	0	36.17	0.21
	1.5	35.13	0.18
	3	35.80	0.14
50	0	36.67	0.24
	1.5	32.67	0.25
	3	34.82	0.18

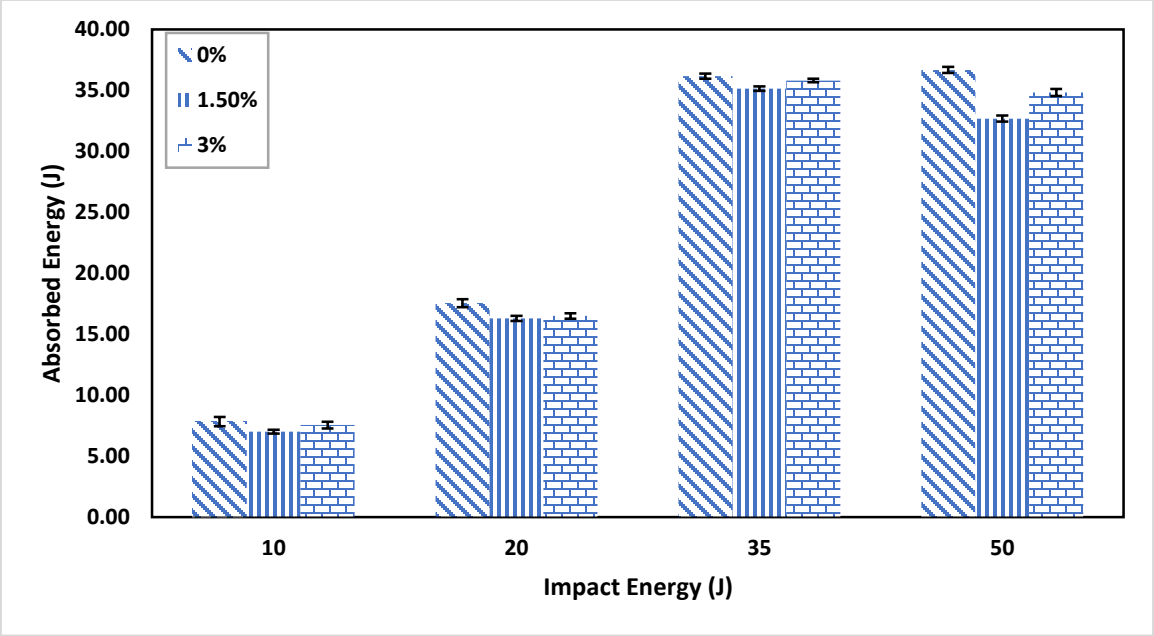

Figure 4.20 Absorbed energy as a function of impact energy.

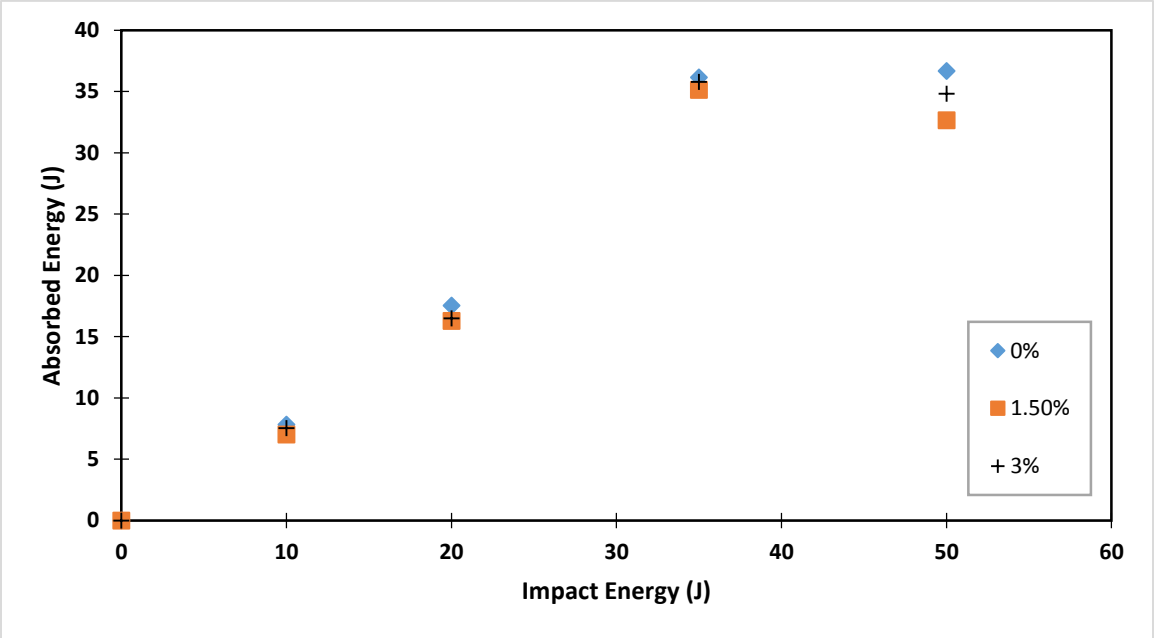

Figure 4.21 Absorbed energy as a function of impact energy.

(c) Deflection-Time Response

Deflection or displacement at peak load is the indicator of the stiffness of the material. Higher the deflection recorded, the lesser is the stiffness and vice versa. Deflection-Time plots for GFRE laminates are shown in Figure 4.22. As can be seen from these plots the deflection of the samples with nanoclay is the lowest and 1.5 wt% samples shows the highest stiffness. For the (a) and (b) plots the samples have returned to original deflection but the higher energy samples of (c) and (d) have seen permanent deflection due to significantly higher damage/perforation. This behavior can be related to energy response as the higher energy absorbed produces higher deflection. The different behavior of 1.5 wt% sample as compared to the rest in (c) is because, as explained in previous section, 1.5 wt% sample had the least amount of energy absorbed and had yet not reached its energy absorption limit and thus also had the lowest damage. The deflection of the samples with nanoclay is lower due to increased stiffness of the nanoclay.

Table 4.9 shows the values of deflection at peak load and total impact duration. These values are plotted in Figure 4.23 and 4.24. The deflection is seen to be increasing steadily until it reaches the saturation energy of 35 J after which it is constant. This is also confirmed by the total impact duration which is also given as a plot in Figure 4.24. More compliant the sample the more time it takes to complete the impact event and also has higher deflection at peak load [37]. The total time is higher for GFRE 0 wt% epoxy samples as compared to those with clay which means that addition of clay makes the samples stiffer. Based on these parameters, 1.5 wt% samples are found to be the stiffest which also agrees with the flexural modulus results discussed earlier.

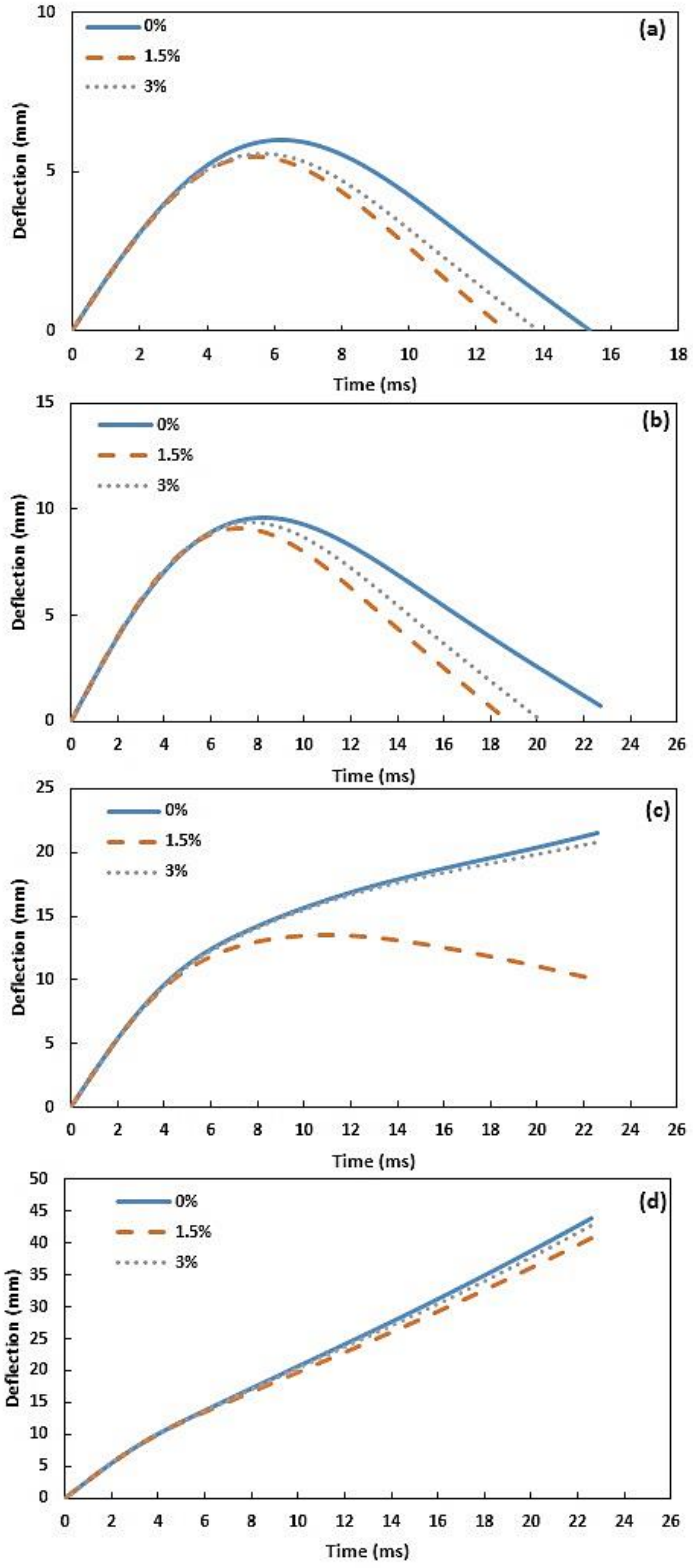

Figure 4.22 Deflection profile with time for laminates impacted with (a) 10J (b) 20J (c) 35 J and (d) 50 J.

TABLE 4.9 Deflection and impact durations for different laminates.

Energy (J)	Clay (wt%)	Impact Duration (ms)	Standard Deviation	Deflection (mm)	Standard Deviation	Improvement (%)
10	0	11.07	0.78	5.15	0.32	-
	1.5	10.00	0.45	4.16	0.01	10.46
	3	10.29	0.31	5.07	0.17	1.56
20	0	14.88	0.98	7.84	0.09	-
	1.5	13.31	0.54	7.33	0.10	6.50
	3	13.87	0.78	7.35	0.03	6.25
35	0	22.64	0.69	9.32	0.14	-
	1.5	18.50	0.95	8.83	0.06	5.25
	3	19.96	0.44	9.16	0.11	1.72
50	0	11.65	0.24	9.33	0.13	-
	1.5	8.35	0.68	8.60	0.10	7.82
	3	11.57	0.33	8.92	0.21	4.39

Table 4.9 above shows that, based on the value of the deflection, the addition of 1.5 wt% of nanoclay improves the stiffness of GFRE by about 10.5%. The decrease in stiffness on further clay addition (beyond 1.5 wt%) can again be attributed to clay agglomeration and micro void formation which reduces the adhesion between resin and fibers and thus reduce the stiffness. A similar trend in stiffness for drop weight impact response is observed by Avila et al. [38] for GFRE samples prepared using C.30B nanoclay and DGEBA epoxy. The authors also found that 5 wt% samples were recorded to have the least impact duration amongst 0 to 10 wt% nanoclay loading samples. Similarly, Kosar et al. [35] reported that

for carbon fiber samples containing 3 wt% of I.30P nanoclay, the stiffness is highest as compared to 0 wt% and 5 wt% samples.

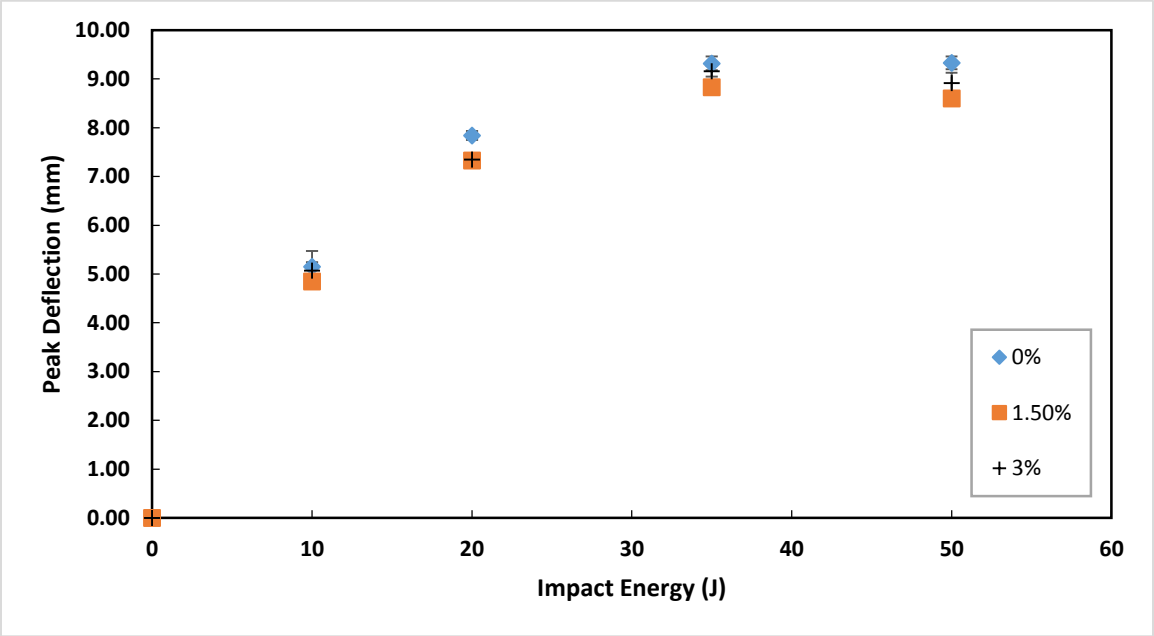

Figure 4.23 Peak deflection as a function of impact energy.

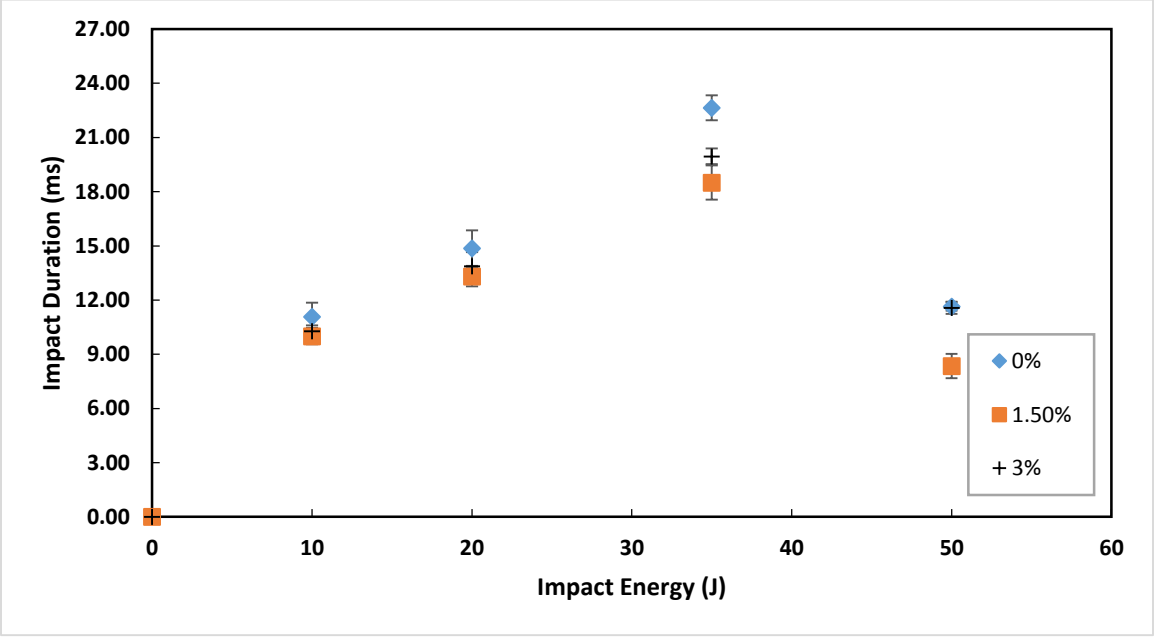

Figure 4.24 Impact duration as a function of impact energy.

4.3.2. Damage Characterization

The above results showed that the higher that impact energy, the higher the absorbed energy and the resulting deflection. These variations are directly related to the physical damage that a sample undergoes. To characterize the extent of the damage, the affected area is measured according to ASTM D7136 [65]. Damage induced by impact is non-destructively observed using strong back lighting, by exploiting the translucency of the material. The front and bottom damage images are taken using Pixera microscope camera and in selected samples (BVID), the internal damage is also directly observed by SEM after sectioning is done using liquid nitrogen.

Figure 4.25 (a) and (b) shows that the front damage is characterized mainly by a dent made by the falling tup which is hardly visible in the case of 10J impacts and thus can be classified as Barely Visible Impact Damage (BVID). The 20J samples appears to have made more contact with the tup as compared to 10J and are found to have higher amount of damage. In the case of 35J and 50J there is a complete puncture in the plates with the hole diameter nearly the size of tup/impactor.

For the back face (Fig. 4.26) the shape and extent of damage varies more profoundly with the impact energy as compared to the front face. Although on the front side the impact of 10 J is barely noticeable but on the back there are visible cracks and dents. The damage induced is somewhat between circular and split shape of cracks and delamination is visible in strong backlight. With 20 J the cross shaped cracks are more prominent with higher damage area. The effect of impact energy and clay loading on damage area will be covered shortly. Higher impact energies of 35J and 50 J result in the most observable damage with large cracks, fiber breakage and puncture.

According to Aktas et al. [55] fiber breakage is the main energy absorption mechanism for glass fiber reinforced composites. Matrix cracking and delamination also occur as matrix cracking initiates delamination and therefore both are taken to be present simultaneously. As can be seen by comparing images 4.20 and 4.21, there is higher damage on the back side as compared to front because the delamination is initiated at the middle plane and proceeds towards the tensile side. The cracks and fiber breakage are much more evident in GFRE 0% samples as compared to those with clay which shows the enforcing behavior of clay.

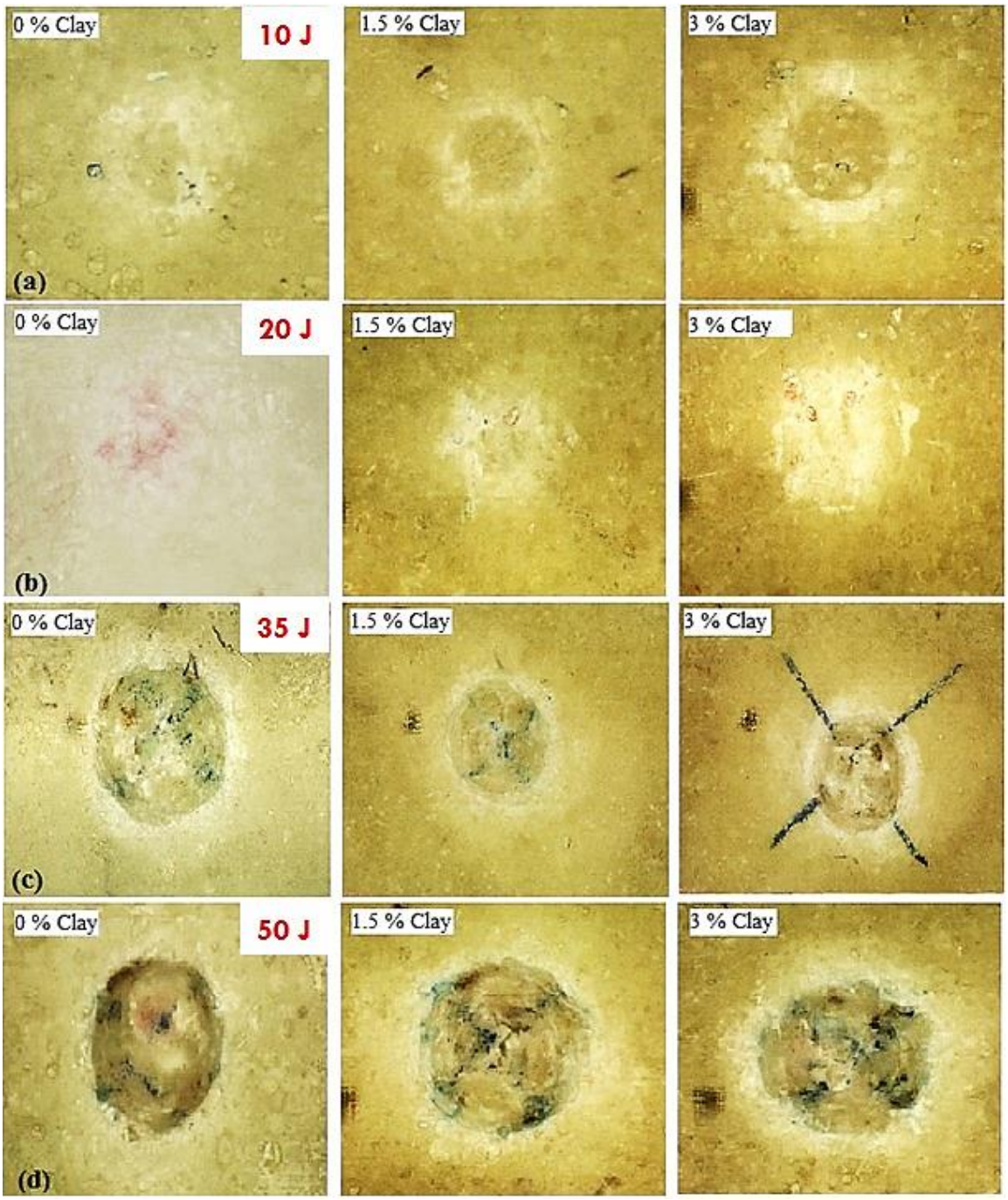

Figure 4.25 Optical images of front side of composite laminates impacted at (a) 10 J (b) 20 J (c) 35 and (d) 50 J.

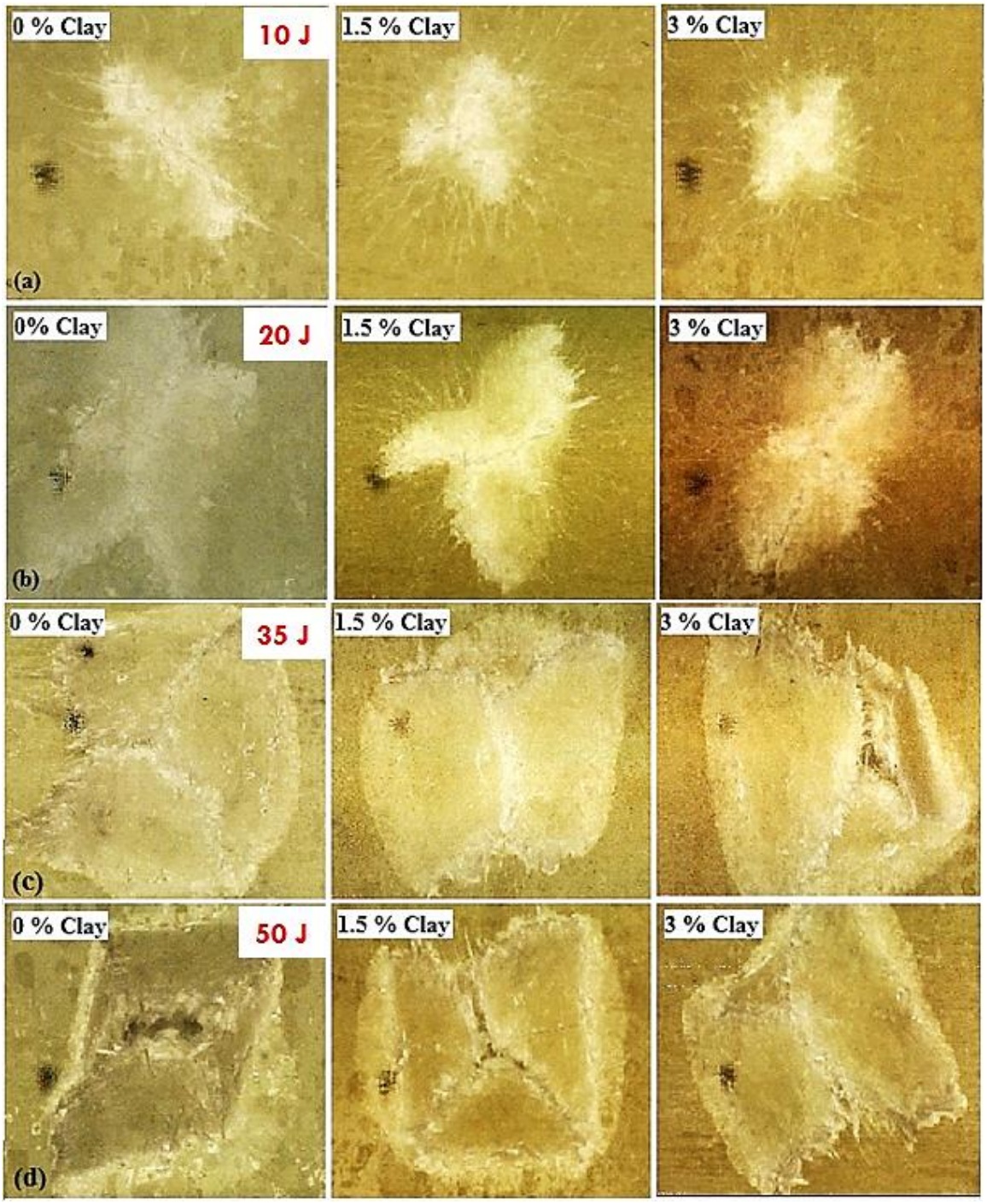

Figure 4.26 Optical images of back side of composite laminates impacted at (a) 10 J (b) 20 J (c) 35 and (d) 50 J

Figure 4.27 shows 'Total Damage Area' which includes the damage resulting from all modes including fiber breakage, matrix cracking and delamination etc. Samples impacted with 10J show the lowest damage area. The damage area increases with impact energy as the absorbed energy also increases which results in higher damage. At 10 J the damage is nearly the same for all clay loadings but as the impact energy increases the difference becomes more profound and 1.5 wt% shows the least damage. At 35 J and 50 J the impact damage is observed to be nearly the same as predicted by the energy time plots which were the same for both of these impact energies. There was improvement in impact damage resistance as explained earlier using force, energy and deflection plots. The improvement in impact damage resistance is mainly because of increase in stiffness due to addition of nanoclay which improves the resistance to fiber buckling under compression which offers enhanced interfacial adhesion [35]. It has also been reported by Caprino [56] and Hirai et al. [58] that the delamination increases with absorbed energy which in turn is associated with impact energy. For 3 % there is clay agglomeration which decreases the effectiveness of clay and results in higher impact damage and lower load bearing as compared to the optimum clay loading of 1.5%.

It can be further observed from the plot that 1.5 wt% and 3 wt% samples are seen to be grouped together as compared to 0 wt% samples. This is due to the fact that clay addition results in lower energy absorption which results in lower damage since impact damage is directly proportional to energy absorbed. This is a major improvement over other studies conducted by Aymerich et al. [40] and Avila et al. [33] which showed that addition of nanoclay increases the energy absorption and subsequently the damage increases as well, which is not desirable.

Table 4.10 Damage area of GFRE nanocomposites at different impact loadings.

Impact Energy (J)	Clay (%)	Damage Area (mm^2)	Standard Deviation
10	0	126.01	0.35
	1.5	86.59	0.71
	3	95.03	0.71
20	0	804.25	0.71
	1.5	268.80	0.35
	3	380.13	2.12
35	0	1288.25	0.71
	1.5	1104.47	0.71
	3	1104.47	0.71
50	0	1288.25	0.71
	1.5	1075.21	0.35
	3	1075.21	0.35

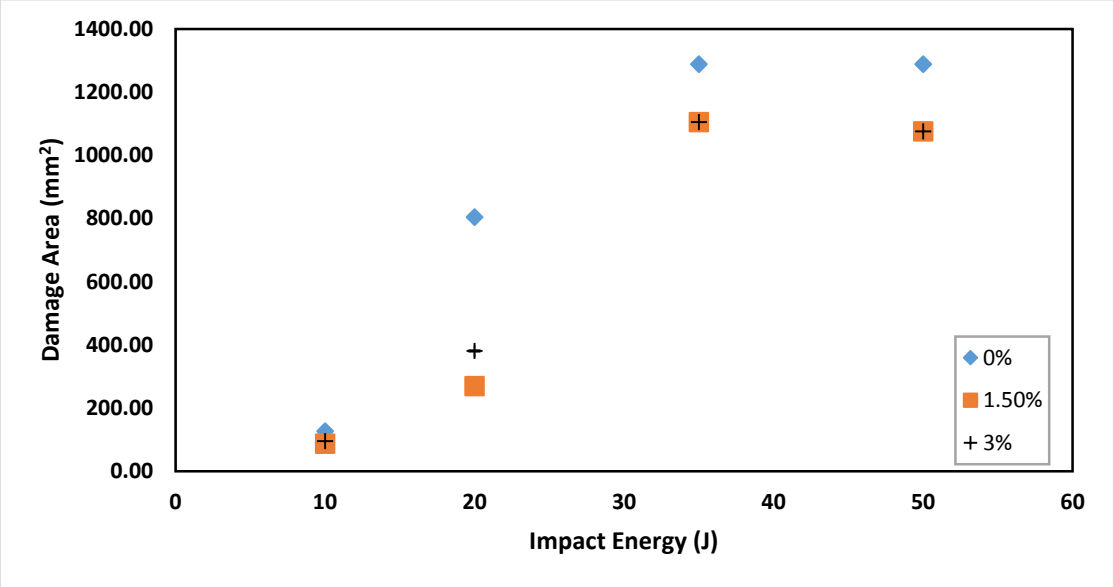

Figure 4.27 Damage area for different impact energies and clay loadings.

In order to observe internal damage, the drop weight impact samples are fractured using liquid nitrogen and fracture surfaces are then observed using SEM. The main purpose of this analysis is to confirm the presence of internal damage in BVID samples of 10J as the damage is very clear in case of higher impact energies. Figures 4.28 (a) and (c) show horizontal and transverse cracks across the matrix which shows matrix cracking. (b) and (d) shows delamination for 0% and 1.5% at 10J which is evident by horizontal delamination of glass fibers sandwiched between two layers of epoxy and epoxy/clay matrix. The evidence for delamination is clearly visible in (b) where one layer has shifted with respect to the other and the fiber impressions can also be seen. Although the damage is not evident on top surface in case of 10J (BVID) but this internal sectioning confirms presence of delamination and matrix cracking which makes these types of damages very dangerous.

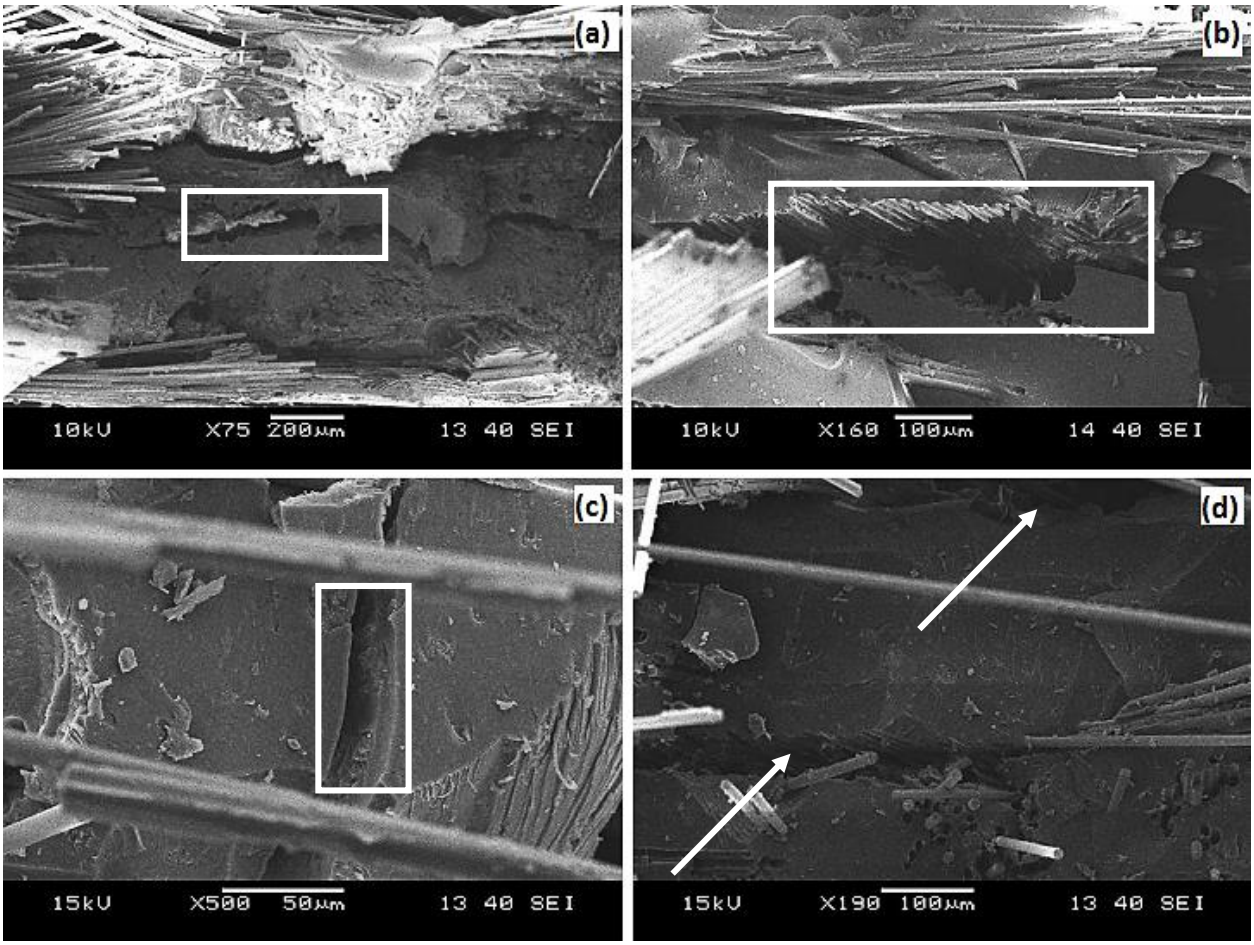

Figure 4.28 SEM images of drop weight impact samples for (a) & (b) 0% and (C) & (d) 1.5% showing delamination and matrix cracking.

CHAPTER 5

CONCLUSIONS & RECOMMENDATIONS

5.1. Conclusions

The focus of this study was to develop fiber reinforced epoxy clay nanocomposites with optimized mechanical and physical properties which could be used in piping systems. In the first part of this work, the fiber reinforced composites were developed using hand layup and hot pressing. As a result, successful hybrid composites of upto 30 fiber volume percent were prepared using ECR Chopped Strand (CSM) glass fiber mats and I.30E nanoclay. Optimal processing of epoxy-nanoclay resulted in exfoliated disorder intercalated structure.

Nanocomposite samples containing ECR Glass fiber (30 vol%) and nanoclay (0-5 wt%) were tested for flexural strength and modulus. The results revealed that clay addition had a positive effect on both properties. Upto 11% improvement was obtained for flexural strength while 14 % improvement was observed for flexural modulus at the optimum clay loading of 1.5 wt%. The SEM analysis showed that the improvement in flexural strength and modulus were mainly due to epoxy-clay morphology and improved interfacial adhesion of clay with glass fibers as well as inherent superior compression properties of clay. After 1.5 wt% the flexural properties were found to decrease reaching values lower than those of neat epoxy samples. The decrease in flexural properties was mainly due to the increase in viscosity at high clay loading which made the degassing and High Shear Mixing much more difficult resulting in increased clay agglomeration and voids as observed by SEM analysis.

The effect of moisture uptake on the flexural strength and modulus was studied by immersing GFRE and GFRE nanoclay samples in tap water at room temperature and at 80°C. The samples were immersed over a period of four months and none of the samples reached saturation. Two distinct regions were observed in the water uptake curve (i) Fickian diffusion and (ii) gradual increase due to polymer relaxation and molecular motion. The addition of both clay and glass fibers had a positive effect on water uptake behavior. Neat epoxy samples absorbed the most water while increasing clay loading upto 5 wt% saw a decrease in water uptake. The water uptake ranged between 0.8 – 1% by weight for different clay loadings. The decrease in water uptake of GFRE containing nanoclay was attributed to the increase in tortuosity in the path of water molecules around the clay platelets. Clay agglomeration at higher wt% resulted in a decrease in effectiveness against water uptake. For high temperature samples the initial diffusion was seen to be many times more than those at room temperature. Although these samples also did not reach complete equilibrium, the water uptake at the end of 4 month period was about 80% higher than those immersed in water at room temperature. At higher temperature the increase in water uptake was due to increase in diffusion.

Afterwards, these samples were then tested for flexural properties in order to determine the impact of water uptake on flexural properties. A similar trend to dry samples was observed with 1.5 wt% being the optimum clay loading. Generally, the room temperature water uptake samples with clay loading did not lose much of their flexural properties but the high temperature water uptake samples showed more profound decrease in flexural strength. GFRE samples lost the most strength while 1.5 wt% samples lost the least strength and were still 3% better than the unexposed GFRE. There was a 10% decrease in strength and

5% flexural modulus for samples immersed in water at room temperature while the samples immersed in water at 80°C showed 36% decrease in strength and 14% decrease in modulus. The decrease in mechanical properties was attributed to the plasticizing effect of water as well as matrix swelling which also reduces the interaction between epoxy-clay and glass fibers. The degradation in mechanical properties of samples immersed in water at 80°C was because of synergistic effect large decrease in mechanical properties at high temperature was because of synergistic effect of both high-temperature and higher water content absorbed.

The low-velocity impact response of epoxy-clay nanocomposites was determined using drop weight impact tests. Four different energies ranging between 10 and 50 J were used to determine the load, energy and deflection response as well as damage caused. GFRE samples with nanoclay exhibited better impact resistance as compared to GFRE 0 wt% samples. 1.5 wt% samples showed an increase in maximum load upto 23% while 3 wt% showed upto 14% improvement. Hybrid composites absorbed less energy as compared to those without clay which led to lesser damage. 35 J was found to be the threshold energy beyond which samples gave in and had complete failure. The absorbed energy increased with increasing impact energy and 1.5 wt% samples were observed to have lowest absorbed energy due to uniform dispersion of nanoclay. The stiffness of samples were determined using deflection at peak load and total impact duration. Both peak deflection and impact time were lowest for samples with nanoclay from which it was concluded that adding nanoclay made the sample stiffer. It was further observed that stiffness of these samples increased upto 1.5 wt% after which the stiffness decreased due to clay agglomeration. These results were in agreement with those obtained from flexural modulus.

The samples contained all types of damage including delamination, matrix cracking, fiber buckling and fracture. The 10 and 20 J samples only had delamination and matrix cracking with only a slight amount of fiber breakage while 35J and 50 J samples went through complete failure and significant fiber damage was also observed. Damage area increased with impact energy but it became constant at impact energy of 35J and above because of the same amount of energy absorbed (saturation limit). It was observed that back side had the largest amount of damage because the damage proceeded towards the tensile side. The 10 J test did not leave any observable mark on the front surface due to which it was characterized as Barely Visible Impact Damage (BVID). This damage was of utmost interest as it was hardest to detect and therefore SEM evaluation was done after cryogenic fracturing of the sample and it confirmed that 10 J BVID samples had delamination as well matrix cracking.

To summarize, fiber based epoxy clay nanocomposites were developed and were tested for flexural properties before and after water uptake. The role of fibers and nanoclay in water uptake behavior was investigated as well. Impact response of different clay loadings at different impact energies were studied for load, energy, deflection and the resulting damage. Therefore, it can be concluded that the objectives outlined for the present work were successfully achieved.

5.2.Recommendations for Future Work

Although a wide variety of tests were performed and a good understanding was developed, still further improvements can be made in the work. The author recommends the following:

1. Vacuum bagging technique can be employed for manufacturing the composites which will reduce the production time and will also increase the fiber percentage and thus increasing the mechanical properties.
2. Different types of fibers can be used e.g woven rovings which will give better properties in specific direction.
3. Instead of using epoxy clay mixture in all of the layers of nanocomposite it can be tested that what is the effect on mechanical properties if only the top and bottom layers are used as it will be much more feasible for industry as it will save overall time and cost.
4. Impact response of water/oil absorbed composites will also give a better insight into the behavior of these composites.

REFERENCES

1. *Effect of water absorption on the mechanical properties of nanoclay filled recycled cellulose fiber reinforced epoxy hybrid nanocomposites.* **H. Alamri, I.M. Low.** s.l. : Composites : Part A, 2012, Vol. 44, pp. 23-31.

2. *Characterizan techniques for nanotechnology applications in textiles.* **M Joshi, A Bhattacharyya, S Wazed Ali.** s.l. : Indian Journal of Fiber & Textile Research, 2008, Vol. 33, pp. 304-317.

3. **Koo, Joseph H.** *Polymer Nanocomposites Processing, Characterization and Applications.* s.l. : McGraw-Hill, 2006. pp. 81-86. 0-07-145821-2.

4. *High-resolution scanning electron microscopy of immunogold-labelled cells by the use of thin plasma coating of osmium.* **Suzuki, E.** s.l. : Journal of Microscopy, 2002, Vol. 208.

5. *Mecahnical and Thermal Behaviours of Glass Fiber Reinforced Epoxy Hybrid Composites Containing Organo-Motmorillonite Clay.* **Mohd. Zulfli, N. H., Abu Bakar A. and Chow W. S.** s.l. : Malaysian Polymer Journal, 2012, Vol. 7, pp. 8-15.

6. *Influence of the addition of montmorillonite to the matrix of unidirectional glass fiber/epoxy composites on their mechanical and water absorption properties.* **L.B. Manfredi, H. De Santis, A. Vázquez.** s.l. : Composites: Part A, 2008, Vol. 39, pp. 1726–1731.

7. *Epoxy-layered silicate nanocompostes as matrix of unidirectional glass fiber/epoxy composites on their mechanical and water absorption properties.* **X. Kornmann, M. Rees,**

Y. Thomann, A. Necola, M. Barbezat, R.Thomann. 2005, Composites Science and Technology, Vol. 65, pp. 2259–2268.

8. *Study of mechanical properties of epoxy/glass/nanoclay hybrid composites.* **Karippal, J.J., Narasimha Murthy, H.N., Rai, K.S., Sreejith, M., and Krishna, M.** Vol. 45, pp. 1893-1899, 2011 2011, Journal of Composites Materials., Vol. 45, pp. 1893-1899.

9. *Mechanical and thermal behavior of clay/epoxy nanocomposites.* **Yasmin, A., Lou, J.J., Abot, J.L., and Daniel I.M.** 2006, Composites Science and Technology, Vol. 66, pp. 2415-2422.

10. *Glass Fiber Reinforced Polymer-Clay Nanocomposites:Processing, Structure and Hygrothermal Effects on Mechanical Properties.* **B. Sharmaa, S. Mahajana, R. Chhibbera, R. Mehtab.** s.l. : Procedia Chemistry, 2012, Vol. 4, pp. 39 – 46.

11. *Effects of moisture on properties of epoxy molding.* **Lu MG, Shim MJ, Kim SW.** 2001, Journal of Applied Polymer Science, Vol. 81, pp. 2253–2259.

12. *Influence of water absorption on the mechanical properties of a DGEBA (n = 0)/1,2 DCH epoxy system.* **Nunez L, Villanueva M, Fraga F, Nunez MR.** 1999, Journal of Applied Polymer Science, Vol. 74, pp. 353-358.

13. *Organoclay-modified high performance epoxy nanocomposites.* **Weiping Lie, Suong V. Hoa, Martin Pugh.** 2005, Composites Science and Technology., Vol. 65, pp. 307–16.

14. *A discussion of the molecular mechanisms of moisture transport in epoxy resins.* **Soles CL, Yee AF.** 2000, Journal of Polymer Science Part B: Polymer Physics, Vol. 38, pp. 792–802.

15. *Nanocomposite.* **Wikipedia.** [Online] [Cited: April 13, 2014.] http://en.wikipedia.org/wiki/Nanocomposite**.**

16. *Mechanical behavior of various nanoparticle filled composites at low-velocity impact.* **Jin-Chein Lin, L.C. Chang, M.H. Nien, H.L. Ho.** 2006, Composite Structures, Vol. 74, pp. 30-36.

17. *An Experimental Study on Clay/Epoxy Nanocomposites Produced in a Centrifuge.* **Saeed Saber-Samandari, Akbar Afaghi Khatibi, and Domagoj Basic.** 2007, Composites: Part B, Vol. 38, pp. 102-107.

18. *Characterization and Modeling of Mechanical Behavior of Polymer/Clay Nanocomposites.* **Daniel, Jyi-Jiin Luo and Isaac M.** 2003, Composites Science and Technology., Vol. 63, pp. 1607–16.

19. *Fracture toughness and water uptake of high-performance epoxy/nanoclay nanocomposites.* **Weiping Liu, Suong V. Hoa, Martin Pugh.** 2005, Composites Science and Technology., Vol. 65, pp. 2364–73.

20. *Preparation and characterization of layered silicate/glass fiber/epoxy hybrid nanocomposites via vacuum-assisted resin transfer molding (VARTM).* **Li-Yu Lin, Joong-Hee Lee , Chang-Eui Hong , Gye-Hyoung Yoo , Suresh G. Advani.** s.l. : Composites Science and Technology, 2006, Vol. 66, pp. 2116–2125.

21. *Understanding the effect of nano-modifier addition upon the properties of fiber reinforced laminates.* **Marino Quaresimin, Russell J. Varley.** s.l. : Composites Science and Technology, 2008, Vol. 68, pp. 718–726.

22. *Modelling the flow of particle-filled resin through a fibrous preform in liquid composite molding technologies.* **Delphine Lefevre, Se´bastien Comas-Cardona , Christophe Bine´truy, Patricia Krawczak.** s.l. : Composites: Part A, 2007, Vol. 38, pp. 2154–2163.

23. *Enhancing compressive strength of unidirectional polymeric composites using nanoclay.* **Arun K. Subramaniyan, C.T. Sun.** s.l. : Composites: Part A, 2006, Vol. 37, pp. 2257–2268.

24. *Mechanical properties of carbon fiber reinforced epoxy/clay nanocomposites.* **Yuan Xu, Suong Van Hoa.** s.l. : Composites Science and Technology, 2008, Vol. 68, pp. 854–861.

25. *Mechanical and thermal behavior of non-crimp glass fiber reinforced layered clay/epoxy nanocomposites.* **Emrah Bozkurt, Elcin Kaya, Metin Tanoglu.** s.l. : Composites Science and Technology, 2007, Vol. 67, pp. 3394-3403.

26. *Influence of montmorillonite clay on the thermal and mechanical properties of conventional carbon fiber reinforced composites.* **Yuanxin Zhou, Farhana Pervin, Vijaya K. Rangari, Shaik Jeelani.** s.l. : Material Processing Technology, 2007, Vol. 191, pp. 347–351.

27. *Investigation of organo-modified montmorillonite loading effect on the abrasion resistance of hybrid composites.* **B. Suresha, R.M. Devarajaiah , T. Pasang , C. Ranganathaiah.** s.l. : Metrials and Design, 2013, Vol. 47, pp. 750–758.

28. *Strength of unidirectional glass/epoxy composite with silica nanoparticle-enhanced matrix.* **Mohammed F. Uddin, C.T. Sun.** s.l. : Composites Science & Technology, 2008, Vol. 68, pp. 1637–1643.

29. *Studies on the flexural and thermomechanical properties of woven carbon/nanoclay-epoxy laminates.* **F.H. Chowdhury, M.V. Hosur, S. Jeelani.** s.l. : Materials Science & Engineering, 2006, Vol. 421, pp. 298–306.

30. *Mechanical, thermal and microstructural characteristics of cellulose fiber reinforced epoxy/organoclay nanocomposites.* **H. Alamri, I.M. Low, Z. Alothman.** s.l. : Composites : Part B, 2012, Vol. 43, pp. 2762–2771.

31. *Impact damage resistance of CFRP with nanoclay-filled epoxy matrix.* **Kosar Iqbal, Shafi-Ullah Khan, Arshad Munir, Jang-Kyo Kim.** 2009, Composites Science and Technology, Vol. 69, pp. 1949-1957.

32. *Drop-weight impact response of hybrid composites impacted by impactor of various geometries.* **Ercan Sevkat, Benjamin Liaw, Feridun Delale.** 2013, Materials and Design, Vol. 52, pp. 57-77.

33. *A study on nanostructured laminated plates behavior under low-velocity impact loadings.* **Antonio F. Avila, Marcelo I. Soares, Almir Silva Neto.** 2007, International Journal of Impact Engineering, Vol. 34, pp. 28-41.

34. *Experimental investigation of the low speed impact characteristics of nanocomposites.* **Ammar Alomari, Saud Aldajah, Saleh Hayek, Kamal Moustafa, Yousef Haik.** 2013, Materials and Design, Vol. 47, pp. 836-841.

35. *Impact damage resistance of CFRP with nanoclay-filled epoxy matrix.* **Kosar Iqbal, Shafi-Ullah Khan, Arshad Munir, Jang-Kyo Kim.** s.l. : Composites Science and Technology., 2009, Vol. 69, pp. 1949–1957.

36. *Mechanical behavior of various nanoparticle filled composites at low-velocity impact.* **Jin-Chein Lin, L.C. Chang, M.H. Nien, H.L. Ho.** 2006, Composite Structures, Vol. 74, pp. 30-36.

37. *Processing of nanoclay filled sandwich composites and their response to low-velocity impact loading.* **M.V. Hosur, A.A. Mohammed, S. Zainuddin, S. Jeelani.** 2008, Composite Structures, Vol. 82, pp. 101-116.

38. *Nano-structured sandwich composites response to low-velocity impact.* **Antonio F. Ávila, Maria Gabriela R. Carvalho, Eder C. Dias, Diego T.L. da Cruz.** 2010, Composite Structures, Vol. 92, pp. 745–751.

39. *Impact response of Kevlar composites with filled epoxy matrix.* **P.N.B. Reis, J.A.M. Ferreira, P. Santos, M.O.W. Richardson, J.B. Santos.** 2012, Composite Structures, Vol. 94, pp. 3520–3528.

40. *Energy absorption capability of nanomodified glass/epoxy laminates.* **F. Aymerich, A. Dalla Via, M. Quaresimin.** 2011, Procedia Engineering, Vol. 10, pp. 780–785.

41. *Thermal stability and water uptake of high performance epoxy layered silicate nanocomposites.* **Ole Becker, Russell J. Varley , George P. Simon.** 2004, European Polymer Journal, Vol. 40, pp. 187–195.

42. *Water absorption of epoxy/glass fiber/organo-montmorillonite nanocomposites.* **Chow, W. S. 2**007, Polymer Letters, Vol. 1, pp. 104–108**.**

43. *Water barrier properties of nanoclay filled sisal fiber reinforced epoxy composites.* **T.P. Mohan, K. Kanny.** 2011, Composites: Part A, Vol. 42, pp. 385–393.

44. *Moisture barrier characteristics of organoclay–epoxy nanocomposites.* **Jang-Kyo Kim, Chugang Hu, Ricky S.C. Woo, Man-Lung Sham.** 2005, Composites Science and Technology, Vol. 65, pp. 805–813.

45. *Effect of water absorption on the mechanical properties of hemp fiber reinforced unsaturated polyester composites.* **H.N. Dhakal, Z.Y. Zhang, M.O.W. Richardson.** 2007, Composites Science and Technology, Vol. 67, pp. 1674–1683.

46. Al-Qadhi, Muneer Abdulrahman. *Development And Characterization Of Epoxy-Clay Nanocomposites.* Mechanical Engineering. s.l. : KFUPM, 2012. PhD Dissertation.

47. *Montmorillonite.* **Wikipedia.** [Online] [Cited: April 13, 2014.] http://en.wikipedia.org/wiki/Montmorillonite.

48. *Low Velocity impact behavior of composite pipes.* **Naik, M. K., Al-Sulaiman F., Khan z., Merah N., mehdi M. Australia :** s.n., 2006. 2nd Conference on: Applications of Traditional and High Performance Materials in Harsh Environments. 9948-42704-1.

49. Khan Z., Merah N., K. Mezghani, Al-Sulaiman F. *Environmental Degradation and its Effect on Long-Term Performance and Durability of Glass Fiber Reinforced Composite used in Oil Production/Transportation pipes.* 2010. #ME2236.

50. *Optimizing the Curing Process of Epoxy-Clay Nanocomposites.* **Al-Qadhi, M., Merah, N. and Mezghani, K.** 2011, Key Engineering Materials, Vols. 471-472, pp. 415-419.

51. *Effect of organo-montmorillonite on the mechanical and morphological properties of epoxy/glass fiber composites.* **M. Norkhairunnisa, A. B. Azhar, and W. S. Chow.** 2007, Polymer International, Vol. 56, pp. 512–517.

52. *Mechanical properties of carbon fiber reinforced epoxy/clay nanocomposites.* **Hoa, Y. Xu and S. V.** 2008, Composites Science and Technology, Vol. 68, pp. 854–861.

53. *Mechanical Properties and water uptake of epoxy-clay nanocomposites containing different clay loadings.* **M. Al-Qadhi, N. Merah, Z. M. Gasem.** 2013, Journal of Material Sceince, Vol. 48, pp. 3798-3804.

54. *Energy-absorption mechanisms in Kevlar multiaxial warp-knit fabric composites under impact loading.* **Kang TJ, Kim C.** 2000, Composite Science and Technology, Vol. 60, pp. 773–84.

55. *An experimental investigation of the impact response of composite laminates.* **Aktas M, Atas C, Icten BM, Karakuzu R.** 2009, Composite Structures, Vol. 87, pp. 307–13.

56. *Residual strength prediction on impacted CFRP laminates.* **G., Caprino.** 1984, Journal of Composite Materials, Vol. 18, pp. 508-518.

57. *Mode I interlaminar fracture behavior and mechanical properties of CFRPs with nanoclay-filled epoxy matrix.* **Naveed A. Siddiqui, Ricky S.C. Woo, Jang-Kyo Kim, Christopher C.K. Leung.** 2007, Composites: Part A, Vol. 38, pp. 449-460.

58. *Effect of Clay Addition on Mechanical Properties of Unsaturated Polyester/Glass Fiber Composites.* **Kusmono and Zainal ArifinMohd Ishak.** 2013, International Journal of Polymer Science.

59**.** *Effect of low velocity impact responses on durability of conventional and nanophased CFRP composites exposed to seawater.* **Mohammad K. Hossain, Md. Mahmudur R. Chowdhury, Kazi A. Imran, Mahmud B. Salam, Arefin Tauhid, Mahesh Hosur, Shaik Jeelani.** 2014, Polymer Degradation and Stability, Vol. 99, pp. 180-189.

60. *Influence of Clay Concentration on the Morphology and Properties of Clay-Epoxy Nanocomposites Prepared by In-situ Polymerization under Ultrasonication.* **Jinwei Wang, Xianghua Kong, Lei Cheng and Yedong He.** 2008, Journal of University of Science and Technology Beijing, Vol. 15, No. 3, pp. 320–23.

61. *Nanoscale***. Freie Universitat, Berlin.** [Online] [Cited: April 29, 2014.] http://www.nanoscale.fu-berlin.de/

62. *Effect of water absorption on the mechanical properties of nano-filler reinforced epoxy nanocomposites.* **H. Alamri, I.M. Low.** 2012, Journal of Materials and Design, Vol. 42, pp. 214–222.

63. *Applications of nanotechnology for the food sector***. Nanowiki.no.** [Online] [Cited: May 01, 2014.] http://www.nanowiki.no/wiki/Applications_of_nanotechnology_for_food_sector.

64. *Delamination threshold loads for low velocity impact on composite laminates.*. **Schoeppner GA, Abrate S.** 2000, Composites Part A : Applied Science, Vol. 31, pp. 903–915.

65. *Measuring the Damage Resistance of a Fiber-Reinforced Polymer Matrix Composite to a Drop-Weight Impact Event*.ASTM D7136/D 7136M, May 2005.

66. *Annual Book of ASTM Standards,* Plastics Materials, 1995

67. **Ali, Yasir Abdelhafiz.** *Enhancement of Mechanical and Physical Properties of Silicate Based Epoxy Nanocomposites.* Mechanical Engineering. s.l. : KFUPM, 2014. MS Dissertation.

VITAE

PERSONAL

Date and Place of Birth: 08/Feb/1990, Bahawalpur (Pakistan)
Nationality: Pakistani
Status: Single
Present Address: KFUPM P.O.Box 8083
King Fahd University of Petroleum and Minerals
Dhahran 31261, Saudi Arabia
Mobile: +966-55-739-3188
E-mail: ahmadrafiq90@gmail.com

EDUCATION

M.S., Mechanical Engineering: May 2014
King Fahd University of Petroleum & Minerals, Saudi Arabia CGPA 3.79/4.00
Thesis: Development and Characterization of Hybrid Glass Fibre and Epoxy Clay Nanocomposite.
B.S., Mechanical Engineering: September 2011
National University of Sciences and Technology, Islamabad, Pakistan CGPA 3.36/4.00
Project: Parametric Study, Design and Fabrication of Dynamometer for Automotive Engines.

PUBLICATIONS

Journal

- Ahmad Rafiq, Muneer Al-Qadhi, Nesar Merah and Yasir Ali, "*Mechanical Behavior of Hybrid Glass Fibre and Epoxy Clay Nanocomposites*', Advanced Materials Research, vol. 894, pp 336-341.

Conference

- Ahmad Rafiq, Muneer Al-Qadhi, Nesar Merah and Yasir Ali. "*Drop Weight Impact Response of Hybrid Glass Fibre and Epoxy Clay Nanocomposites on Low Velocity Impact*", Advances in Material & Processing Technology Conference, Dubai, United Arab Emirates, November 16– 20, 2014. (Submitted)